Control of a dynamic brake to reduce turbine-generator shaft transient torques
by Matthew Kenneth Donnelly

A thesis submitted in partial fulfillment of the requirements for the degree of Doctor of Philosophy in Electrical Engineering
Montana State University

Abstract:
The feasibility of applying a resistive dynamic brake to damp turbine shaft torsional oscillations is studied. In cases where series-compensated transmission lines increase the likelihood of subsynchronous resonance phenomena, the damping of one or more of the torsional modes of the shaft may prove to be inadequate. This is particularly so when high-speed reclosing of transmission lines near a generator is practiced. In this thesis, various control strategies and brake configurations are studied and simulation results are shown. The simulations are performed using the ElectroMagnetic Transients Program (EMTP) on models ranging from one machine, infinite bus (the IEEE Second Benchmark) to multiple machines in a complex network. A derivative of Prony's method for signal analysis is used to find a linearized transfer function of the system for controller design and implementation. Methods for reducing the complexity of the results of a Prony analysis are presented. It is seen both empirically and intuitively that a simple control law does an effective job of damping turbine shaft torques throughout the range of subsynchronous frequencies. The empirical evidence is gained through comparisons with a Generalized Predictive Control (GPC) algorithm implemented on a linearized model of the test system. Discrete-level GPC is seen to have sensitivity problems in this application. The thesis goes on to analyze and document these sensitivity problems. Recommendations are made as to size, placement, and construction of the brake for adequate damping. Studies incorporating multiple brakes are also conducted revealing that, with few exceptions, the interaction between brakes operating on non-identical machines is negligible and that the interaction between brakes operating on identical machines is substantial and desirable. Computer code for implementing a brake in the EMTP is included as an appendix.

Control of a Dynamic Brake to Reduce Turbine-Generator Shaft Transient Torques

by

Matthew Kenneth Donnelly

A thesis submitted in partial fulfillment
of the requirements for the degree
of

Doctor of Philosophy

in

Electrical Engineering

MONTANA STATE UNIVERSITY
Bozeman, Montana

November 1991

APPROVAL

of a thesis submitted by

Matthew K. Donnelly

This thesis has been read by each member of the thesis committee and has been found to be satisfactory regarding content, English usage, format, citations, bibliographic style, and consistency, and is ready for submission to the College of Graduate Studies.

Nov. 13, 1991
Date

Roy M. Johnson
Chairman, Graduate Committee

Approved for the Major Department

Nov. 13, 1991
Date

Head, Major Department

Approved for the College of Graduate Studies

November 14, 1991
Date

Henry L. Parsons
Graduate Dean

STATEMENT OF PERMISSION TO USE

In presenting this thesis in partial fulfillment of the requirements for a doctoral degree at Montana State University, I agree that the Library shall make it available to borrowers under the rules of the Library. I further agree that copying of this thesis is allowable only for scholarly purposes, consistent with "fair use" as prescribed in the U.S. Copyright Law. Requests for extensive copying or reproduction of this thesis should be referred to University Microfilms International, 300 North Zeeb Road, Ann Arbor, Michigan 48106, to whom I have granted "the exclusive right to reproduce and distribute copies of the dissertation in and from microfilm and the right to reproduce and distribute by abstract in any format."

Signature Matth K. Donald

Date NOVEMBER 12, 1991

ACKNOWLEDGMENTS

My sincere gratitude is extended to my thesis advisor, Dr. Roy Johnson. His faith in my abilities has motivated me in every phase of my research, and his personal friendship will be valued for many years to come. The help of Dr. Jim Smith and Dr. Don Pierre in the areas of system identification and control system design is also acknowledged. Further, I am indebted to Dr. John Lund and Dr. Ken Bowers for sparking in me an intense interest in the mathematical sciences which will stay with me forever.

In addition to the funding provided by the Electric Power Research Institute, I would like to acknowledge the financial contributions made by the Montana Electric Power Research Affiliates (MEPRA) and the Montana State University Engineering Experiment Station (EES). The guidance provided by my industrial advisors is also appreciated. Mr. Ray Brush of Montana Power Company supplied me with much needed practical information. Dr. John Hauer of Bonneville Power Administration provided insight at our meetings and has been an inspiration in developing some system identification routines.

Lastly, I would like to thank my fiance', Toni Crosby, for enduring the long days and late nights associated with graduate study. Her interest in the work and her support and understanding have made this research enjoyable.

TABLE OF CONTENTS

TABLE OF CONTENTS -- Continued

LIST OF TABLES

LIST OF FIGURES

LIST OF FIGURES -- Continued

LIST OF FIGURES -- Continued

NOMENCLATURE

$\mathcal{L}\mathbf{f}$	The LaPlace transform of **f**
$\mathcal{L}^{-1}\mathbf{g}$	The inverse LaPlace transform of **g**
$\| \ \|$	Any induced matrix norm
$\kappa(A)$	The condition number of A
B^{+}	The Moore-Penrose Inverse of B
Q^{H}	The conjugate-transpose of Q

ABSTRACT

The feasibility of applying a resistive dynamic brake to damp turbine shaft torsional oscillations is studied. In cases where series-compensated transmission lines increase the likelihood of subsynchronous resonance phenomena, the damping of one or more of the torsional modes of the shaft may prove to be inadequate. This is particularly so when high-speed reclosing of transmission lines near a generator is practiced. In this thesis, various control strategies and brake configurations are studied and simulation results are shown. The simulations are performed using the ElectroMagnetic Transients Program (EMTP) on models ranging from one machine, infinite bus (the IEEE Second Benchmark) to multiple machines in a complex network. A derivative of Prony's method for signal analysis is used to find a linearized transfer function of the system for controller design and implementation. Methods for reducing the complexity of the results of a Prony analysis are presented. It is seen both empirically and intuitively that a simple control law does an effective job of damping turbine shaft torques throughout the range of subsynchronous frequencies. The empirical evidence is gained through comparisons with a Generalized Predictive Control (GPC) algorithm implemented on a linearized model of the test system. Discrete-level GPC is seen to have sensitivity problems in this application. The thesis goes on to analyze and document these sensitivity problems. Recommendations are made as to size, placement, and construction of the brake for adequate damping. Studies incorporating multiple brakes are also conducted revealing that, with few exceptions, the interaction between brakes operating on non-identical machines is negligible and that the interaction between brakes operating on identical machines is substantial and desirable. Computer code for implementing a brake in the EMTP is included as an appendix.

CHAPTER 1

INTRODUCTION

The primary focus of this thesis is the damping of transient torques in turbine-generator shafts following electrical network system disturbances. The damping is to be improved by means of a dynamic resistive brake located near to the generator. Transient torques are oscillatory in nature. It is desirable to damp these oscillations as quickly as possible, particularly in the case where high speed reclosing is employed on transmission lines emanating from the generator.

This dissertation contains seven chapters. Chapter 1 is an introduction to the problem along with a brief history and literature review. Chapter 2 describes the models used in the research and the associated modeling techniques. Because of the complexity of the electrical network and the cost of lost generation, accurate and realistic modeling is a crucial task. Therefore, a significant amount of work was spent in developing appropriate models and simulation routines. This effort should prove to be a great benefit to other researchers in this area. Chapter 3 discusses some of the techniques that are useful in the analysis of subsynchronous resonance

problems. Specifically, the analysis techniques used in determining appropriate feedback signals for the dynamic brake and for sizing the brake are explained. Chapters 4 and 5 describe the control techniques, controller analysis and simulation results. In Chapter 6, some special cases are examined to determine the effectiveness of the control algorithm over a wide range of conditions. Finally, Chapter 7 offers some conclusions relating to the project and provides some direction for future work. Following Chapter 7, a list of references is provided.

In addition to the text, four appendices are included showing some representative computer code used in this research. Appendices A and B contain data files for the "IEEE Second Subsynchronous Benchmark" model and the Montana Power Company Colstrip model. Appendix C shows the interface and controller subroutines. Appendix D contains computer code implementing a numerical integration technique along with a sample data file described in Chapter 2.

History of the Problem

The notion of series compensation to increase the carrying capacity in electric power transmission lines beyond what is considered the uncompensated stability limit was developed almost simultaneously with the widespread adoption of alternating current as the transmission standard in the US.

Dr. Charles Concordia recognized as early as 1937 that series compensation would set up a resonance in the electrical network and that this was a potential problem [1]. Dr. Concordia and other early researchers saw this resonance as a problem only with respect to the electrical network. It was not until 33 years later when a turbine-generator was actually damaged in operation that researchers began to look at the interaction between the electrical network and the turbine-generator shaft mechanical system.

In 1970, the first of two shaft failures occurred at the Mohave plant in southern Nevada. By 1972, a consortium of engineers had determined that the cause of the 1970 shaft failure and the second failure in 1971 were due to interactions between the electrical network and the mechanical system at certain frequencies where both systems showed a tendency to resonate [2], [3]. This phenomenon has been the topic of much research since that time.

Description of the Problem

Power system network disturbances create several distinct transients in nearby generation units. One such transient occurs in steam-driven generators as the separate masses along the turbine-generator (TG) shaft oscillate against each other. The magnitude of the inertias of these masses along with the

spring constant of the connecting shaft determine the frequencies of oscillation according to Newtons Law for torsional mechanics,

$$Torque = Inertia \times angular\ acceleration .$$

Current technology in the field of turbine design is such that these natural frequencies of oscillation fall into the range of 10 to 50 Hertz. Power system transmission networks are relatively poorly damped at frequencies below synchronous speed. In some cases the combination of the network and turbine shaft resonances at a frequency can be negatively damped. It is this interaction between the poorly damped network and the turbine shaft natural frequencies that has been described as *Subsynchronous Resonance* or SSR.

The phenomena of subsynchronous resonance can be divided into two main areas for the purpose of analysis. These are generally recognized in the literature as being self-excitation phenomena and transient torque phenomena. The area of self-excitation effects is often further divided into induction motor effects and torsional interactions. In the cases that have been reported, both conditions occur simultaneously [4]. From a control perspective self-excitation phenomena is not a separate issue from transient torque phenomena but rather the issue is how these electrical and mechanical interactions affect the damping of turbine shaft oscillations. A shaft system with very low or no damping

will exhibit steady-state instability. A system with larger damping factors for each natural mode will not exhibit steady state oscillations, but may experience damaging shaft torques for a given sequence of network events.

The practice of transmission line high-speed reclosing may fatigue some turbine-generator shaft systems [5], [6]. Although the shaft is sufficiently damped so as to prevent steady state oscillation, the damping factors are small enough that damaging shaft torques can be created by a high speed reclosing operation. A system with natural modes of oscillation will always respond more actively to inputs that contain frequencies near to the natural modes. High-speed reclosing involves faster operation of breakers which necessarily means creating shocks to a shaft system that contain a larger amount of energy at frequencies nearer to the natural shaft modes.

Generator shaft torsional damping results from both mechanical and electrical factors. The mechanical factors include windage, bearing friction, and natural damping of the shaft material. The windage on turbine blades is cited as the major factor which causes shaft systems to exhibit more damping at higher machine loadings [7]. Electrical factors contributing to damping are predominated by the electrical resonance points of the network. Maintaining a high electrical impedance at all frequencies within the SSR range will eliminate problems of steady state shaft oscillations but may

not be sufficient to produce enough damping to safely allow for high speed reclosing. This may be an important consideration for a control strategy which is intended to produce enough damping to allow for high speed reclosure. Such a strategy will likely have to provide much more damping than would be obtained passively by changing the apparent network impedance over the range of subsynchronous frequencies.

It is also important to realize that during a typical short circuit disturbance with fault clearing and reclosing, the generator shaft system is exposed to three suddenly different electrical networks. These correspond to the apparent impedances seen during the short, those seen during clearing and those seen upon reclosure. These three networks are very likely to have different resonant characteristics and result in different damping factors for each of the shaft natural modes. With this in mind a controller that will produce good damping must be able to operate on the shaft system during as much of these three time periods as possible.

This study examines the use of a resistive brake at the terminals of a large synchronous generator which is activated in such a way and at such a time so as to provide additional damping to the turbine-generator shaft during critical transients. Only steam-powered generators (thermal units)

are considered since hydro-electric generators do not exhibit mechanical oscillations in the frequency range of concern for this work.

Pertinent Literature

There is an abundance of literature dealing with the topic of subsynchronous resonance. The vast majority of these papers treat SSR as a sustained phenomenon and do not discuss the transient torque problem associated with turbine-generator shaft fatigue. The reader is referred to the IEEE working group bibliographies on SSR for an exhaustive list of references in this area [8]-[11]. The IEEE working group has also published a reference of terms, definitions, and symbols relating to SSR phenomena [12]. In [13], Bowler gives a concise summary of the various aspects of SSR that will provide the reader with a familiarity of the topic without thorough research. In his text on power system dynamics [14], Yu also gives an excellent summary. Hamouda, Iravani, and Hackam give insight into the specific problem of torsional oscillations and provide an integrated study model in [15]. Agrawal, et al., [16], explain some of the evaluation tools available to researchers in this field.

Several papers have investigated the use of braking technologies to improve power system stability in the "transient stability" sense. Traditionally, transient sta-

bility has referred to the ability of synchronous generators to return to the system synchronous frequency following a major disturbance. In [17], [18], and [19], some optimal control strategies are developed to damp low frequency swings using braking resistors. These strategies are implemented in computer simulations to evaluate their effectiveness. Yoshida's work, [20], is more functional in that he discusses some implementation issues with respect to resistive devices in the network. A resistive brake acting alone may not provide the optimal amount of damping in transient stability studies. The coordination of system components such as exciters with a braking resistor is discussed in [21]. Of equal interest to the theoretical studies, the testing of braking resistors on the actual system is always enlightening. In [22] and [23], the results of testing at two sites which have installed large braking resistors are discussed.

Additionally, several methods have been proposed to address the problem of damping transient torques in TG shafts. Hingorani, et al. discuss the possibility of using a series device to damp transient torques [24], [25]. The referenced device appears to be better suited for damping the sustained oscillations commonly associated with severe SSR. In [26], the generator field is adjusted to attempt to compensate for torsional oscillations with some success. The use of a resistive brake to damp higher frequency oscillations such

as can be seen in the mechanical mass-spring system of a turbine shaft was first researched at Purdue University [27], [28]. No other recent literature has been found dealing specifically with this topic. Generally, the brake size may be smaller than would be seen in a brake designed to improve transient stability, but expensive thyristors must be used to switch the brake. The low frequencies involved in traditional transient stability studies allow the use of circuit breakers to switch these resistors.

CHAPTER 2

MODELS AND MODELING

The development, testing and verification of models and modeling techniques make up a large percentage of the work performed in this research. This chapter provides the documentation for the two test systems that were developed for use in the study of transient torque. The information provided herein should be useful as a starting point in any future studies involving turbine-generator shaft oscillations and the transient torque phenomena.

A one-line diagram of the first test system examined is shown in Figure 1. The basis for this model is the IEEE Second Subsynchronous Benchmark case as reported in [29]. This system provides a benchmark by which all studies in this area can be compared. The machine and line parameters found in the paper are implemented in an Electromagnetic Transients Program (EMTP) [32], [34], [37]. The damping factors for the generator shaft system in this study have been increased over what is specified for a self-excitation case. The actual damping values used are as specified in [29] under the section titled "Torque Amplification Studies." The IEEE First

Subsynchronous Benchmark [30] was not deemed to be suitable for these studies because the authors made no provision for simulating transient SSR (torque) problems.

The Second Subsynchronous Benchmark model is useful in testing various control strategies on a single machine system and in comparing the effectiveness of one control technique over another. The system is fairly simple and as an IEEE benchmark it can lend credibility to simulation results. The basic EMTP data file used to implement this benchmark is shown in Appendix A.

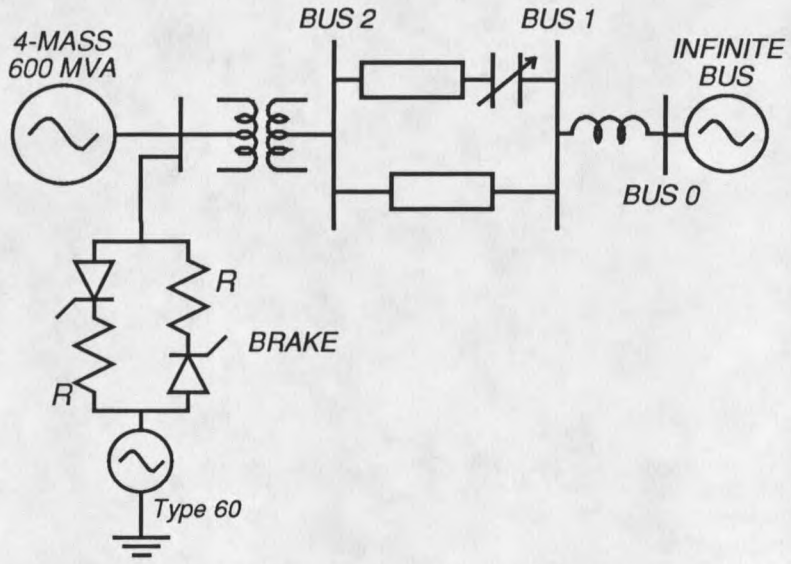

Figure 1. The IEEE Second Subsynchronous Benchmark.

A second test system developed for the braking studies is the Montana Power Company (MPC) Colstrip Model and associated 500 kV transmission lines. This system has several

advantages over the benchmark system which make it more useful as the primary test bed for the dynamic brake stability studies presented here. The basis for the model was provided by Ray Brush of MPC in late 1989. Though significantly modified from the original MPC data for the purposes of this study, the current model has retained enough major features of the original to make it a realistic facsimile.

The MPC Colstrip Model

Three major modifications to the original model stand out as being significant. They are: 1) the inclusion of the J. Marti line models [31] on the 500 kV lines replacing Π sections, 2) the elimination of the zinc oxide varistors used as series capacitor protection, and 3) creation of Thevenin equivalents at the 230 kV buses and at Dworshack and Bell substations. Numerous other less dramatic changes were made in converting the files to EMTP version 2.0 and tuning the simulations. The current model is well suited to studies on transient torque and dynamic braking. A one-line diagram of the system is shown in Figure 2. The Colstrip generators appear on the right as synchronous machines and are labeled *SM*.

The model, implemented in the Electric Power Research Institute's (EPRI's) version of EMTP, consists of two sets of two identical turbine-generators for a total of four

machines at the generating facility. Two machines, Colstrip #1 and Colstrip #2, feed a 230 kV bus located at Colstrip and are each rated at 377 MVA. An autotransformer then feeds the 500 kV bus at Colstrip from the 230 kV bus. These are three mass machines. The masses consist of two turbines and a generator. Colstrip #3 and Colstrip #4 are two larger machines, each rated at 818 MVA, that feed the 500 kV bus at Colstrip directly. These are six mass machines consisting of four turbines, a generator, and an exciter.

The machines can be configured in several different ways depending on the type of study desired. One common configuration in the preliminary studies was to combine the two large units into one 1636 MVA conglomerate machine and implement the brake at the terminals of this machine. In previous studies on the topic, the case with multiple machines -- particularly closely coupled machines -- has not been considered.

The bulk of the energy from Colstrip is carried on twin 500 kV circuits, both of which are series compensated. The series compensation can provide a turbine-generator mass-spring system with negative damping under certain circumstances as identified in numerous papers on SSR. In almost all cases, the presence of series compensation on a transmission line has the effect of reducing the damping of at least one mode of a turbine-generators natural frequencies

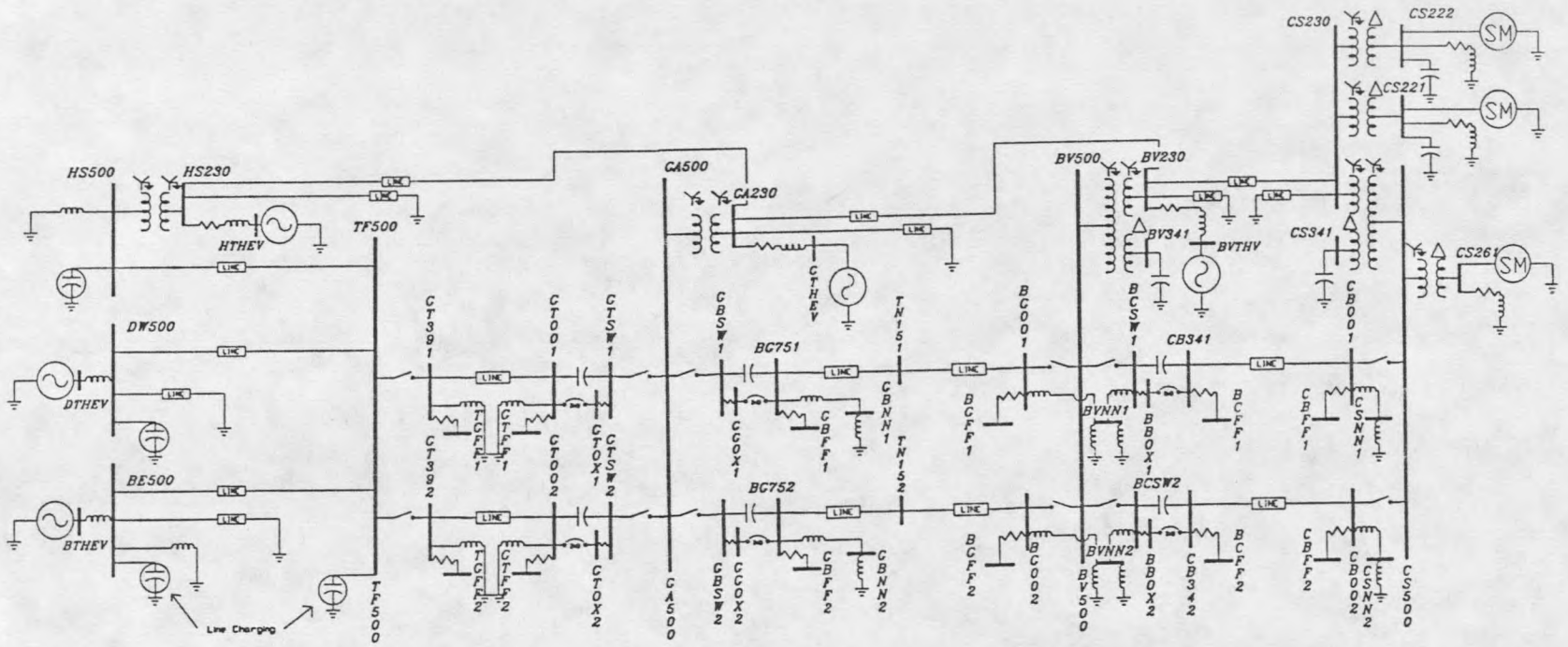

Figure 2. MPC Colstrip Model

of oscillation. This reduction in damping can in turn create problems with transient torques in turbine-generator shafts following system disturbances. Again, the Purdue studies do not incorporate series compensation into their systems for studying transient torques.

The basic EMTP data file for the MPC Colstrip model is included in Appendix B.

The Dynamic Brake

The resistive brake is connected to the system in wye at the generator terminals. The wye connected brake is shown in Figure 3.

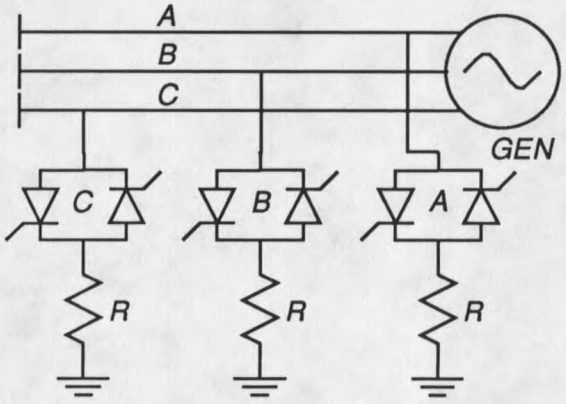

Figure 3. Wye Connected Dynamic Brake.

Historically, resistive brakes have been placed at higher voltages than is seen at the terminals of a synchronous machine. The Peace River 600 MW brake is at 138 kV [22] and

the BPA 1400 MW brake is at 230 kV [23]. Since the primary function of these devices has been for improving transient stability, they are large and employ circuit breakers as switching devices. The brake presented here utilizes thyristors as switching devices, and so a lower operating voltage may be considered advantageous. Circuit breakers may still be employed in a normally closed position to protect the system against thyristor failure.

The size of the brake is determined by the value of resistance. In this study, brakes ranging from 41 MW to 850 MW were used. It is difficult to put a percent rating on these values when dealing with multiple machines, however 850 MW is approximately 50% of the conglomerate Colstrip machine rated MVA.

Implementation of the Brake in EMTP

The brake is implemented in the EMTP as shown in Figure 4. The EMTP Type 60 sources connected in each phase to ground are TACS controlled sources. TACS is a sub-program of the EMTP that implements controllers on the simulated systems [32]. TACS is an acronym for Transient Analysis of Control Systems. In this case, these sources are always proportional to the voltage at their respective generator terminals. The relationship between the generator bus voltage and the Type

60 source is

$$V_{Type60\ A} = V_{Bus\ A}(1-\sqrt{u})$$
$$V_{Type60\ B} = V_{Bus\ B}(1-\sqrt{u}) \qquad (2.1)$$
$$V_{Type60\ C} = V_{Bus\ C}(1-\sqrt{u})$$

where

$$0 \le u \le 1.$$

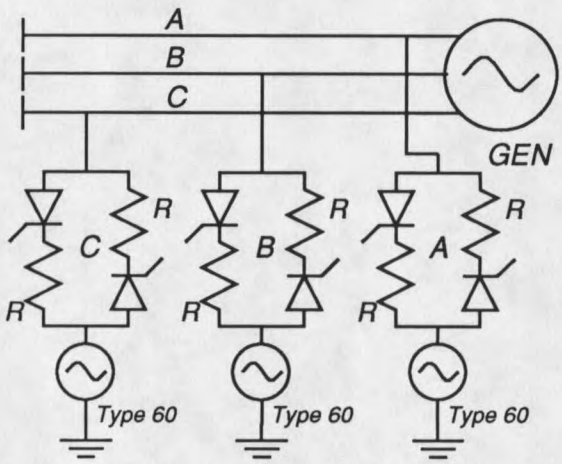

Figure 4. Dynamic Brake With Type 60 Sources.

For "bang-bang" control of the type employed in [27], let $u = 1$ in (2.1). Then the status of the thyristors only determine whether the brake is off or fully on. Bang-bang control refers to a control law which provides maximum control action for a period of time and then switches to minimum control action without taking on any intermediate values. Now for a value of $u = 0.5$,

$$P = \frac{(V_{Busi} - V_{Type60i})^2}{R}$$

$$= \frac{\left(V_{Busi} - V_{Busi}\left(1 - \sqrt{\frac{1}{2}}\right)\right)^2}{R}$$

$$= \frac{V_{Busi}^2}{2R} \quad .$$

Should the thyristors now gate the brake, it would be supplying only one half of the potential braking power. The Type 60 source therefore gives the flexibility to design controllers of the conventional type as well as looking into bang-bang control.

Although nonlinear systems are in general difficult to analyze, they often can be accurately approximated by linear systems. A control strategy with the objective of damping oscillations in a minimum amount of time is referred to as time optimal control. Time optimal control of systems with limited control actuator energy are usually bang-bang controllers [33]. For this reason, the most effective control strategy for damping shaft transient torques for fast reclosing will likely involve bang-bang control of the brake. The Type 60 sources described above are used as a starting point for brake modeling and research into the possible uses of the brake in improving shaft damping and transient stability. In the bang-bang implementation, the Type 60 sources are unnecessary but are included for consistency.

Long term damping in the transient stability case may not be most readily obtained from bang-bang control. Thyristor firing angle control could be used to implement such a long term braking action in which case the Type 60 source concept may be an adequate model. If the controller called for $u = 0.5$ in (2.1), the firing of the appropriate thyristor would be delayed long enough to admit only "half power" through its resistor in any given half cycle of the 60 Hz bus voltage.

The thyristor models and the Type 60 sources are each controlled in this study by TACS supplemental variables. The determination of the Type 60 source amplitude and the firing angle of the thyristors are computed using various control strategies which will be discussed later. These calculations are conducted in a FORTRAN subroutine which is linked with the EMTP. The EMTP support subroutine CSUP is used to place the software interface "hooks" to the user written controller. Subroutine CSUP is called at each integration time step to calculate the values of some of the TACS supplemental variables. Node voltages are brought in to the user written subroutine via three supplemental variables, one per phase, defined in the EMTP data file. Synchronous machine variables are brought in via the common block SMTACS with the array ETACS. With this information, the controller subroutine delivers the Type 60 source amplitudes and the status of the thyristor gate firing signals through other supplemental

variables defined in the EMTP data file. The array containing the supplemental variables at this point in the time step integration is called XTCS. A block diagram containing the pertinent calls at each time step is shown in Figure 5.

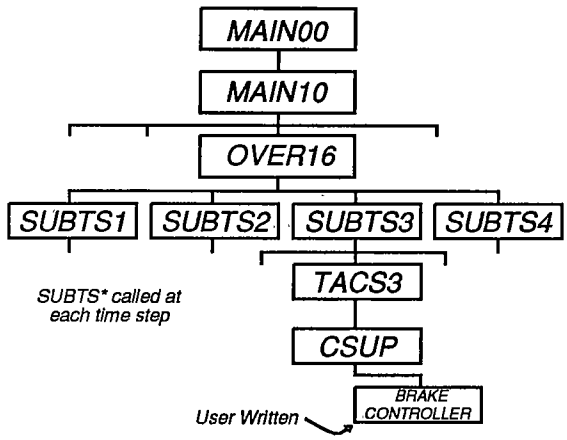

Figure 5. EMTP Calls To Control Subroutine.

A description and listing of the modifications made to the EMTP source code is included in Appendix C. The new external subroutine called from the EMTP contains the control algorithm and is discussed in Chapter 4.

An Alternative Integration Technique for Time-Domain Simulation

The EMTP uses a trapezoidal integration rule to solve the network equations representing the modeled system. This choice has historically been motivated by the robustness of the trapezoidal rule in the face of complexities often found in power system models such as nonlinearities, switching

actions which create time-domain discontinuities, and wave phenomena [34]. The trapezoidal rule can be placed in a broader category of numerical schemes known as Adams methods. The particular rule used in the EMTP is known as a second-order Adams-Moulton scheme. Some steps that are common in the development of all Adams methods are shown below [35].

Writing the differential equation

$$\frac{dx}{dt} = f(t,x) \tag{2.2}$$

in the form

$$dx = f(t,x)dt \tag{2.3}$$

one integrates (2.3) between t_k and t_{k+1}

$$\int_{t_k}^{t_{k+1}} dx = x_{k+1} - x_k = \int_{t_k}^{t_{k+1}} f(t,x)dt \quad . \tag{2.4}$$

The function $f(t,x)$ is now approximated as a polynomial so that the integral on the right-hand side of (2.4) may be evaluated. If Newton-Gregory backward interpolating polynomials fitting at $t_k, t_{k-1}, \ldots, t_{k-n}$ are used to approximate $f(t,x)$ and the integration in (2.4) is carried out, the result is a $k+1^{st}$ order Adams-Bashforth predictor scheme. Now if $f(t,x)$ is approximated using a $(k+1)^{st}$ degree polynomial fit at $t_{k+1}, t_k, \ldots, t_{k-n+1}$, a different scheme called an Adams-Moulton corrector is obtained.

The fourth-order Adams-Bashforth predictor is

$$\tilde{x}_k = x_{k-1} + \frac{h}{24}(55f_{k-1} - 59f_{k-2} + 37f_{k-3} - 9f_{k-4}) \tag{2.5}$$

and the fourth-order Adams-Moulton corrector is

$$x_k = x_{k-1} + \frac{h}{24}(9f_k + 19f_{k-1} - 5f_{k-2} + f_{k-3}) \quad . \tag{2.6}$$

In (2.5) and (2.6), h denotes the step size.

In standard practice, (2.5) would be applied to the set of system equations constituting the system model. Once $\tilde{x}_k$ is obtained from the predictor, it is used to estimate f_k and (2.6) is applied to the system equations. The x_k obtained from the corrector is a better estimate of the actual value at t_k than is $\tilde{x}_k$.

The higher order predictor-corrector schemes provide more accurate estimates of the true system, but they suffer one major drawback. For the fourth-order scheme shown in (2.5) and (2.6), four past values of f are required to initiate the simulation. Since it is already a difficult task to formulate a three-phase load-flow to find initial conditions for the trapezoidal rule, the higher order predictor-corrector schemes are not implemented in the EMTP.

There are cases ideally suited for predictor-corrector integration schemes. In some simulations, the user is interested in transients occurring during the start-up of a system as well as the steady-state. In many cases, the

transients are fast and the steady-state can be reached in a minimum of computation time. In these situations, one can set all of the initial conditions to zero and start the simulation from rest. Such is the case with the "PASC" converter described in [36].

Appendix D contains the source code for a model of the PASC system overlaid on a generic implementation of a fourth-order Adams predictor-corrector. The PASC model proved to be difficult to simulate using some implementations of standard integration routines. The Adams routines had the advantage of being a-stable and simple. These are the features noted by the authors of the EMTP in defending their choice of integration routines also [37]. Should a greater amount of accuracy be required in the future, it may be worthwhile to re-write the EMTP to incorporate a higher order Adams scheme. Such a re-write is beyond the scope of the present work.

CHAPTER 3

SYSTEM ANALYSIS TECHNIQUES

There are several system analysis techniques which are suggested in the open literature for studies dealing with SSR phenomena. Three of these techniques, frequency scan, EMTP, and eigenvalue analysis, have been widely used in previous research on the topic. Agrawal et al. have done an excellent job of summarizing these in a paper submitted at the 1989 IEEE Power Engineering Society Summer Meeting [16]. In addition to these conventional analysis techniques, system identification methods resulting in identified models have proven to be useful tools in the design of controllers for the brake. The identified models are obtained using an off-line system identification routine. The three conventional methods and the identified model are discussed in more detail in this section.

Frequency Scan

Frequency scanning is a technique which can be used to identify frequencies in the electrical network that pose potential SSR problems. A frequency scan shows the equivalent

network resistance and reactance "looking out" from a point in the network as a function of frequency. For SSR analysis, this point in the network is invariably at the terminals of the generator under study. One can obtain a plot of resistance and reactance versus frequency for a particular generator and determine whether the electrical network, as seen from that generator, will exhibit any resonances within a certain frequency range -- typically 10 to 50 Hertz. A resonance occurs where the reactance at a frequency is identically zero. The effects of this network resonance on the stability of a turbine-generator shaft system are amplified if the network resistance at the resonant frequency is small or perhaps even negative. Agrawal and Farmer comment on the use of frequency scanning in SSR analysis in [38].

Commonly, the mechanical mass-spring system consisting of the turbine shaft is analyzed separately for the mechanical resonances. These frequencies are then reflected to the electrical network using frequency-domain convolution [see 39, p.451]. Convolution is appropriate because the action of the generator mass oscillating at some frequency while rotating at synchronous speed modulates the magnetic flux acting on the machine stator. This process amounts to the equivalent of amplitude modulation in communication theory. The net effect of this convolution is the appearance of two "sideband" frequencies in the electrical network. One sideband

can be seen at $f_{synchronous} - f_{mechanical}$ and one can be seen at $f_{synchronous} + f_{mechanical}$. The latter frequency is of no interest in SSR studies due to the high network damping at supersynchronous frequencies [40]. The resulting subsynchronous frequency is normally called the "compliment" frequency.

The mechanical system compliment frequencies are drawn on the frequency scan plots as vertical lines for a visual aid in identifying potential problems. Figures 6 and 7 show frequency scans from the terminals of Colstrip #1 and Colstrip #3 respectively. These plots were obtained using the FREQUENCY SCAN option of the EMTP. As would be expected for machines which are electrically close together, the two plots are similar. Figure 6, however, contains more inductive reactance than does Figure 7. This is due to the presence of the 230/500 kV auto-transformer between the two machines.

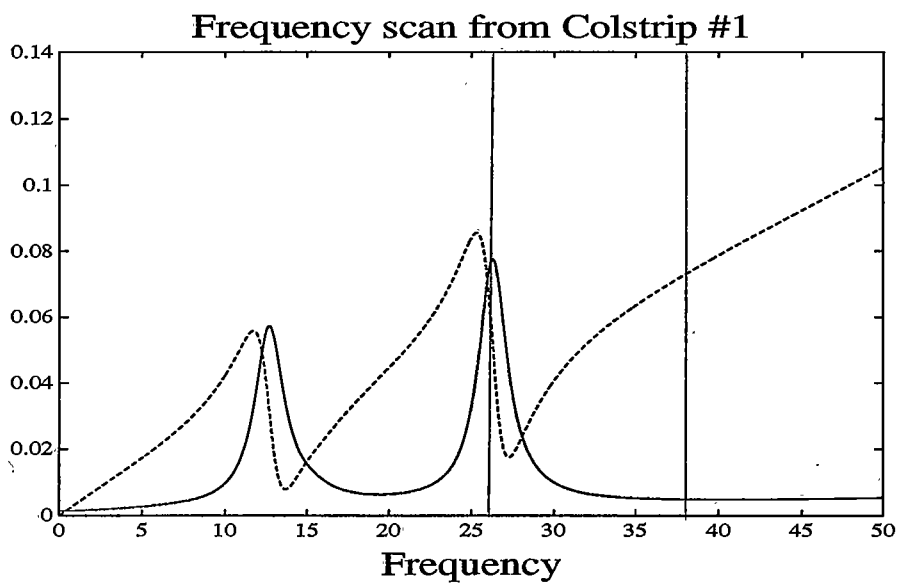

Figure 6. Frequency Scan From Colstrip #1.

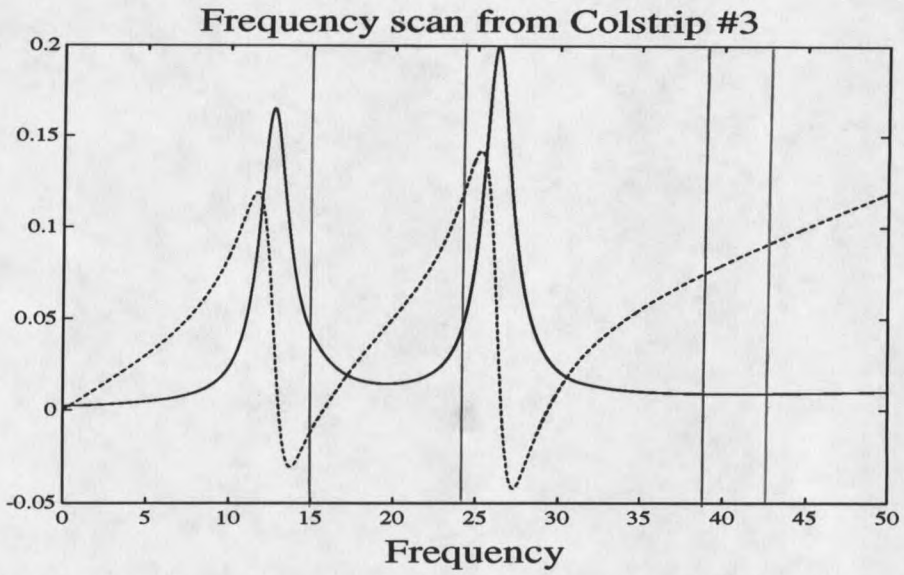

Figure 7. Frequency Scan From Colstrip #3.

Sharp fluctuations in the reactance curve indicate the presence of a network resonance at the corresponding frequency. This is analogous to the "Q" factor of an oscillator in circuit theory. In Figure 7, the points at which the reactance is zero are resonant points. Although the network as seen from Colstrip #1 (Figure 6) has no genuine resonant points, there may still be considerable energy present at certain frequencies. This is important to remember for transient torque studies. Lightly damped oscillations of this nature in the network at one of the turbine shaft compliment frequencies would tend to prolong oscillations in the shaft itself.

Colstrip #1 has three masses and therefore three resonant frequencies or modes. One mode is always a result of all of the masses on a turbine-generator shaft oscillating together.

This mode creates no torque on the shaft and so is of no interest in these studies. The compliment of the two remaining modes are shown in Figure 6. The mode at approximately 26 Hertz is seen to fall close to a network resonance. In Figure 7, the modes at approximately 15 and 24 Hertz fall close to network resonant points.

Frequency scanning can be seen to be a useful tool in the preliminary analysis of SSR studies. By this analysis the Colstrip machines would seem to be fairly safe from SSR problems of the sustained type, but susceptible to high transient torques at one or more modes. It can also be seen that the auto-transformer plays an important attenuation role in the suppression of sustained SSR. Should Colstrip #1 ever be moved to the 500 kV bus directly, severe SSR problems might result.

Electromagnetic Transients Program (EMTP)

A time-domain analysis capability is essential in determining the effectiveness of any proposed control action particularly for nonlinear systems. The EMTP provides this capability with the advantage of having validated, built-in models for all of the generation and transmission components. The EMTP accomplishes this by integrating a large set of differential equations and solving them simultaneously with a set of algebraic -- and sometimes nonlinear -- auxiliary

or constraint equations. In conventional SSR studies, the EMTP can provide valuable information on the magnitude of oscillations at a particular frequency and for a particular disturbance. None of the other analysis techniques discussed here can do the same.

The EMTP is used exclusively in Chapter 5 to carry out system and controller simulations.

Eigenvalue Analysis

Eigenvalue analysis can provide more information about potential problems than can a frequency scan because the eigenvalue analysis includes generator models. One can readily obtain the network resonant frequencies (the imaginary part of the eigenvalues) from a frequency scan and then compute the shaft resonant frequencies as was shown in Figures 6 and 7. In addition to all this information, an eigenvalue analysis provides the damping information at each resonant frequency.

Many computer programs exist and are widely used that can perform these analyses. Eigenvalues can also be obtained from an EMTP study as is described in the next section. This is the approach taken in this work.

System Identification and Modeling

System identification is important in this research in that one of the primary control algorithms to be studied

requires the knowledge of a system transfer function from input to output. The transfer function we seek is a ratio of polynomials in the Laplace complex variable s. The roots of the denominator polynomial of this transfer function are the eigenvalues of the system as described earlier.

Assuming valid results, the transfer function obtained from a system identification routine is a linear model of the original system. The nonlinear power system is of extremely high order so any model, particularly a linear one, is of a reduced order. The identified model is useful in system analysis and in designing controllers.

An extension of the Prony signal analysis work completed in [41] is used as a system identification routine. More information on Prony analysis can be found in [42] through [45]. The results of a Prony analysis used to identify a transfer function can be put in the form

$$\mathbf{G(s)} = \sum_{i=1}^{m} \frac{R_i}{s - \lambda_i}, \quad \lambda_i \neq \lambda_j \forall i \neq j \tag{3.1}$$

where R_i are the residues of the transfer function **G** at the eigenvalues λ_i. For the single input, single output case,

$$\mathbf{G(s)} = \frac{\mathcal{L}[y(t)]}{\mathcal{L}[u(t)]} \tag{3.2}$$

where here $y(t)$ is the output response to the input signal $u(t)$.

The identification is performed by first giving the system an input signal. The input signal should contain components of all of the frequencies of interest in the study. The systems output response to the signal is observed and recorded. Finally, using the known input signal and the observed response the identification routine computes a transfer function. The eigenvalues of a 12^{th} order model of the MPC system as seen from the terminals of Colstrip #3 are shown as x's in Figure 8. The o's represent the roots of the numerator polynomial of **G**, commonly referred to as zero's.

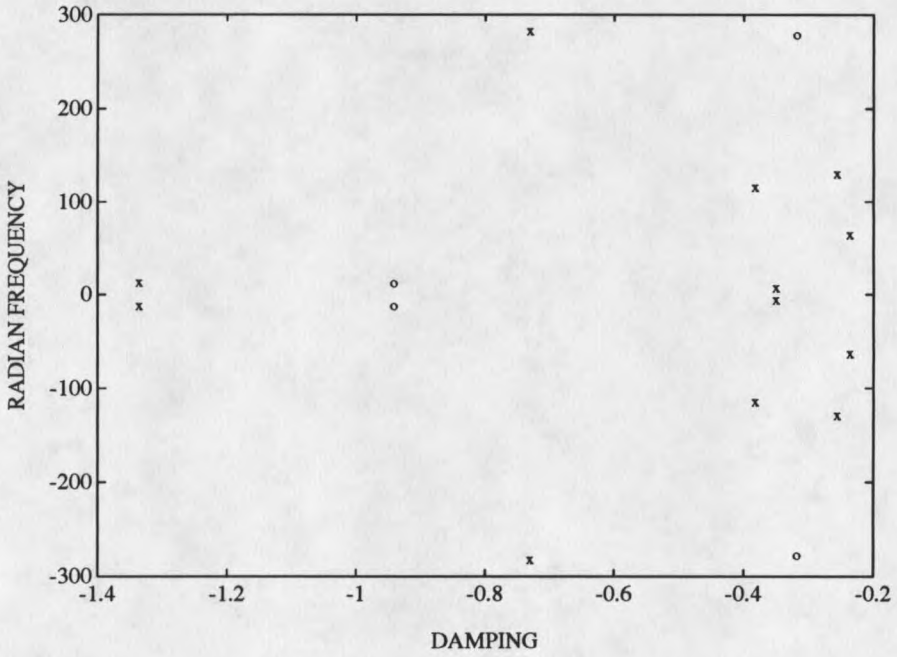

Figure 8. Eigenvalues of the MPC System from Colstrip #3.

Output Analysis of Prony Identification Routine

In the application presented by Trudnowski in [41], the number of eigenvalues contained in **G** are wholly determined by the number of data points in the output response $y(t)$. The number **m** in (3.1) is chosen so as to optimize the numerical robustness of the singular value decomposition (SVD) which is an integral part of the Prony package. The SVD is used to fit the eigenvalues of the system in a least-squares sense. The ordering of the eigenvalues from 1 to **m** is somewhat arbitrary. It is determined by the order in which the roots are taken from the SVD. A difficulty arises in truncating the transfer function **G** to a reasonable order for control calculations. One would like to order the eigenvalues so that a minimum error exists between the known response $y(t)$ and the response predicted by **G** for a similar input $u(t)$ for any given transfer function order $n < m$.

A first step in ordering the **m** eigenvalues is commonly to group the conjugate eigenvalue pairs together. A real-valued output response will always present complex eigenvalues in conjugate pairs. Following this grouping, Trudnowski uses a search technique reported by Hocking and Leslie [46] to complete the ordering. Though this technique works well for the majority of systems, a major problem was encountered using this simple search on some of the systems in this study.

To use the Hocking and Leslie search technique, one would group the conjugate pole-pairs together and apply the known input signal $u(t)$ to each pole-pair individually. If the pole is not complex, $u(t)$ would be applied to the real pole separately from the conjugate poles. The error is tabulated between the known output response $y(t)$ and the computed output response for each pole or pole-pair given the known input. The pole or pole-pair having the least error is ranked first. The process is repeated for each of the remaining poles or pole-pairs using the known input signal on the combination of the first **k** ranked poles along with each of the unranked poles or pole-pairs individually. The process can be described iteratively as follows:

$$\hat{\mathbf{G}}_k(s) = \sum_{i=1}^{k} \frac{R_i}{s-\lambda_i}$$

$$E_j = \left\{ y(t) - \mathcal{L}^{-1}\left[\mathbf{U}(s)\left[\hat{\mathbf{G}}_k(s) + \frac{R_j}{s-\lambda_j} \right] \right] \right\}^2 ; j = k+1, k+2, \ldots, m$$

$$E_r = \min_{k<j\le m} [E_j] \qquad (3.3)$$

$$\hat{\mathbf{G}}_{k+1}(s) = \hat{\mathbf{G}}_k(s) + \frac{R_r}{s-\lambda_r} \quad .$$

Where the j^{th} eigenvalue is complex, its conjugate, the $j+1^{st}$ eigenvalue, must also be included implicitly in the iteration.

The problem in using this type of search technique is best described by example. Consider the fourth order system described by

$$\mathbf{G}(s)=\frac{1}{s+0.1+j150}+\frac{1}{s+0.1-j150}+\frac{-1}{s+0.11+j150}+\frac{-1}{s+0.11-j150} \quad . \quad (3.4)$$

It is readily seen from the imaginary part of the eigenvalues in (3.4) that the oscillators in this system operate at the same radian frequency in the s-plane. The sign of the residue of an eigenvalue indicates which direction the system response will take due to an external input with respect to that eigenvalue. Opposite signs indicate opposite directions. With the radian frequency the same and opposite sign residues, one can expect some cancellation in the output waveform for a net reduction in output magnitude. In fact, if the damping in (3.4) were to be equal throughout, the output response would be identically zero for any input indicating complete cancellation. In this example, the damping has been chosen to be slightly different in the last two terms of (3.4) because the Prony routine cannot identify non-distinct poles.

This test system was excited by a short series of input pulses and simulated at 100 Hertz using a commercial numerical package [47]. An output sequence 350 samples long was entered into the Prony identification routine. Table 1 shows the partial results of the Prony analysis. The true and estimated residues and poles for the pertinent elements of **G** are shown.

Table 1. Prony Analysis Results for Example System.

Pole #		Residues		Eigenvalues	
		Real Part	Imag. Part	Real Part	Imag. Part
1	(true)	1.0000000	0.0000000	-0.1000000	150.00000
	(est.)	0.9974675	0.0407073	-0.0999565	149.99980
2	(true)	1.0000000	0.0000000	-0.1000000	-150.00000
	(est.)	0.9974675	-0.0407073	-0.0999565	-149.99980
3	(true)	-1.0000000	0.0000000	-0.1100000	150.00000
	(est.)	-0.9974675	-0.0407073	-0.1100044	150.00020
4	(true)	-1.0000000	0.0000000	-0.1100000	-150.00000
	(est.)	-0.9974675	0.0407073	-0.1100044	-150.00020

Since the order of the system is not *a priori* knowledge when performing a Prony analysis, the Prony algorithm identifies many extraneous eigenvalues in addition to the ones shown in Table 1. In this case, some potential eigenvalues were discarded in the singular value decomposition and 52 eigenvalues were listed in the final Prony output. A suitable ordering scheme would put the four valid eigenvalues ahead of any extraneous ones. The Hocking and Leslie scheme, however, ordered the four eigenvalues shown in Table 1 in last place -- behind the 48 other invalid eigenvalues. This is because the cancellation due to the presence of similar eigenvalues with opposite-sign residues creates an output waveform which is generally small in magnitude while the response of a valid pole-pair is comparatively larger. Each of the valid pole-pairs taken individually create a +34 to

+40 dB error between the actual system output and the estimated output using that pole-pair. Both pole-pairs taken together estimate the actual system extremely well. The error between actual and estimated is -260 dB. Figure 9 shows a plot of the error as the poles were ordered by the Hocking and Leslie search technique.

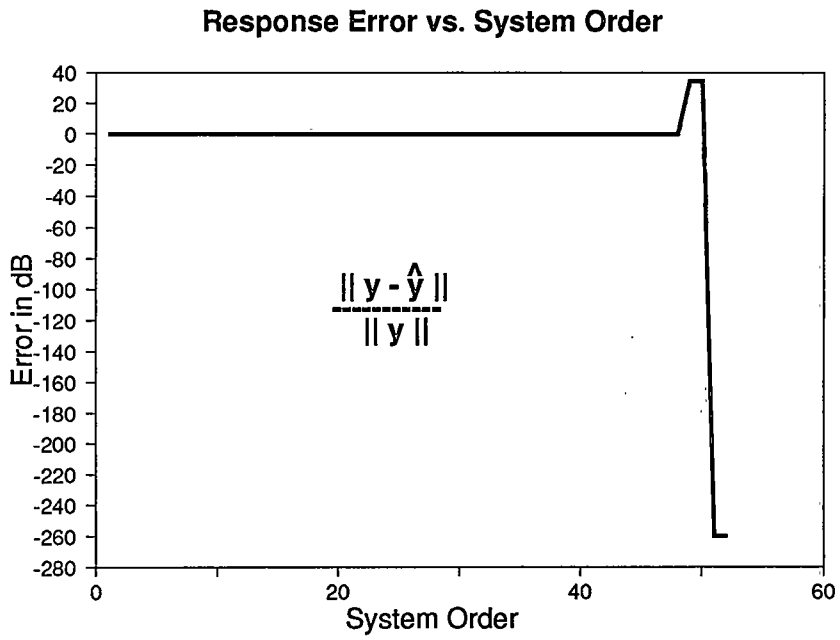

Figure 9. Errors Between Actual and Estimated Response for the System in (3.4).

One of the greatest benefits of Prony analysis over other identification routines is in the partial-fraction expansion form of the program output. Each eigenvalue is isolated from the others along with its residue. This property makes for easy interpretation of the results. It can generally be said that a large residue will elicit a large response from its

eigenvalue due to a given input. This is certainly true for eigenvalues of similar frequency and damping. One may be tempted to order the eigenvalues in a Prony analysis according to the magnitude of their residues. This approach would certainly solve the problem of the example described by (3.4). While the residues of the valid poles have magnitudes of approximately one, the residues of the eigenvalues that the Hocking and Leslie scheme ranked first had a magnitude of 10^{-15}. In fact, the largest residue of the 48 invalid poles had a magnitude of 10^{-14}. Although encouraging in this case, ordering the eigenvalues according to the magnitude of the residues has a distinct disadvantage in that it does nothing to try to control the error between the actual and estimated outputs.

The method used in this research was a combination of the two techniques. It was felt that the additional complexity involved in changing the Hocking and Leslie scheme to accommodate opposite-sign residues would not enhance the overall Prony package and may in fact have long-term detrimental effects on the robustness of the computer code. Once this "patch" was made it would be tempting to use more patches to fix future unforeseen problems. With this in mind, the Prony code was modified to order the eigenvalues according to the magnitude of the residues and separately, according to the original Hocking and Leslie scheme. When the user

wishes to select an appropriate model order, a computer program performs an error analysis on the two files containing the separately ordered eigenvalues and choses the model exhibiting the least amount of error. This method seems to incorporate the benefits of both ordering schemes while not adding significantly to the complexity of the code.

It should be noted in closing this chapter that, as always, there is no substitute for "engineering judgement" in selecting the order of the system model and the eigenvalues that should be included in that model. Where there is no knowledge of the system to be identified, the Prony identification package discussed herein works well. In other cases, one is wise to use Prony in conjunction with judgement.

CHAPTER 4

CONTROLLER DESIGN

Four analysis techniques for determining the existence and severity of SSR problems in electric power systems were described in Chapter 3. A powerful approach in dealing with the task of designing a controller is the last technique described -- system identification and modeling. Almost all classical control theory, and most modern control theory, assumes a known linear "plant" which is to be controlled. The plant in the case of these studies is the turbine shaft mass-spring system coupled magnetically to the electrical network.

An identified model obtained from a Prony analysis is a linear model which can be taken to be an accurate representation of the plant within a small operating region. A controller can be designed to act on the identified model in such a way as to increase the damping of the system at the frequencies associated with the turbine shaft modes. When the controller is implemented on the actual system, it can be expected to improve the damping of the system within a certain region

where the plant behaves linearly. If this region is very large, the controller is said to be "robust" in its operation on the plant.

The major goal of this research is to design a robust controller to control a resistive brake while meeting certain performance criteria. The brake should provide enough damping at frequencies within the realm of SSR to allow for the reliable use of high-speed reclosing of transmission lines emanating from the generator. This is to say that high-speed reclosing could be applied without fear of turbine shaft damage.

A good starting point in searching for an appropriate control law would seem to be straight feedback control. The Purdue studies used this approach and showed reasonable damping in the turbine shaft following a disturbance [27]. In these studies, the deviation from synchronous speed ($\Delta\omega = \omega_{gen} - \omega_o$) of the generator mass is used as a feedback signal. The author best describes the control action in the published results of the studies in saying, "... power is dissipated whenever the generator speed exceeds synchronous." In other words, the brake is turned on whenever $\Delta\omega > 0$.

In retrospect, this starting point has emerged as the preferred strategy for control of the brake. This report will promote the conclusion that the strategy outlined above is one of the best possible control algorithms to achieve the

damping goal. The Purdue studies give only intuitive evidence that suggests straight feedback control on the generator $\Delta\omega$ would be a good control strategy. This research lays the theoretical foundation that appears to validate the premise.

Straight Feedback Control

There are several questions that may be asked regarding the use of generator $\Delta\omega$ as a feedback signal. Two important ones are: "Why does generator $\Delta\omega$ work well?" and "Are there any other signals that are better?". These questions will be addressed in this section and the advantages of using generator $\Delta\omega$ as a feedback signal will be demonstrated.

Insight into the first question may be gained by using an identified model to obtain a root locus plot of the system. The open-loop poles for a 12^{th} order model are shown in Figure 8. A root locus plot extends the results shown in Figure 8 to include the closed-loop poles of the system. The closed-loop poles are the eigenvalues of the closed-loop system. To satisfy the design goal, an engineer would like to place the closed-loop poles as far into the left half-plane as possible. This would provide maximum damping. Figure 10 shows a root locus plot of the identified model of the MPC Colstrip test system. As in Figure 8, the x's represent the open-loop poles

and the o's represent the open-loop zeros. The dots represent the location of the closed-loop poles as the feedback gain is increased from 0.1 to 1.0.

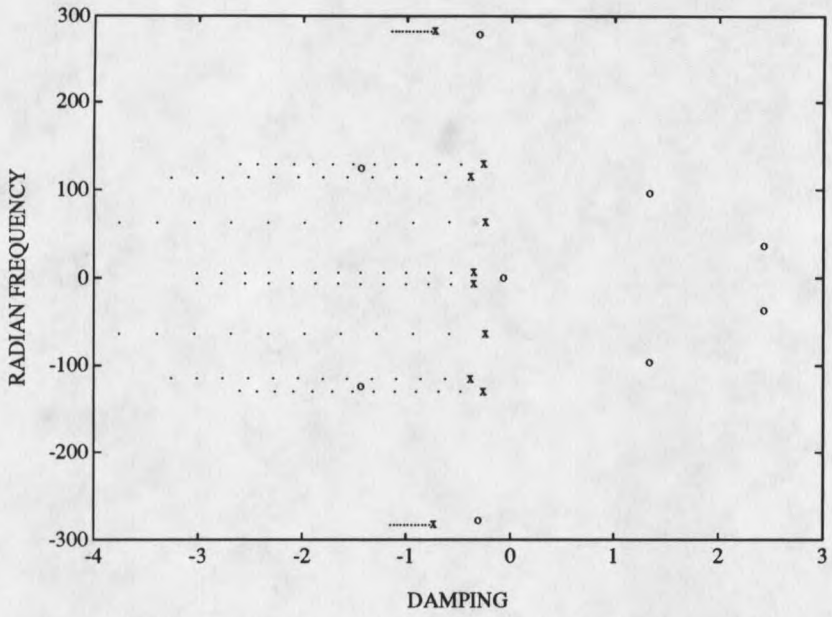

Figure 10. Root Locus of the MPC Colstrip Test System at Colstrip #3 using Generator $\Delta\omega$ as a Feedback Signal.

All of the closed-loop poles move farther into the left half-plane as gain is increased indicating improved damping. In fact, this feedback is having a dramatic effect on the closed-loop poles. An indication of how far the closed-loop poles will move for a given change in feedback gain can be gained by examining the magnitude of the residues associated with a given set of poles. The residues are the R_i's shown

in (3-1). The generator $\Delta\omega$ as a feedback signal provides for relatively large residues at the poles corresponding to the turbine shaft natural frequencies.

An example of a feedback signal that provides for smaller residues at the shaft modes is seen in Figure 11. This figure shows a root locus of the same system for the same range of gains using generator acceleration as a feedback signal. The open-loop poles are in virtually the same location as in Figure 10. The fact that the Prony analysis identified the same open-loop poles for both cases is an indication that the identified models are accurate.

For the moment we ignore the direction in which the closed-loop poles are moving and focus attention on the distance that the poles move for a given control action. The assumption is that with the proper control law, it is possible to get the poles moving into the left half-plane. Even with this generous assumption, it would be impossible to achieve the same amount of damping as can be seen in Figure 10. The magnitudes of the residues in the latter case indicate that it is more difficult to control the shaft modes using this feedback signal.

Another example of testing the various feedback signals for suitability in controlling the brake is seen in Figure 12. This case shows the high pressure turbine $\Delta\omega$ with the

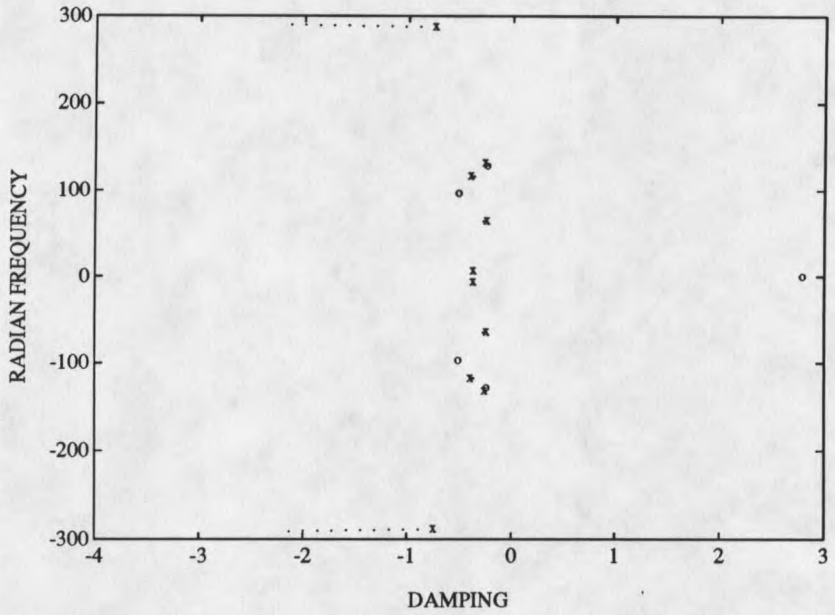

Figure 11. Root Locus of the MPC Colstrip Test System at Colstrip #3 using Generator Acceleration as a Feedback Signal.

same range of gains. The HP turbine is on the opposite end of the turbine shaft from the generator and is therefore readily accessible for speed measurement.

Most of the residues are of large magnitude in this case, but it would be nearly impossible to design a control strategy that would send all of the closed-loop poles into the left half-plane. Thus, it makes little sense to develop a complex control strategy when a feedback signal is available which does not require complexity as is illustrated in Figure 10.

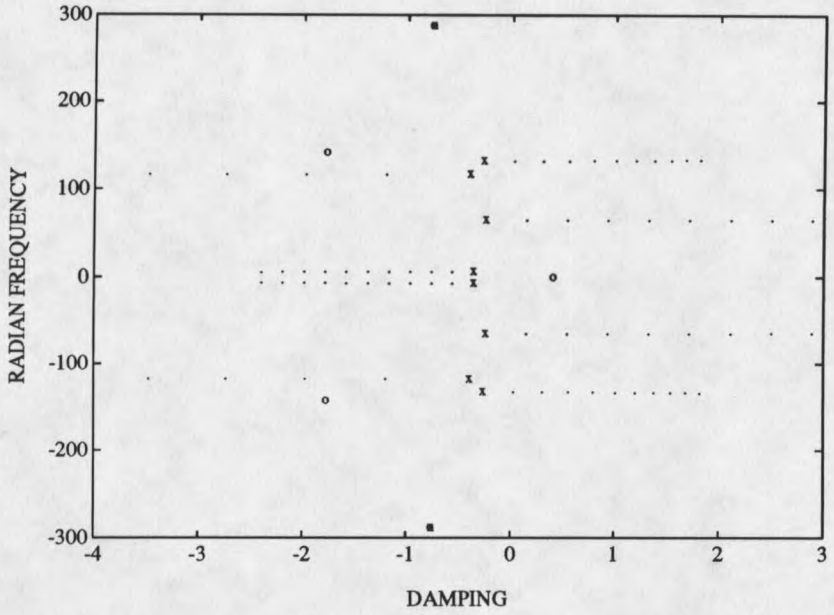

Figure 12. Root Locus of the MPC Colstrip Test System at Colstrip #3 using High Pressure Turbine $\Delta\omega$ as a Feedback Signal.

It should be noted that in all cases, the closed-loop poles must eventually end up on the open-loop zeros when the feedback gain is increased to infinity. In the three previous figures, this means that as gain is increased, the closed-loop poles will enter the right half-plane and the system will go unstable. One must be careful to remember that the identified models used to produce the root locus plots are only good for a finite operating range. Hence, as the gain is increased, nonlinearities in the system will make the use of root locus as an analysis tool unreliable.

Filtering the Feedback Signal

It was mentioned in Chapter 3 that one of the modes of a turbine shaft mass-spring system involves all of the masses on the shaft oscillating in unison with each other. This mode has been called an electromechanical mode in some circles, or "hunting" mode as in [27]. Since all of the masses on the shaft participate in phase with each other for this mode, no torques are induced on the shaft. The hunting mode is more of a concern in transient stability studies than in transient torque studies. This mode is seen as the slow mode which is closest to the real axis (zero radians) in Figures 10 through 12.

In Figure 10 it can be seen that this mode is well damped in the closed-loop. The damping which is added to the hunting mode represents wasted energy if the goal is simply to reduce transient torques. To this end, it makes sense to let the hunting mode maintain its original damping and expend more energy damping the other shaft modes. A filter is employed for this purpose. The filter acts to remove the hunting mode from the generator $\Delta\omega$ before it is fed back to the brake. Energy saved by not having to damp the hunting mode is expended on damping the SSR modes. In Figure 13 a high-pass filter has been added in the feedback loop. It can be seen that the

filter has very little effect on the higher frequency shaft modes, but the hunting mode is effectively stopped from moving left.

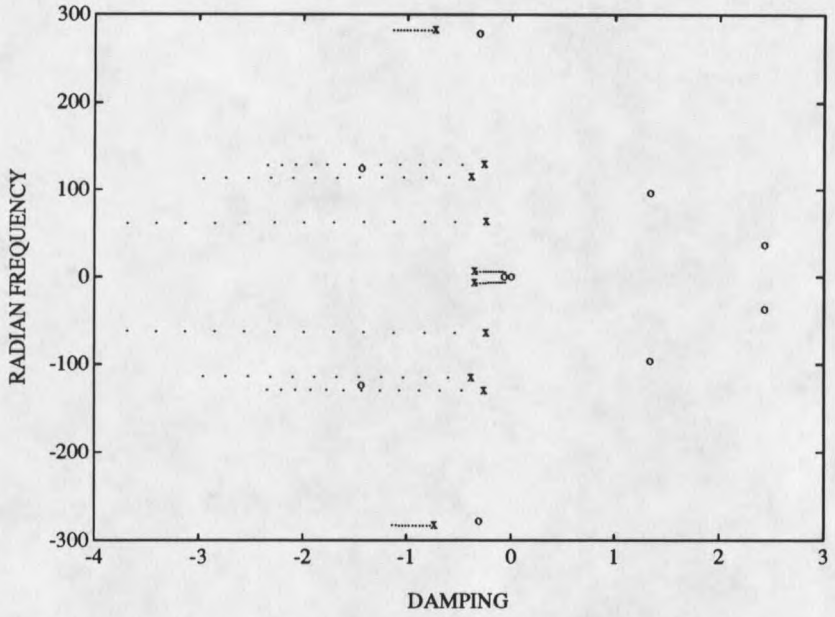

Figure 13. Root Locus of the MPC Colstrip Test System at Colstrip #3 using the Filtered Generator $\Delta\omega$ as a Feedback Signal.

The elimination of the hunting mode should be evaluated on a case-by-case basis. Figure 10 and Chapter 5 show that the hunting mode can be damped with a resistive brake. Many different strategies could be employed in the specific design of a brake. A design engineer could decide that transient stability is a big enough problem to warrant leaving out the high-pass filter. This approach would tend to damp the hunting

mode along with the torsional modes. Another design might filter the feedback signal just until the torsional modes achieve a set amount of damping and then switch the filter out of the circuit to attack the hunting mode.

Optimal Control

We have seen that the generator $\Delta\omega$ may be the best feedback signal to use in controlling the brake, but is a straight feedback gain the best strategy in using the signal? It is common in power system control applications such as exciters and PSS units to condition the feedback signal before applying it to the controlled input. In addition, optimal control theory would suggest that there is a single, unique set of control actions which will bring a disturbed output signal to zero in a minimum amount of time. In this section, these topics are discussed and straight feedback control using the generator $\Delta\omega$ is again shown to be extremely suitable to achieve the design goals.

Conditioning of the feedback signal was discussed in the previous two sections. There is no need for complex control strategies to be employed in the feedback loop when all of the closed-loop poles satisfy the design goal with a simple feedback gain. There may be, however, a call for a high-pass filter to remove the hunting mode from the feedback signal. The hunting mode is well below the lowest SSR frequency and

so a second order filter should be adequate. The only strict requirement would be to induce a minimum phase error into the feedback signal in the SSR range.

The topic of optimality may deserve a more detailed explanation. An effort has been made in this research to find an optimal control law which would work well with the generator $\Delta\omega$ as a feedback signal in damping the transient torques. A recently developed theory called Generalized Predictive Control (GPC) was evaluated as to its usefulness in this respect. While GPC researchers make no claims that the technique results in the unique optimal control for a given circumstance, it can be thought of as a "quasi-optimal" control. GPC is formulated for use with digital controllers.

GPC was originally developed by D. W. Clarke of Oxford University and his associates in 1985 [48]. Bitmead et al. give a more comprehensive discussion of the technique in making strong comparisons to linear quadratic control [49]. The development of the theory is somewhat similar to that of linear quadratic control in that one forms a quadratic cost function, J, and attempts to minimize J throughout time. Since GPC is a discrete-time algorithm, the cost function takes on the general form

$$J = \sum_{j=N_1}^{N_2} y^2(j) + \sum_{k=1}^{NU} \alpha u^2(k) \quad . \tag{4.1}$$

At each successive time step, the objective is to find the set of control actions $u(i), i = 1,2,...,NU$ that minimize J. The control action taken at the next time step is then $u(1)$. The parameters N_1, N_2, and NU are somewhat arbitrary, however there are some guidelines that can be followed in choosing them. Let us assume that $N_1 = 1$, $N_2 = 10$, and $NU = 1$. Then $y(i), i = 1,2,...,10$ is simply the pulse response to $u(1)$ predicted over the next 10 time steps given the initial conditions $y(i), i = -n, -n+1,...,0$. The control, u, is assumed to be zero for all time subsequent to the control horizon NU i.e. $u(i) = 0, i = 2,3,...,\infty$. Out of all possible choices of $u(1)$, one would choose the one that minimizes J. As Clarke shows, the optimal u can be found by setting the partial derivative of J with respect to u to zero.

GPC has certain properties that make it appealing in situations such as dynamic braking with bang-bang control. Suppose one has a discrete-time transfer function fit of a system such as can be found using Prony analysis. Then given a set of initial conditions, the future values of the output can be predicted by iterating the difference equation specified by the transfer function. In bang-bang control of the brake, there are only two discrete levels of control - the brake is either on or off. In the above example where $NU = 1$, one would iterate the difference equation out 10 steps assuming the brake is on at $u(1)$ and calculate the value of J. Then the

same thing is done assuming the brake is off at $u(1)$. The minimum J of these two possibilities is found and the corresponding control is applied. This method is commonly referred to in the literature as a tree search. If NU is kept fairly small, it can be seen that this would be an extremely fast calculation which is important in discrete-time control. As NU increases, the number of branches to search on the tree increases by L^{NU} where L is the number of discrete levels of control.

Discrete level GPC will theoretically give "more optimal" control of the dynamic brake than would straight feedback gain. This coupled with the ease of computation in the bang-bang case makes GPC look fairly attractive as a control strategy.

Sensitivity Problems with Discrete-Level GPC

Despite its inherent advantages, the GPC control strategy was found to be ineffective when applied to the dynamic brake as specified above. In implementing discrete level GPC, a severe lack of robustness with respect to output initial conditions was encountered. These problems with sensitivity in the algorithm are first illustrated in an example. Following the example, an attempt is made to describe the phenomenon more quantitatively.

The GPC algorithm was implemented on the MPC Colstrip model in the EMTP. No positive effects were observed in damping the generator $\Delta\omega$ for any values of N_1, N_2, and NU. The controller seemed to be acting randomly. After careful study, it was found that the 12^{th} order difference equation was so sensitive to initial conditions as to make the discrete level GPC algorithm inoperable. Ten past values of $\Delta\omega$ were chosen and the cost function was calculated for $u(0)=0$ and for $u(0)=1$. The minimum cost of these two indicated that the brake should be off at $u(0)$. A change of only 0.06% in one of the past $\Delta\omega$ values changed the cost function enough so that the minimum cost now indicated that the brake should be on at $u(0)$. This behavior was verified on a separate case involving only two oscillators and a 5^{th} order system. With this kind of sensitivity, GPC as it was implemented originally had no chance of controlling the nonlinear system.

As it would have to be implemented in controlling the dynamic brake, the GPC algorithm would retrieve past $\Delta\omega$ values and use these to predict the future values. The sensitivity problem surfaces when the noise and nonlinearities in the system slightly distort the past $\Delta\omega$ values which are used as initial conditions in the algorithm. The error in approximation from the system to the model in this case is enough to make the controller ineffective.

While the previous example has illustrated the nature of the sensitivity problem, it is necessary to study the problem analytically in order to fully understand what is happening. The discrete-time equivalent of (3.1), assuming a Zero-Order Hold (ZOH) on the input, can be written

$$\mathbf{G}_{ZOH}(z) = \sum_{i=1}^{m} \frac{-R_i}{\lambda_i} \frac{(1 - e^{\lambda_i T_s}) z^{-1}}{1 - e^{\lambda_i T_s} z^{-1}} \quad . \tag{4.2}$$

Given this linearized transfer function, one is faced with the task of predicting the future values of the system output. Many different formulations of (4.2) can accomplish this task. It is initially tempting to write (4.2) as

$$\mathbf{G}_{ZOH}(z) = \frac{\sum_{i=0}^{m} b_i z^{-i}}{1 - \sum_{i=1}^{m} a_i z^{-i}} \quad . \tag{4.3}$$

With

$$\mathbf{G}(z) = \frac{Y(z)}{U(z)} \tag{4.4}$$

the inverse Z-transform of (4.3) is

$$\tilde{y}(k) = \sum_{i=1}^{m} a_i y(k-i) + \sum_{i=0}^{m} b_i u(k-i) \tag{4.5}$$

where $\tilde{y}(k)$ is the predicted value of the system output at time kT_s.

Iteration of the difference equation (4.5) to find the predicted values of the system output given m past values is referred to in [50, p.215], [51, p.151], [52, p.474] as the Direct Form I formulation.

Another formulation seen commonly in control work stems from the Direct Form II. We first write (4.2) as

$$\mathbf{G}_{ZOH}(z) = b_0 + \sum_{j=1}^{m} \frac{(b_0 a_j + b_j) z^{-j}}{1 - \sum_{i=1}^{m} a_i z^{-i}} \quad . \tag{4.6}$$

The state-space representation of (4.6) is

$$\begin{bmatrix} x_1(k+1) \\ x_2(k+1) \\ x_3(k+1) \\ \cdot \\ \cdot \\ \cdot \\ x_m(k+1) \end{bmatrix} = \begin{bmatrix} a_1 & a_2 & \dots & a_{m-1} & a_m \\ 1 & 0 & \dots & 0 & 0 \\ 0 & 1 & \dots & 0 & 0 \\ \cdot & \cdot & & \cdot & \\ \cdot & \cdot & & \cdot & \\ \cdot & \cdot & & \cdot & \\ 0 & 0 & \dots & 1 & 0 \end{bmatrix} \begin{bmatrix} x_1(k) \\ x_2(k) \\ x_3(k) \\ \cdot \\ \cdot \\ \cdot \\ x_m(k) \end{bmatrix} + \begin{bmatrix} 1 \\ 0 \\ 0 \\ \cdot \\ \cdot \\ \cdot \\ 0 \end{bmatrix} u(k)$$

(4.7)

$$y(k) = [(b_0 a_1 + b_1) \quad (b_0 a_2 + b_2) \quad \dots \quad (b_0 a_m + b_m)] \begin{bmatrix} x_1(k) \\ x_2(k) \\ x_3(k) \\ \cdot \\ \cdot \\ \cdot \\ x_m(k) \end{bmatrix} + b_0 u(k).$$

Though (4.7) is straightforward and easily implemented on a digital computer, severe numerical problems are encountered as the model order, m , is increased. These

numerical difficulties are almost wholly due to parameter quantization effects in the "a" coefficients. This becomes evident through a derivation by Oppenheim [51, p.167] which shows the sensitivity of the discrete pole location due to small deviations in a coefficient of the denominator polynomial of (4.6). It is shown that the sensitivity problem is particularly acute when the poles of the discrete system are tightly clustered. Oppenheim concludes by saying,

> "[t]hen we can expect the poles of the direct-form realization to be quite sensitive to quantization errors in the coefficients. Furthermore, it is evident that the larger the number of roots, the greater the sensitivity."

While Oppenheim speaks of sensitivity in terms of errors in the coefficients of polynomials, another measure of sensitivity is commonly applied to matrices. The condition number of a matrix A, $\kappa(A)$, indicates the sensitivity of the solution vector $\mathbf{x}$ to small changes in the entries of the coefficient matrix A and of the vector $\mathbf{b}$ in the solution of the matrix equation

$$A\mathbf{x} = \mathbf{b}.$$

Lancaster [53, p.385] defines the condition number to be

$$\kappa(A) \equiv \|A\| \, \|A^{-1}\| \tag{4.8}$$

where $\|\|$ denotes any matrix norm. Let us use the spectral norm (the matrix 2-norm) to define the condition number. We know that

$$\|A\|_s = \max_{1 \le i \le n} \mathcal{S}_i \tag{4.9}$$

where the subscript s denotes the spectral norm and the script $\mathcal{S}_i$ denotes a singular value of A. We can see that

$$\|A^{-1}\|_s = \mathcal{S}_{\max}(A^{-1}) = \frac{1}{\mathcal{S}_{\min}(A)} \tag{4.10}$$

and therefore, at least for invertible matrices,

$$\kappa(A) = \frac{\mathcal{S}_{\max}(A)}{\mathcal{S}_{\min}(A)} \quad . \tag{4.11}$$

This tool can now be used to re-examine the twelfth-order system shown in Figure 10.

Oppenheim's sensitivity analysis would lead us to believe that the formulation in (4.7), the state-space realization of Direct Form II, would be a poor implementation of the identified model in predicting future output values. An evaluation of the condition number of the coefficient matrix in (4.7) using the data from Figure 10 yields a κ on the order of 10^7. This relatively large condition number tends to confirm Oppenheim's analysis. Another structure that may be used in the implementation of the identified model eliminates the numerical problems in predicting future output values discussed above. This method is not without its faults, however, in that the numerical conditioning problems are shifted to another phase of the calculations.

The parallel form realization of the identified model is better suited for use with the Prony identification routine because it implements the system in the partial-fraction expansion form characteristic of Prony. Each of the terms in the partial fraction expansion is implemented separately so that "the error in a given pole is independent of its distance from other poles in the system." Oppenheim goes on to say, "For this reason, it can be stated that in general the ... parallel form [is] to be preferred over the direct forms from the viewpoint of parameter quantization." [51, p.169]. The conjugate poles can be grouped together in the parallel form to avoid complex arithmetic. (4.2) is then written

$$\mathbf{G}_{ZOH}(z) = C_0 + \sum_{j=1}^{m_1} \frac{\beta_{1j} z^{-1}}{1 - \alpha_{1j} z^{-1}} + \sum_{\ell=m_1}^{m_1+\frac{m_2}{2}} \frac{\beta_{1\ell} z^{-1} + \beta_{2\ell} z^{-2}}{1 - \alpha_{1\ell} z^{-1} - \alpha_{2\ell} z^{-2}} \tag{4.12}$$

where m_1 is the number of real poles, m_2 is the number of complex poles, and $m = m_1 + m_2$. Now form the sub-matrices

$$\mathcal{A}_j = [\alpha_{1j}] \quad 1 \le j \le m_1 \tag{4.13a}$$

$$\mathcal{A}_\ell = \begin{bmatrix} \alpha_{1\ell} & \alpha_{2\ell} \\ 1 & 0 \end{bmatrix} \quad m_1 < \ell \le m_1 + \frac{m_2}{2} \quad . \tag{4.13b}$$

The coefficient matrix for the state-space implementation of the parallel form is then

$$\hat{A} = \begin{bmatrix} \mathcal{A}_1 & 0 & \dots & 0 \\ 0 & \mathcal{A}_2 & \dots & 0 \\ \cdot & \cdot & & \cdot \\ \cdot & \cdot & & \cdot \\ \cdot & \cdot & & \cdot \\ 0 & 0 & \dots & \mathcal{A}_{m_1+\frac{m_2}{2}} \end{bmatrix}_{mxm} \qquad (4.14)$$

For equivalent systems, the coefficient matrix (4.14) and the coefficient matrix in (4.7) are similar matrices in that one can be obtained from the other through an invertible, linear transformation. While it is known that the eigenvalues of similar matrices are identical, their singular values are generally not. The condition number of this matrix for the system shown in Figure 10 is 5.8 -- seven orders of magnitude less than the coefficient matrix for the direct-form implementation.

In order to use the parallel form in a GPC application, a method must be found to enable us to determine the initial conditions of the state variables in their new form. With the direct method, the state variables are directly related to the m past output values and past input values. These

being known quantities, the prediction algorithm is straightforward. With the parallel form, however, the past output and input values are related to the initial conditions of the state variables by a transformation matrix. If we denote the transformation matrix as $\boldsymbol{P}$, then let

$$\mathbf{x} = P\hat{\mathbf{x}} \tag{4.15}$$

then

$$\hat{\mathbf{x}}(k+1) = P^{-1}AP\hat{\mathbf{x}}(k) + P^{-1}B\mathbf{u}(k) \tag{4.16}$$

and

$$\hat{A} = P^{-1}AP \quad . \tag{4.17}$$

To find the initial conditions of the state variables in the parallel form, let

$$\hat{\mathbf{x}}(0) = P^{-1}\mathbf{x}(0) \quad . \tag{4.18}$$

A modification of the method used in Ogata [50, p.571] is used to find the appropriate transformation matrix, P. Let

$$\frac{Y(z)}{U(z)} = \sum_{k=1}^{n} \frac{b_{1k}z^{-1} + b_{2k}z^{-2}}{1 + a_{1k}z^{-1} + a_{2k}z^{-2}} \tag{4.19}$$

where $n = m/2$ and m is the system order. This formulation is sufficient for the work described in this dissertation since all of the modes of interest are oscillatory. The formulation could be easily generalized to include real roots by assuming $\frac{Y}{U}$ in the form of (4.12). Now multiplying both sides of (4.19) by z^{-l} with $l = 1,2,\ldots,2n-1$ yields

$$\frac{z^{-1}Y(z)}{U(z)} = C_1 z^{-1} + \sum_{k=1}^{n} \frac{\frac{-b_{2k}}{a_{2k}} z^{-1} + \left(b_{1k} - \frac{b_{2k}a_{1k}}{a_{2k}}\right) z^{-2}}{1 + a_{1k}z^{-1} + a_{2k}z^{-2}}$$

$$\frac{z^{-2}Y(z)}{U(z)} = C_1 z^{-2} + C_2 z^{-1} + \sum_{k=1}^{n} \frac{-\left(\frac{b_{1k} - \frac{b_{2k}a_{1k}}{a_{2k}}}{a_{2k}}\right) z^{-1} - \left(\frac{b_{2k} + a_{1k}\left(b_{1k} - \frac{b_{2k}a_{1k}}{a_{2k}}\right)}{a_{2k}}\right) z^{-2}}{1 + a_{1k}z^{-1} + a_{2k}z^{-2}} \qquad (4.20)$$

$$\frac{z^{-(2n-1)}Y(z)}{U(z)} = C_1 z^{-(2n-1)} + C_2 z^{-(2n-2)} + \ldots$$

where

$$C_1 = \sum_{k=1}^{n} \frac{b_{2k}}{a_{2k}} \quad ; \quad C_2 = \sum_{k=1}^{n} \left(\frac{b_{1k} - \frac{b_{2k}a_{1k}}{a_{2k}}}{a_{2k}}\right) \quad ; \quad etc.$$

In matrix notation, (4.19) and (4.20) can be written

$$\begin{bmatrix} \dfrac{Y(z)}{U(z)} \\ \dfrac{z^{-1}Y(z)-z^{-1}C_1U(z)}{U(z)} \\ \dfrac{z^{-2}Y(z)-z^{-2}C_1U(z)-z^{-1}C_2U(z)}{U(z)} \\ \vdots \end{bmatrix} \tag{4.21}$$

$$= \begin{bmatrix} b_{11} & b_{21} & b_{12} & \cdots \\ \dfrac{-b_{21}}{a_{21}} & \left(b_{11}-\dfrac{b_{21}a_{11}}{a_{21}}\right) & \dfrac{-b_{22}}{a_{22}} & \cdots \\ -\left(\dfrac{b_{11}-\frac{b_{21}a_{11}}{a_{21}}}{a_{21}}\right) & -\left(\dfrac{b_{21}+a_{11}\left(b_{11}-\frac{b_{21}a_{11}}{a_{21}}\right)}{a_{21}}\right) & -\left(\dfrac{b_{12}-\frac{b_{22}a_{12}}{a_{22}}}{a_{22}}\right) & \cdots \\ \vdots & \vdots & \vdots & \cdots \end{bmatrix} \begin{bmatrix} \dfrac{z^{-1}}{1+a_{11}z^{-1}+a_{21}z^{-2}} \\ \dfrac{z^{-2}}{1+a_{11}z^{-1}+a_{21}z^{-2}} \\ \dfrac{z^{-1}}{1+a_{12}z^{-1}+a_{22}z^{-2}} \\ \vdots \end{bmatrix}$$

Now define

$$\begin{bmatrix} \dfrac{X_1(z)}{U(z)} \\ \dfrac{X_2(z)}{U(z)} \\ \dfrac{X_3(z)}{U(z)} \\ \vdots \end{bmatrix} = \begin{bmatrix} \dfrac{z^{-1}}{1+a_{11}z^{-1}+a_{21}z^{-2}} \\ \dfrac{z^{-2}}{1+a_{11}z^{-1}+a_{21}z^{-2}} \\ \dfrac{z^{-1}}{1+a_{12}z^{-1}+a_{22}z^{-2}} \\ \vdots \end{bmatrix}. \tag{4.22}$$

Then from (4.21) and (4.22)

$$\begin{bmatrix} Y(z) \\ z^{-1}Y(z)-z^{-1}C_1U(z) \\ z^{-2}Y(z)-z^{-2}C_1U(z)-z^{-1}C_2U(z) \\ \cdot \\ \cdot \\ \cdot \end{bmatrix} = \mathcal{B} \begin{bmatrix} X_1(z) \\ X_2(z) \\ X_3(z) \\ \cdot \\ \cdot \\ \cdot \end{bmatrix} \tag{4.23}$$

where $\mathcal{B}$ is the first matrix on the right-hand side of (4.21). (4.23) defines the m states used in the state-space formulation

$$x_{k+1} = \hat{A}x_k + Bu_k$$

where $\hat{A}$ is as shown in (4.14). To illustrate this, the first two elements of (4.22) are written as

$$(1 + a_{11}z^{-1} + a_{21}z^{-2})X_1(z) = z^{-1}U(z)$$

$$(1 + a_{11}z^{-1} + a_{21}z^{-2})X_2(z) = z^{-2}U(z) \quad .$$

Simple substitution yields

$$X_2(z) = z^{-1}X_1(z)$$

$$X_1(z) = z^{-1}(-a_{11}X_1(z) - a_{21}X_2(z) + U(z))$$

which correspond to a sub-block of $\hat{A}$ as shown in (4.13b). As an aside, the $\mathcal{B}$ matrix is easily programmed since each row builds upon the previous one.

A check of the condition number of P revealed that the transformation to parallel form had simply shifted the conditioning problem to another place. The condition number of

P for the system shown in Figure 10 is on the order of 10^{11}. It can be shown that this must be the case when a transformation is used to improve the condition of A. From (4.8),

$$\kappa(A) \equiv \|A\| \|A^{-1}\| \quad .$$

Now (4.17) into (4.8) yields

$$\begin{aligned} \kappa(A) &= \|P\hat{A}P^{-1}\| \|P^{-1}\hat{A}^{-1}P\| \\ &\leq \|P\|^2 \|P^{-1}\|^2 \kappa(\hat{A}) \\ &= [\kappa(P)]^2 \kappa(\hat{A}) \quad . \end{aligned}$$

It follows directly that

$$\kappa(P) \geq \left(\frac{\kappa(A)}{\kappa(\hat{A})} \right)^{\frac{1}{2}} \quad . \tag{4.24}$$

(4.24) shows that at least some of the conditioning problem is shifted to the transformation matrix when an ill-conditioned matrix is transformed to a matrix which is more manageable computationally.

There is theoretically no reason to stop at $2n-1$ in (4.20). The method can be extended to attempt a "least-squares" fit of past data to the m initial conditions. As an example, let

$$\begin{bmatrix} Y(z) \\ z^{-1}Y(z)-F_0(U) \\ z^{-2}Y(z)-F_1(U) \\ \cdot \\ \cdot \\ \cdot \\ z^{-(r-1)}Y(z)-F_{r-2}(U) \end{bmatrix} = \mathcal{B}_{rX2n} \begin{bmatrix} X_1(z) \\ X_2(z) \\ X_3(z) \\ \cdot \\ \cdot \\ \cdot \\ X_{2n}(z) \end{bmatrix} \tag{4.25}$$

Now $\mathcal{B}$ can be written as

$$\mathcal{B} = Q\,\mathcal{D}(S_i)V^H$$

where $\mathcal{D}(S_i)$ is a diagonal matrix of the singular values of $\mathcal{B}$. The Moore-Penrose inverse [53, p.432] of $\mathcal{B}$ is then

$$\mathcal{B}^+ = V\mathcal{D}^{-1}(S_i)Q^H \quad .$$

Finally, the initial conditions are found by taking the Moore-Penrose inverse of (4.24)

$$\mathbf{x}_{init}^{opt} = \mathcal{B}_{2nXr}^{+}\mathbf{y}_{past} \quad . \tag{4.26}$$

In (4.26), $\mathbf{y}_{past}$ is the left-hand side of (4.25).

This extension improves the condition number of $\mathcal{B}$, but in practice it was found to weight the past **y** values too heavily. From a control perspective, the controller was not allowed to respond quickly to a sudden disturbance because only a minor change is immediately seen in the initial conditions due to the weighting.

Notwithstanding these problems with the numerical implementation of GPC, GPC itself proves to be a powerful control strategy. The potential effectiveness of GPC is illustrated in the following example. A case was run on the linear model in the absence of noise. The control values were saved at each time step. These control values were fed back into the nonlinear system running in the EMTP for the same disturbance. The EMTP output for this case is shown in Figures 14 and 15. The series of control actions from the separate linear model case worked even in the EMTP, but the discrete level GPC could not calculate them given the EMTP output data.

Figure 15 shows basically no difference between the straight feedback gain strategy and GPC. Although the sensitivity problems with GPC have not yet been worked out, the results shown in Figure 15 would lend credence to the claim that straight feedback control on the generator $\Delta\omega$ in the case of a resistive dynamic brake is in itself "nearly" optimal control. For this reason and for reasons discussed in the next section, the effort to overcome the sensitivity problem of GPC seems to be no more than an academic exercise. Straight feedback gain may be as optimal a strategy as can be expected for this situation.

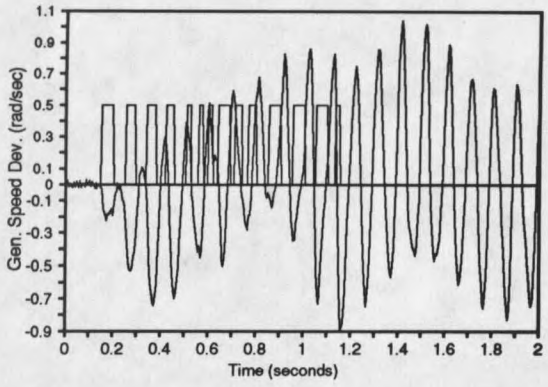

Figure 14. Uncontrolled Response of System Due to Pulse Disturbances.

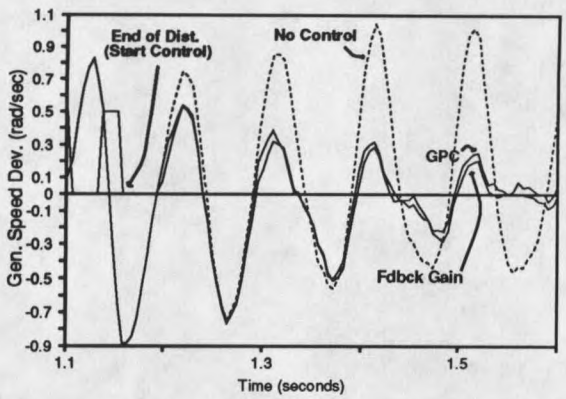

Figure 15. Damping of System from Feedback Gain and GPC.

Sizing the Brake

As related in the introduction, the primary focus of this work is in relation to high speed reclosure of circuit breakers on series compensated lines. High speed reclosure is a technique used to improve system stability by restoring the structural integrity of a system as rapidly as possible following a temporary fault. A 1979 AEP/MIT paper by Dunlop et al. reports experiences reclosing a 765 kV AEP line at 30 cycles [54]. Previous work suggests that the magnitude of damping of transient torques at or near 0.5 seconds after the initiating disturbance must be considered in choosing resistor values for braking transient torques in a system of this type.

Figures 16 and 17 show the generator $\Delta\omega$ and torque between the generator and the low pressure turbine of the synchronous machine shown in the IEEE Second Subsynchronous Benchmark (Figure 1). The disturbance is a three phase bolted fault lasting 4.5 cycles at bus 2. The fault naturally extinguishes at 0.0916 seconds with no circuit breaker operation. No effort has been made to determine a worst case scenario. The above fault scenario was used merely to produce a large torque in the generator-LP shaft section. Straight feedback of the generator speed signal is used to obtain the damped response shown in the plots. The thyristors are gated when the generator $\Delta\omega$ is greater than zero. The brake size is 240 MW or 40% of rated generator MVA.

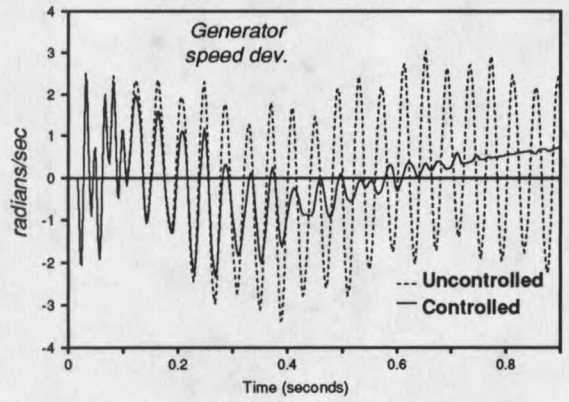

Figure 16. Second Benchmark Generator Speed Deviation.

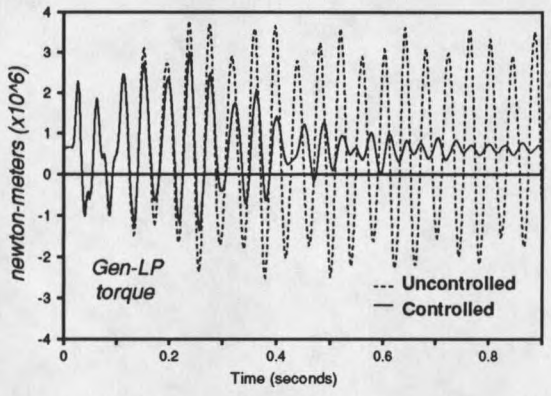

Figure 17. Second Benchmark gen-LP Torque.

Studies to date indicate that a major factor in determining the size of the brake will be the amount of "dead-time" allowed in the reclosure scheme. Dead-time as used in [54] means the amount of time which elapses between a circuit breaker trip to clear a fault and the subsequent reclose. Less dead-time in the reclosure scheme indicates the need for a larger brake. In the figures above, a value of 240 MW was chosen for the brake to meet a design goal of a maximum of 0.75 p.u. torque at 0.5 seconds. Maximum peak to peak torque of 0.70 p.u. occurs in the damped curve at 0.6 seconds. Half this value is added to the steady-state torque value of 0.38 p.u. to get a theoretical maximum of 0.73 p.u. Torque at 0.5 seconds. An unsuccessful reclose in the no control case could seriously damage the shaft as there is a possibility that the circuit could reclose into a 2.28 p.u. Torque creating an intolerably high total torque.

Aside from simply satisfying a design goal, the root locus plots could be used as a tool to aid in sizing the brake. In order to end up on the open-loop zeros in Figure 10, the closed-loop poles must change direction at some point and travel to the right half-plane. The value of gain for the point at which the closed-loop poles change direction represents the maximum possible damping for the system. To use the root loci as a tool in determining optimal brake size, an engineer would perform a Prony analysis on a system with

an arbitrary brake size -- say 100 MW. The identified model is used to plot a root locus. The root locus is examined to determine the gain at which the poles change direction. This gain is a multiplier on the control action. If the gain should turn out to be 3.0, the controller would be calling for three times a 100 MW brake or 300 MW. One would have to remember in using this approach that the identified model is only valid for a small operating region. The brake size determined using this method would have to be confirmed using other means.

We have shown that the generator $\Delta\omega$ is an excellent feedback signal to use in controlling the dynamic brake. We have also implied that straight feedback gain on this signal is nearly optimal. This section on sizing the brake lends more credibility to the claim that complex controllers or optimal digital control is not needed in this case. Simply employing a larger brake will have the same effect as implementing a better control law if such a law exists and if economics permit a larger brake.

CHAPTER 5

SIMULATION RESULTS

The simulation results in this section were performed using EPRI's Electromagnetic Transients Program (EMTP) Version 2.0. Synchronous machines in EMTP are modeled in a rotating orthogonal coordinate system using Park's equations and the associated transformation. The mechanical mass-spring system is modeled separately by Newton's laws for rotating bodies. No governor model has been included in the simulations and so the EMTP assumes a constant mechanical input power.

These results were obtained using the straight feedback control strategy discussed in this section and listed in Appendix C. The brake is switched in a bang-bang mode rather than using a sophisticated firing angle thyristor gate control which could simulate a variable resistance and provide smooth control. In addition to simpler operation, bang-bang control should provide faster damping. To implement the algorithm, a gain is set for the feedback loop and a dead-zone is established where the brake will not be turned on. The dead-zone serves the function of disabling the brake when

there is no major disturbance present so that small fluctuations in generator $\Delta\omega$ do not activate the brake. When the feedback signal exceeds the dead-zone limit in the positive direction, the brake thyristors are gated. Dalpaiz [55] shows that the proposed feedback signal, $\Delta\omega$, is accessible on a typical generator. In this paper, the generator $\Delta\omega$ is monitored for subsynchronous oscillations using a PC.

The results in this section have been chosen to illustrate certain points with respect to the application of the brake which have been mentioned in the previous sections. The effects, or lack thereof, of filtering, brake size, control algorithms, and thyristor types are seen in the plots. A discussion of the effects of dynamic braking on nearby machines is also included in this section.

Effects of Filtering

To study the effects of a filtered $\Delta\omega$ as discussed in Chapter 4, a simple second order high-pass filter was designed with a cutoff frequency of 2 Hz. In order to effectively damp the torsional modes, it is imperative that the filter have minimum phase error at 20 Hz and above -- the range of subsynchronous resonance and shaft torsional frequencies. With a decade between the cutoff frequency and the passband, a second order filter can meet these specifications. The

s-plane transfer function was converted to discrete-time using a bilinear transformation and implemented in the controller subroutine shown in Figure 5.

The figures in this chapter were obtained from EMTP simulations of the MPC Colstrip model described in Chapter 2. In the first set of cases to be discussed, Colstrip 3 and 4 are lumped together to form a conglomerate 1638 MVA machine. The brake is operating at the terminals of this machine. Colstrip 1 and 2 are operating separately into the 230 kV bus CS230 (Figure 2). A three phase bolted fault occurs at bus BGFF1 at 0.22 seconds. The fault is cleared at buses BG001 and GBSW1 4.7 cycles later. The circuit breakers at BG001 and GBSW1 then reclose into the same fault at 1.112 seconds. This gives a total dead-time of 0.814 seconds. The fault clears itself 2 cycles later with no further breaker operations. The disturbance was chosen to produce large torques in the turbine shaft. Reclosing into a three phase fault would be expected to be one of the most severe disturbances. The brake is rated at 200 MW or 12 % of the conglomerate rated MVA.

Figure 18 shows the uncontrolled conglomerate machine $\Delta\omega$ for this disturbance while Figure 19 shows the controlled but unfiltered response superimposed on the filtered, controlled response. Of particular interest is the sharp increase in amplitude of the torsional modes at the time of reclosure.

It is this torsional impact that is of major concern in these studies. Both controlled responses show a large amount of damping over the uncontrolled case in the transient modes at 1 second - just before reclosing.

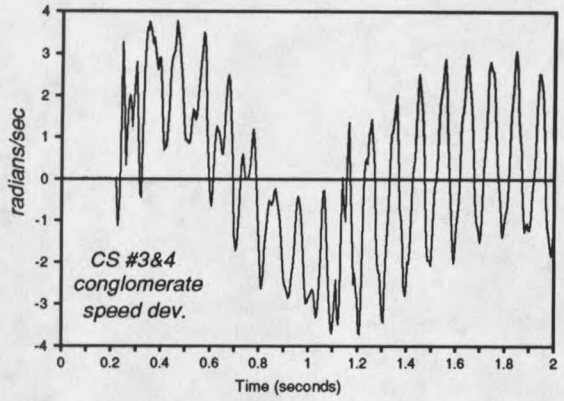

Figure 18. Uncontrolled Generator $\Delta\omega$ for Three Phase Fault With Reclose.

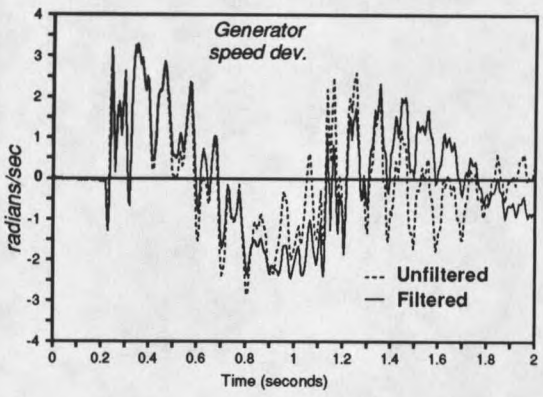

Figure 19. Filtered and Unfiltered Controlled response for Case in Figure 18.

Figures 20 and 21 show the effects of filtering on the control action. The top plot in each figure shows the generator $\Delta\omega$ as seen in Figure 19 while the bottom half shows the A phase brake current. The filtered brake gives more uniform action on the torsional modes with less of the long-term operation seen between 0.2 and 0.6 seconds in Figure 20.

Figure 22 shows the torque on the LP1-LP2 shaft section for both the filtered and unfiltered control. Here the benefits of the filter are evident. The plot shows a 36%

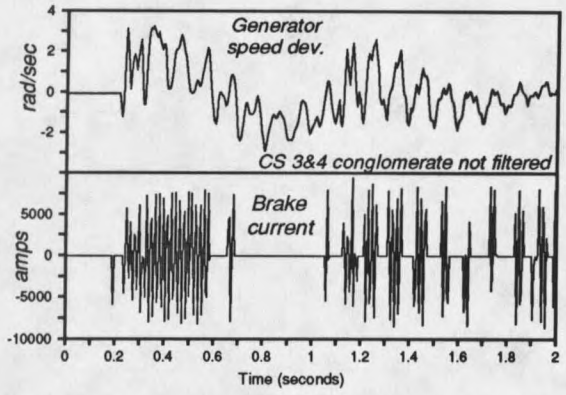

Figure 20. Generator Speed Deviation and Brake Current for Unfiltered Controller.

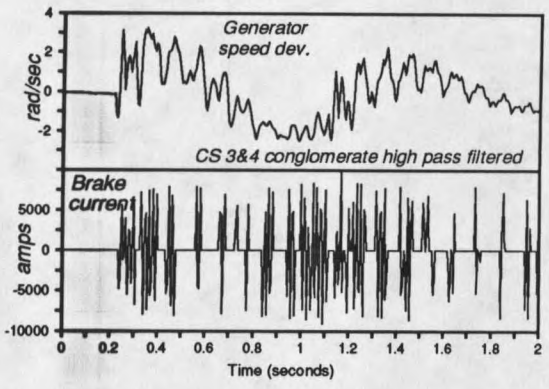

Figure 21. Generator Speed Deviation and Brake Current for High-Pass Filtered Controller.

reduction in total torque at 1.2 seconds through filtering compared to the unfiltered control. Damage to turbine-generator shafts due to excessive torque is known to be exponential in nature so a 36% reduction in torque could correlate to a much larger percent increase in shaft life. Moreover, the filtered signal control case is down 57% from the uncontrolled torque. The 57% figure may be enough to guarantee the safety of the shaft should a high-speed reclosure scheme be considered by a utility.

The filtering discussion in Chapter 4 and the results shown in Figures 18 through 22 demonstrate the effectiveness of employing a high-pass filter on the feedback signal. The amount of filtering and the strategies used may be a matter

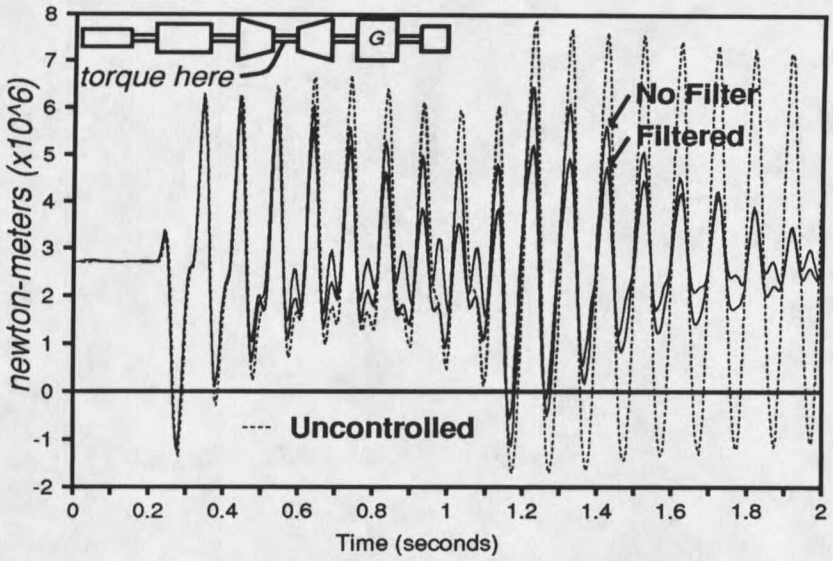

Figure 22. LP1-LP2 Torque for Disturbance in Figure 18 Showing Effect of Filtering.

of engineering judgement in cases where a secondary function of the brake is to improve transient stability. High-pass filtering is used on all of the following plots and those seen in Chapter 6 unless otherwise specifically stated.

Results with a 200 MW Brake

Two additional torque plots are shown below for the same disturbance. Figure 23 shows the HP-IP torque for the uncontrolled response superimposed on the controlled. The LP2-Gen torque for the same case is shown in Figure 24. Special attention is called to the torsional damping at approximately 1.1 seconds. The damping at this time -- just

before reclosing -- should be used as a measure of the effectiveness of the controller since this value can be used to approximate the maximum possible torque at reclosing. Simulation may not show the maximum torque if the oscillations are out of phase with the response due to the reclosing.

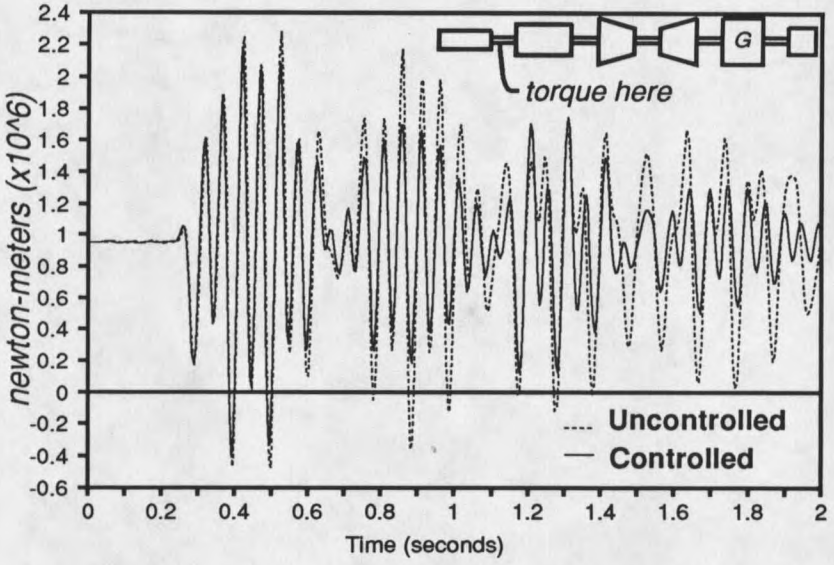

Figure 23. HP-IP Torque for Disturbance in Figure 18.

Damping is seen to have improved in all cases, although perhaps not as dramatically as is seen in Figure 22. One reason for this is that this particular disturbance was "tuned" to create large torques in the LP1-LP2 shaft section. An evaluation of the eigenvectors associated with the mass-spring system has shown this section and the LP2-Gen section to be the two most critical for the Colstrip #3 and #4 machines

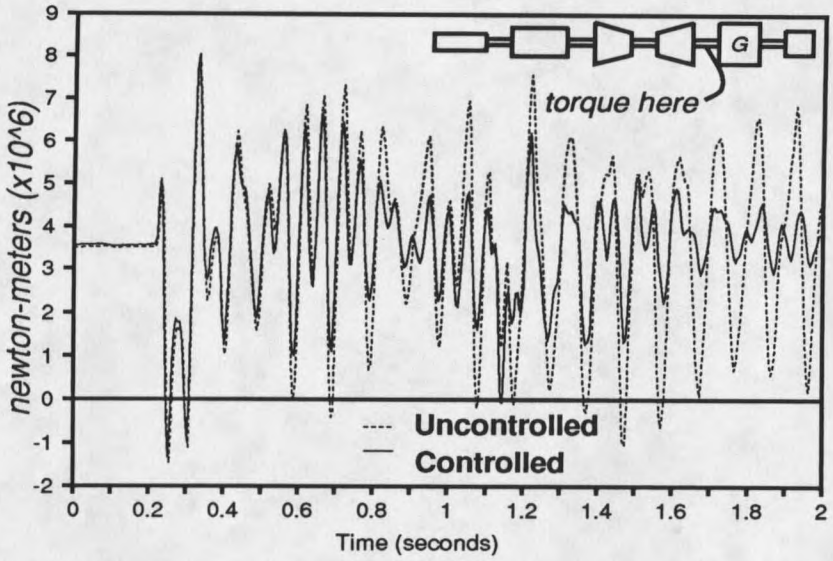

Figure 24. LP2-Gen Torque for Disturbance in Figure 18.

modeled in these simulations. The root locus plots of Chapter 4 and further simulations show that the brake would also be effective in damping the other shaft modes.

Effects of Brake Size

Some factors in determining the size of the brake were discussed in Chapter 4. The following plots were chosen to illustrate some of the benefits and drawbacks of using larger brakes in attempting to damp torsional modes.

Figure 10 shows that the closed-loop system is non-minimum phase i.e. there are zeros in the right half-plane. Arbitrarily increasing the size of the brake will eventually force the

closed-loop poles to change direction and reduce the damping of the system. A reasonable approximation to the point at which the poles in Figure 10 change direction is at a feedback gain of 5.2. The root locus was drawn for a 200 MW brake. From this information a guess might be made as to the optimal size of the brake. To make this guess, two major assumptions must be made. The system must remain at an operating point which is close to the one at which the Prony analysis was made so linearity is maintained. Also, one must assume that the bang-bang action of the brake is a close approximation to the continuous control of the root locus. These being stated, a 1,040 MW brake may seem to be a reasonable choice from the standpoint of maximum damping ability.

Mainly because of the bang-bang restriction, the 1,040 MW estimation is too large. Damping is seen to have decreased from that of brakes with slightly smaller ratings and the large device starts to create some system disturbances of its own. Figures 25 and 26 show the LP1-LP2 torque and the HP-IP torque for the disturbance described in the previous section using an 800 MW brake for damping. In Figure 25, the 800 MW brake is shown on top of the 200 MW brake and the uncontrolled response. Figure 26 shows only the 800 MW brake and the 200 MW brake. 800 MW is 50% of the machine rated MVA.

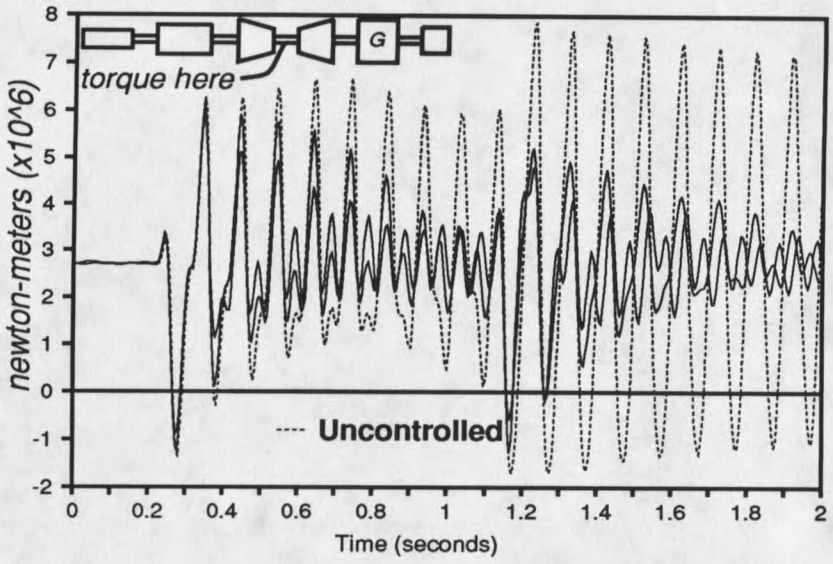

Figure 25. LP1-LP2 Torque for Disturbance in Figure 18 Using 800 MW Brake.

In Figure 25, a large increase in damping can be seen roughly between 0.4 seconds and 0.9 seconds. After this time, the damping achieved using the 200 MW brake almost equals that of the 800 MW brake. This would seem to be a case of the large brake creating a mild disturbance by its own operation after the amplitude of the feedback signal has been reduced a considerable amount. Figure 25 shows that there is no need for a larger brake given the amount of dead-time used in this reclosing scheme. The use of a faster reclosing scheme may warrant the consideration of a brake larger than 200 MW.

Figure 26 tells a different story. There is no indication that the larger brake has improved the damping of this faster

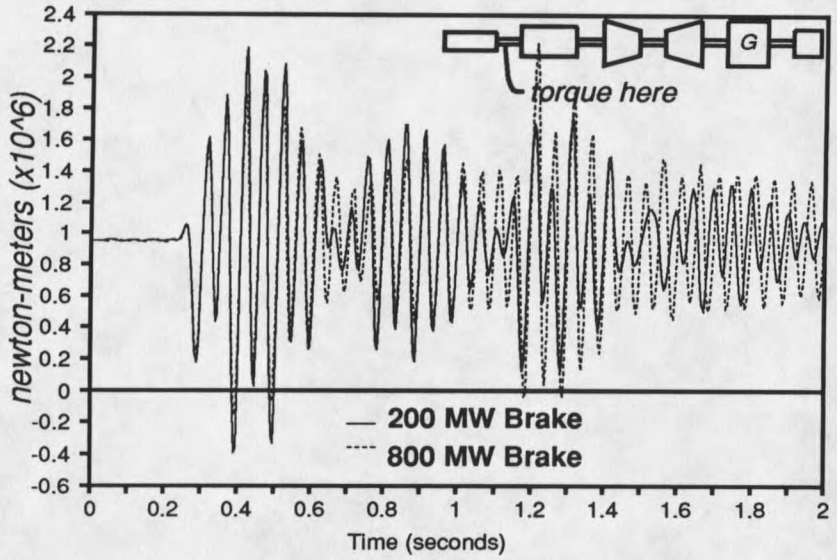

Figure 26. HP-IP Torque for Disturbance in Figure 18 Using 800 MW Brake.

mode. Further studies show that with the given control strategy, maximum damping is achieved for this mode with a 500 MW brake. This may still be larger than is needed given the reclosing scheme employed.

Damping Electromechanical Modes

The root locus of Figure 13 illustrates the usefulness of filtering the feedback signal to direct more energy into the damping of the torsional modes. An undesirable effect of the filter used here is the apparent decrease in damping of the electromechanical mode. The reduction in damping, however, may not be as severe as indicated in Figure 13. If

it were, there would certainly be cause for concern. Simulations bear out that there is little detrimental effect on the electromechanical modes for low power brakes of the kind which would probably be installed specifically to damp transient torques. These brakes would be small in size and would be active for a very short period of time with respect to the frequency ranges of interest in transient stability studies. For larger brakes that are meant to deal with the stability problem as well as transient torques, the controller would be designed so as to provide damping to all of these modes.

Figure 27 shows the generator $\Delta\omega$ for two cases. In the first case, high-pass filtering is employed throughout the simulation. Damping of the electromechanical mode is indeed decreased with this large brake in operation. In the second trace on this plot, the filter was taken out of the feedback loop when the filtered signal was adequately damped. This allowed the brake controller to act on the electromechanical mode with dramatic results.

In damping first the torsional modes and then the electromechanical mode, the dynamic brake is seen to be extremely flexible in its applications. Designs specific to an installation have a wide range of possibilities which need to be considered on a case-by-case basis.

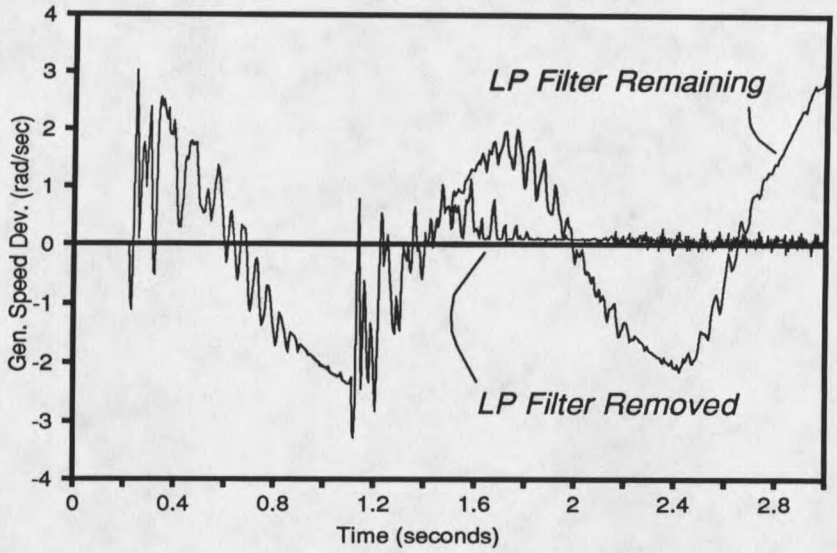

Figure 27. Generator $\Delta\omega$ Signals Showing the Electromechanical Mode Damping.

Thyristor Types

A question which has arisen frequently centers around the type of thyristor needed to obtain effective control using the scheme outlined above. SCR's are commonly used as switches in power system applications. This makes them attractive for use in switching a dynamic brake, but they have the drawback that once gated, they will continue to conduct current until they are line-commutated which must happen at least every 8 milliseconds. Gate Turn-Off thyristors or GTO's are less familiar but they have the advantage that they can be commutated

at any time. This feature is a must for truly optimal control. In this case, the brake cannot continue to conduct after the controller has given the "off" signal.

Figure 28 shows the generator $\Delta\omega$ for two signals in a case for which a 200 MW brake is used to damp the disturbance mentioned for Figure 18. One of these signals is the system response where SCR's were used to switch the brake and one for GTO's.

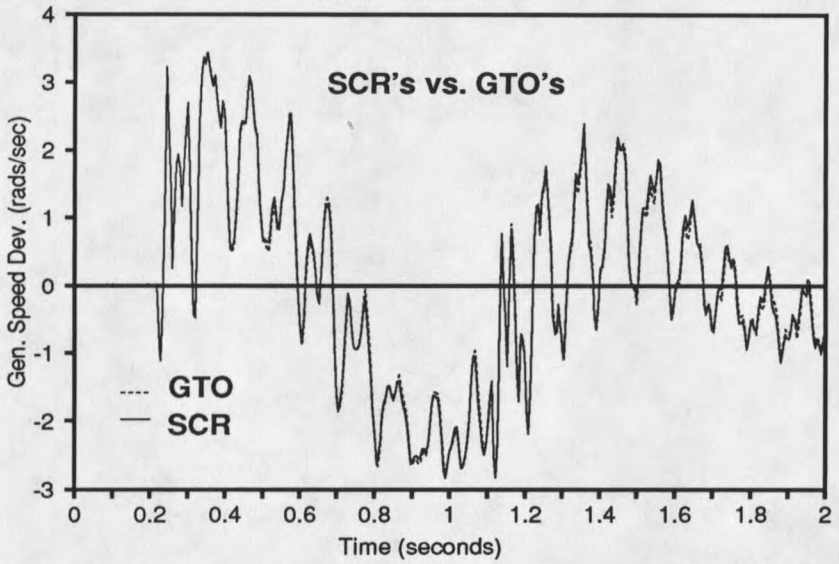

Figure 28. Generator $\Delta\omega$ Signals Showing the Effects of Thyristor Type.

There is little difference in damping between the two signals indicating that SCR's are sufficient in this application. The main reason for the success of SCR's is that the time lag associated with the commutation of these devices is small compared to most of the frequencies being damped. The

SCR's are being commutated at 60 Hertz while most of the torsional frequencies are below 30 Hertz. One may expect to see an advantage in using GTO's if a high torsional frequency is expected to be lightly damped. In addition, because of the large amount of energy being expended in the time between "off" signal and commutation, large brakes may warrant the use of GTO's.

Effects of Braking On Nearby Machines

The use of a braking resistor at the Colstrip #3 conglomerate machine was seen in the simulations as having very little effect on the response of other nearby machines. In the case of the MPC Colstrip model, two smaller machines feed the same bus as does the Colstrip #3 machine where the brake was located. The response from these machines was closely watched for signs of reduced damping in either the torsional modes or the electromechanical modes. No significant effects were seen in either case except that when the brake was used to damp electromechanical oscillations subsequent to its primary purpose, an improvement in the damping of the electromechanical modes at Colstrip #1 and #2 were seen also. Figures 29 and 30 show the generator $\Delta\omega$ of Colstrip #1 for the same disturbance that has been previously cited. In Figure 29, the uncontrolled disturbance is shown as a ref-

erence. Figure 30 shows the same response when a 200 MW brake and a 800 MW brake are used to control the torsional oscillations on Colstrip #3.

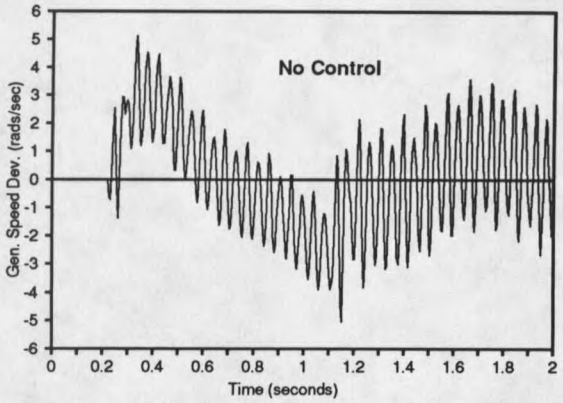

Figure 29. Colstrip #1 Uncontrolled Generator Speed Deviation.

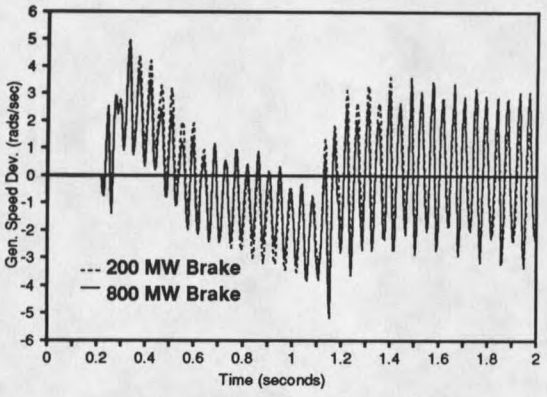

Figure 30. Colstrip #1Generator Speed Deviation for 200 MW and 800 MW Brake.

It can be seen from these figures that the application of a brake acting on one machine has little effect on other nearby machines. In the case of the MPC Colstrip model, this is because the non-controlled machines do not have any shaft modes that are near to the modes of the Colstrip #3 conglomerate machine. The braking action on the Colstrip #3 modes does not excite the modes of Colstrip #1 or #2. If the modes of a nearby machine fall close to those of the machine being controlled, one could expect to see a more significant effect of the brake on the uncontrolled machine.

In this chapter we have shown some standard configurations and attempted to illustrate some of the points which have been brought up in the previous sections. Chapter 6 shows the simulation results for some special configurations and operating conditions which are of interest in this study.

CHAPTER 6

EFFECTS OF FAULT TYPE, POWER FACTOR AND BRAKE ORGANIZATION

It is well known that unbalanced network faults create a negative sequence component of current which can be thought of in the phasor domain as a counter-rotating current. For simplicity, a single-line-to-ground (SLG) fault will be considered in this discussion although equally valid arguments can be made for other unbalanced fault types. The negative sequence current exists in the stator of the generator both during the fault and during the clearing action if single-line clearing is employed.

It is logical to assume that the counter-rotating currents flowing in the stator of the generator as described above will set up a second harmonic torque in the generator rotor as the magnetic fields associated with each will cross twice per revolution of the rotor. It has been suggested that this second harmonic component may have some uses in the feedback control of the dynamic brake to damp transient torques. Overall damping of a machine, however, is said to increase when negative sequence currents are present [56]. With these preliminaries in mind, an EMTP case was set up to simulate

a SLG fault with single-line reclosing for analysis. The brake was not included in this analysis. Fast Fourier transforms were performed on the generator $\Delta\omega$ signal and all of the applicable torques of the single synchronous machine in the simulation. The Montana Power Company Colstrip test system was used as the model. Figures 31 through 35 show the results of these FFT's. A small 120 Hertz component of generator speed deviation is seen in Figure 31 but no significant components are seen in the torque plots.

Further examination of the FFT's reveals that the subsynchronous frequencies corresponding to the turbine shaft modes are prominent and higher frequencies are attenuated greatly. This confirms results and discussions on the topic found in conventional texts and in the open literature. In fact, the supersynchronous component of network resonances set up by such components as series capacitors are not considered to be a problem in SSR studies. This higher frequency component is generally not exciting the turbine shaft at one of the shaft's natural frequencies, which dominate the FFT and so that component is generally neglected. We could find no advantage to utilizing the second harmonic frequency in the control algorithm.

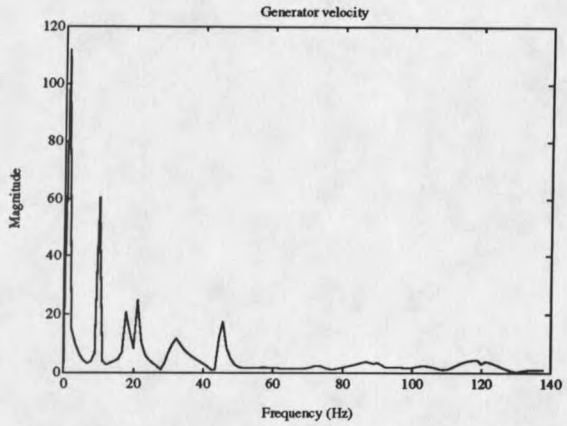

Figure 31. FFT of Generator $\Delta\omega$.

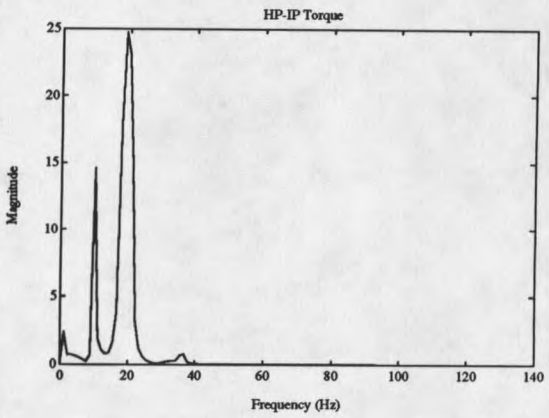

Figure 32. FFT of HP-IP Torque.

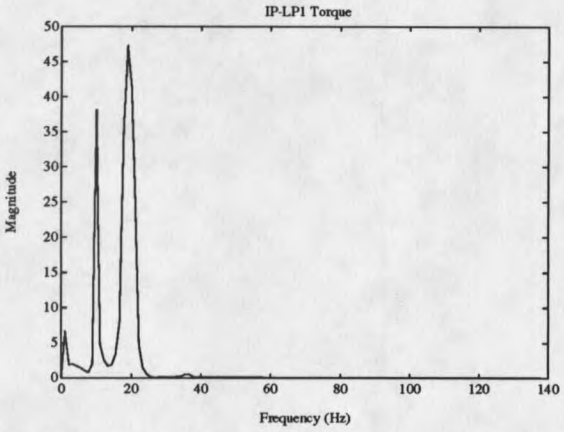

Figure 33. FFT of IP-LP1 Torque.

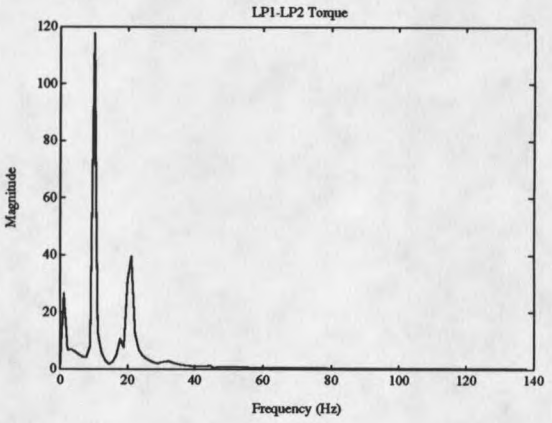

Figure 34. FFT of LP1-LP2 Torque.

The FFT's confirm what is seen from system transfer functions obtained from Prony analysis. Both show an overwhelming dominance of the turbine-generator shaft modes in favor of any network components that the dynamic brake may see. This would suggest that with the given feedback signal, the brake devotes almost all of the available energy to damping

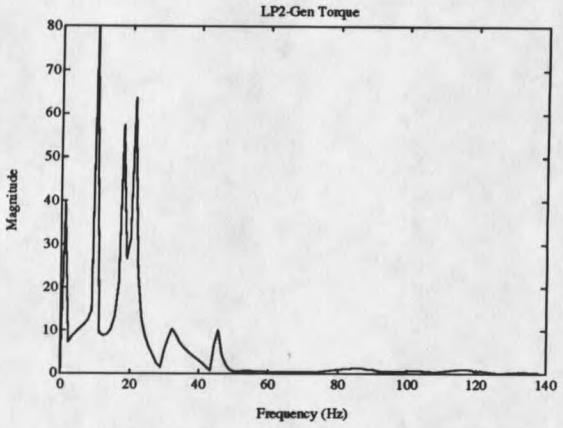

Figure 35. FFT of LP2-Gen Torque.

the particular shaft resonant modes regardless of the network configuration at any given moment in time. In other words, the controller does an effective job of damping the shaft at the frequencies of interest through a disturbance of any type - be it in the electrical network or even a mechanical disturbance.

Figures 36 through 38 compare the uncontrolled response to the controlled response of the Colstrip model when subjected to a SLG fault near to the synchronous machine. The fault occurs at 0.22 seconds and is cleared by a single line opening at 0.30 seconds. An unsuccessful single-line reclose occurs at 1.11 seconds and the fault then extinguishes itself at 1.16 seconds with no further circuit breaker operation. The generator $\Delta\omega$ (feedback) signal is high-pass filtered to block the electromechanical modes of the generator. A "dead-zone"

is employed in the control algorithm to prevent the brake from operating unless there is a significant disturbance in the system. The dead-zone encompasses a region where the filtered signal is approximately ± 0.01 radians per second from synchronous speed. It can be seen that the brake provides excellent damping of the transient torque over the uncontrolled case.

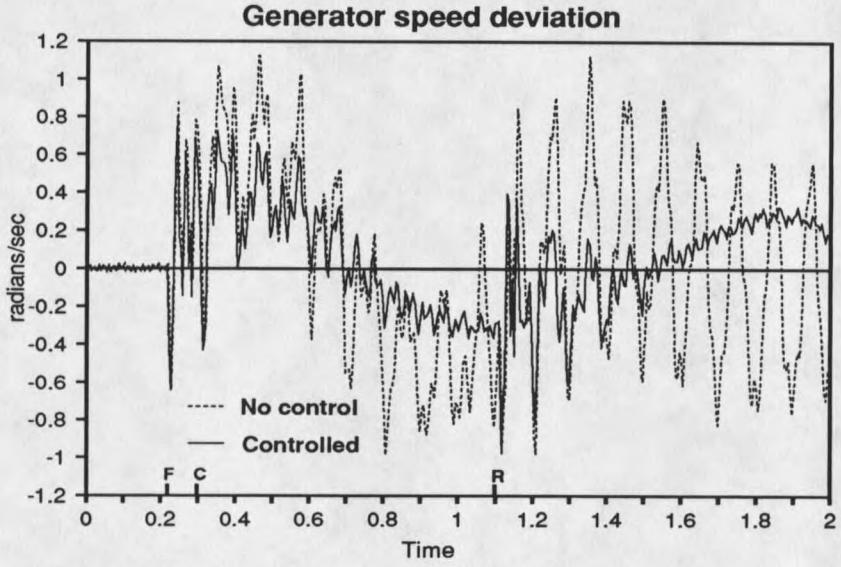

Figure 36. Generator $\Delta\omega$ Signals Showing Damping of SLG Fault.

It should be noted that similar results were obtained from DLG faults which also contain negative sequence currents. As a point of reference, the SLG fault created a disturbance in the generator speed deviation signal which amounted to approximately one third of the magnitude of the same signal

when subjected to a three phase fault at the same bus. The damping ratio appears to be similar in both cases, but the small initial magnitude of the SLG fault allows for a quicker return to steady-state than does the three phase fault.

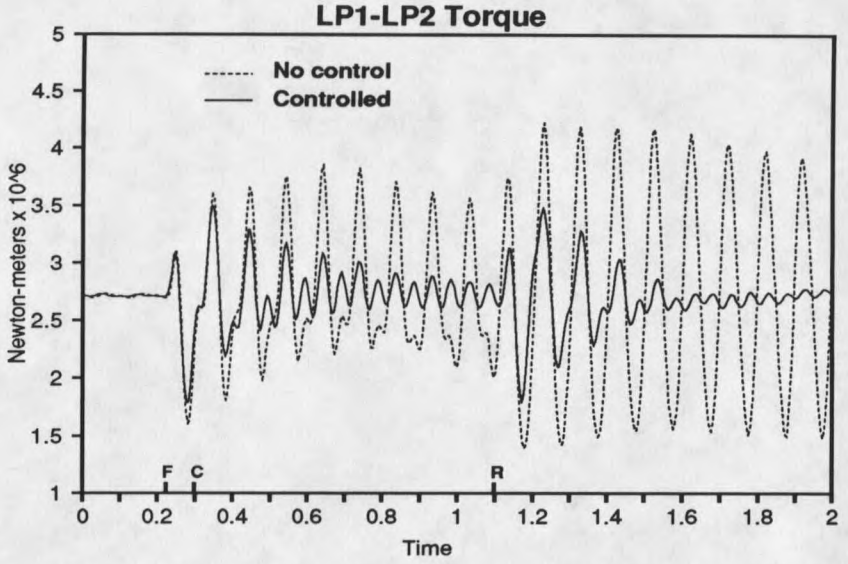

Figure 37. LP1-LP2 Torque Showing Damping of SLG Fault.

The dominance of the shaft torsional modes as seen from the generator $\Delta\omega$ signal in the FFT plots can also be used to explain some of the robustness properties of the control algorithm with respect to other system conditions. Figures 36 through 38 leave little doubt that the controller is robust with respect to fault type. Additional simulations involving the system at different steady-state operating points and for varying generator power factors have resulted in comparable

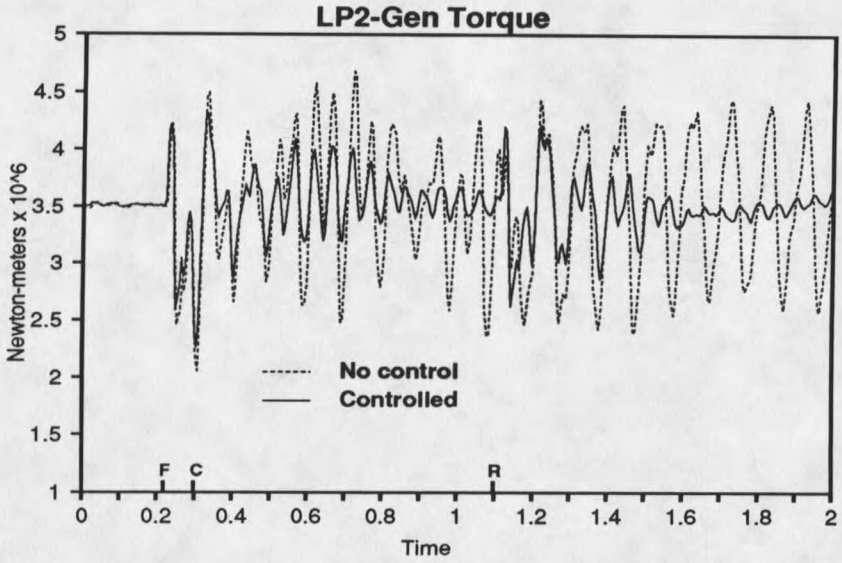

Figure 38. LP2-Gen Torque Showing Damping of SLG Fault.

results to those which have already been illustrated. The choice of generator $\Delta\omega$ as a feedback signal has again proven to be a wise one. Network configurations, fault types, generator loading, and generator power factor are not parameters which can significantly affect the spectrum of this signal. This property is what makes the control algorithm robust through a wide range of conditions.

Several studies were also conducted as part of this project to determine some options for brake configurations at a generation facility. Economic considerations may warrant the use of only a single brake at a given facility if a control algorithm can be found which will damp all of the machines

at that location. A study involving multiple brakes at a single facility and a study for a single brake for multiple machines are described in the remainder of this section.

Multiple Brakes at a Single Location

Optimal braking for any given machine can only be achieved by the use of a dedicated brake for that machine. These studies have shown, however, that sets of identical machines which are electrically close to one another can be controlled effectively from a single brake. The damping seen for these machines closely approximates that of a single brake for a single machine. Even though the identical machines may be loaded differently at any given time, the shafts exhibit the same resonances and can be expected to be in phase in response to a network disturbance. Only the damping may differ due to loading conditions. This analysis is confirmed in [57].

Figures 39 and 40 show the damping of the generator $\Delta\omega$ signals for two non-similar machines for a case in which two dynamic brakes have been used for damping. One of the brakes is a 200 MW brake connected to the 26 kV CS261 bus (see Figure 2) at Colstrip on the MPC model. 200 MW again represents 16 % of the conglomerate machine rated MVA. The other brake is located on the low voltage side of a transformer connected to the 230 kV CS230 bus. This brake operates at 22 kV and is intended to damp the transient torques in both the Colstrip

#1 and #2 machines. These are identical machines which are both rated at 377 MVA. The second brake is rated at 120 MW which is 16 % of the Colstrip #1 and #2 combined rating.

The disturbance is similar to that described in Chapter 5 and the control algorithm for each separate brake is also the same as that discussed in Chapter 5. The Colstrip #3 conglomerate machine $\Delta\omega$ is fed back to control the first brake and the Colstrip #2 $\Delta\omega$ is used to control the second brake.

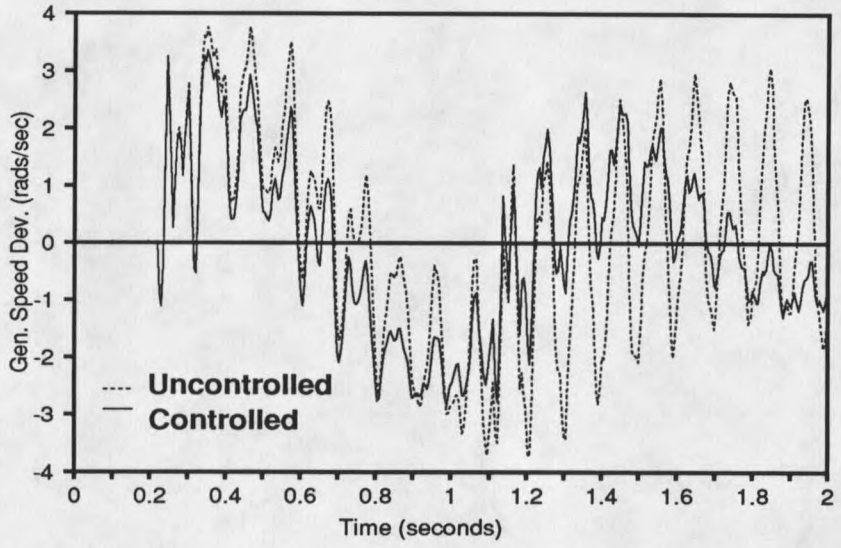

Figure 39. Colstrip #3 $\Delta\omega$ Signals Showing Damping for Multiple Brakes at a Single Location.

Figures 41 and 42 show the LP1-LP2 torque on the Colstrip #3 conglomerate machine and the LP-Gen torque for Colstrip #1. The damping for the Colstrip #2 machine is analogous to that of Colstrip #1.

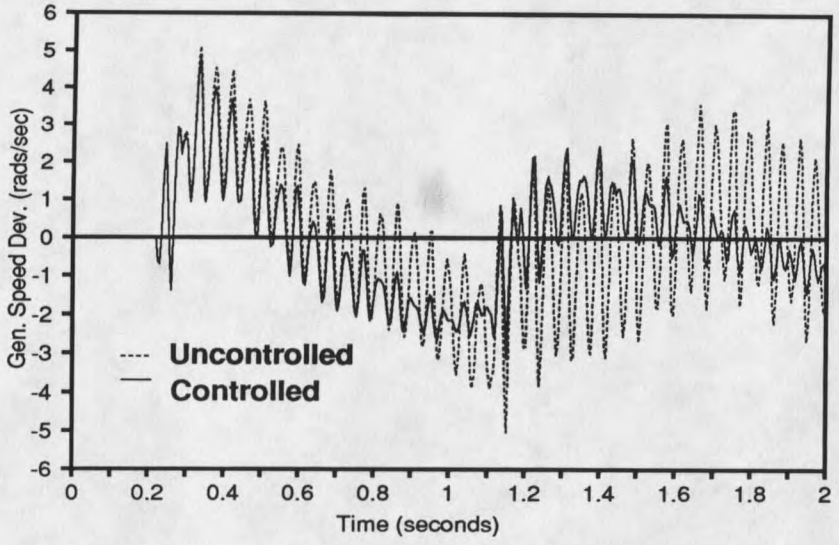

Figure 40. Colstrip #1 $\Delta\omega$ Signals Showing Damping for Multiple Brakes at a Single Location.

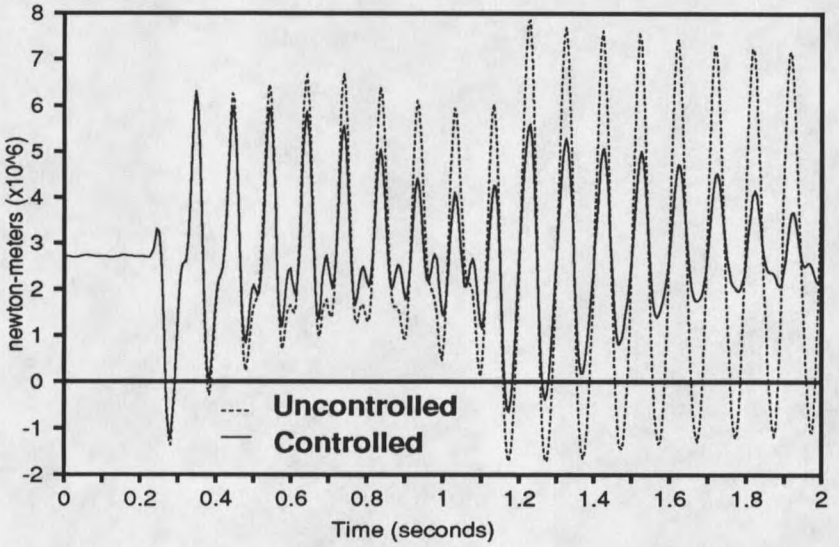

Figure 41. Colstrip #3 LP1-LP2 Torque Showing Damping for Multiple Brakes at a Single Location.

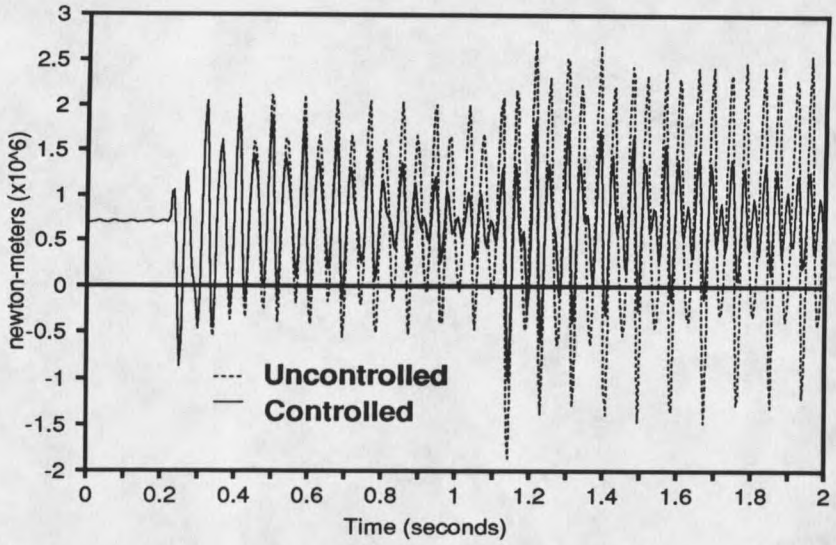

Figure 42. Colstrip #1 LP-Gen Torque Showing Damping for Multiple Brakes at a Single Location.

The results shown above seem to be reasonable given that the Chapter 5 results showed no effect on the damping of the smaller machines using a brake on the larger machines. Special precautions may have to be taken if a resonant mode of one machine matches that of another machine but the machines are otherwise dissimilar.

A Single Brake For Multiple Machines

To complete the study of the various brake configuration, a single brake was placed on the low voltage side of a transformer at the 500 kV CS500 bus. The generator $\Delta\omega$ signals for both the Colstrip #3 conglomerate machine and the Colstrip

#2 machine were fed into a summing junction and then into the controller filter. This simple strategy would have to be re-evaluated if some of the modes of one machines fell close in frequency to those of another machine. In this case, the simple summer may be unpredictable. Components which are in phase will tend to activate the brake for added damping. Weighting factors could be added to one signal should engineering considerations dictate that one machine should receive more damping than others.

A 320 MW brake was used representing 16 % of the total rated MVA of all machines at the facility. Figures 43 and 44 show the generator $\Delta\omega$ for Colstrip #3 and Colstrip #1

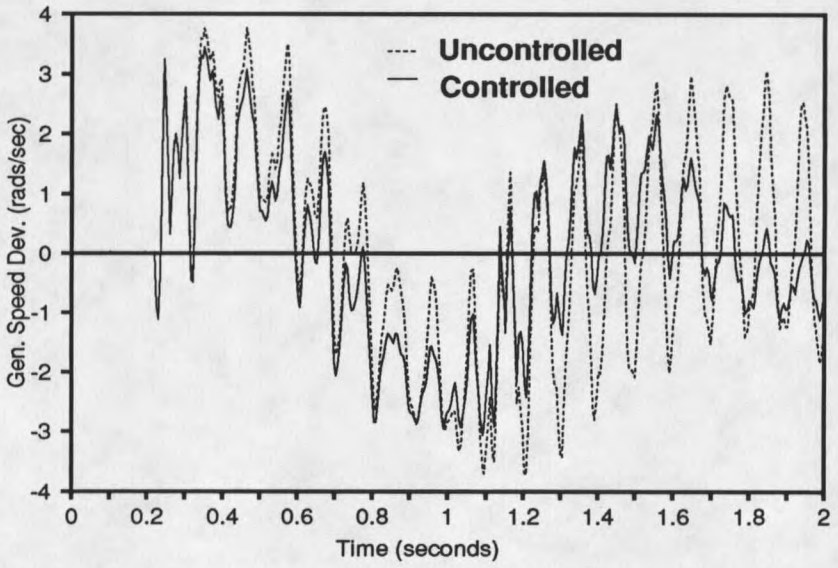

Figure 43. Colstrip #3 $\Delta\omega$ Signals Showing Damping for a Single Brake on Multiple Machines.

respectively. The damping seen in these plots is slightly less than that seen for multiple brakes which can be expected with this strategy. As is consistently the case, the torque plots follow the damping seen in the speed plots and so are not shown here.

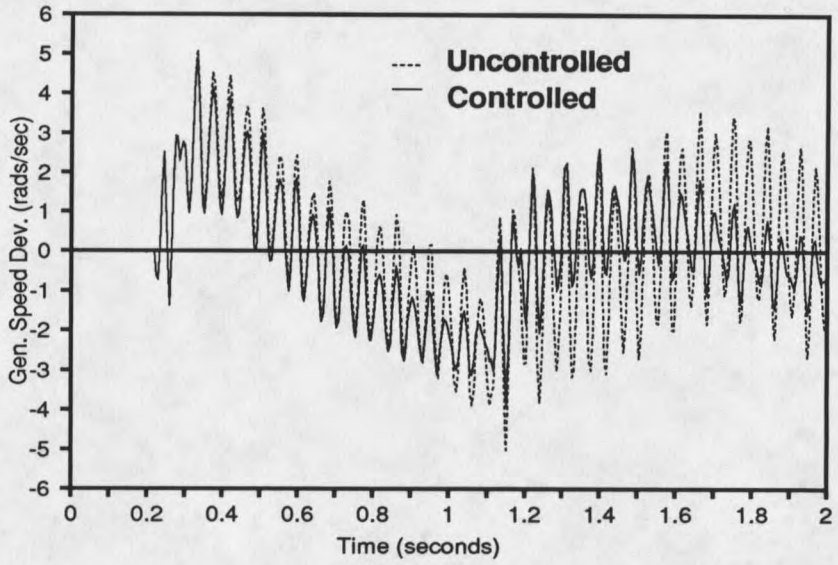

Figure 44. Colstrip #1 $\Delta\omega$ Signals Showing Damping for a Single Brake on Multiple Machines.

This section has highlighted some of the robustness properties of the brake as it is proposed. The control algorithm and feedback signal are seen to adapt well to numerous different situations including operating points, generator power factor, and fault types. It was suggested that this is because the spectrum of the feedback signal is

dominated by the modes of the turbine shaft mass-spring system which are constant and thus can be very accurately represented by linear models.

CHAPTER 7

CONCLUSIONS AND FUTURE WORK

This report has presented discussion and results relating to the application of a dynamic resistive brake to damp torsional oscillations in a synchronous generator. A computer model of a dynamic brake was applied to the EMTP models of two separate test systems in a variety of different conditions. Feasibility of the scheme was demonstrated by time-domain plots showing significant damping of the turbine shaft torsional modes over the uncontrolled case. Some of the benefits of this research and conclusions drawn are summarized in this section.

Dynamic braking of the type employed in this study would be particularly appealing in situations where large turbo-generators are served by series-compensated lines. It is usually the case in these situations that the generators are operating near to their stability limits, and therefore fast reclosing of the series-compensated lines is desirable. Currently, a major concern with fast reclosing is torsional damage to the turbine-generator shaft. The scheme developed

in this thesis will improve the damping of the turbine-generator shaft transient torques providing a larger safety margin for utility engineers contemplating fast reclosing.

The reasons this work should prove to be beneficial in future research involving dynamic braking, transient torque studies, and SSR studies follow.

- Two detailed system models exhibiting moderate to severe transient torques have been developed and implemented in the EMTP. One model is a standard of the IEEE and may be used to verify results from research conducted at various institutions. The other model represents a large system with multiple machines and is a realistic representation of an actual system.
- An EMTP model of a resistive brake was developed and tested. The controller for the brake was made to be extremely flexible by allowing the use of a user-written subroutine interface with the EMTP. This subroutine receives EMTP variables, makes a decision on control action, and transmits the control action to the brake thyristors which are modeled in the EMTP.
- Several traditional SSR analysis techniques were discussed. System identification using Prony's method was introduced and proved to be particularly

useful in developing control strategies. In addition to providing information on the eigenvalues of a system as does the more conventional Eigenvalue Analysis technique, Prony's method provides the user with the residues associated with those eigenvalues. The residues and eigenvalues can be combined to form a transfer function that represents the system as seen from the brake.

- Two schemes for ordering the eigenvalues in the partial-fraction expansion form of the transfer function which is characteristic of the output of a Prony analysis were shown. Potential problems with these schemes were identified and a compromise solution was proposed.
- Sensitivity problems in implementing discrete-level GPC on high-order systems were identified. The discussion and analysis of these sensitivity problems should prove to be beneficial in future work relating to optimal control and the use of high-order models in control engineering.
- Some techniques for determining appropriate feedback signals and control strategies were discussed. Root locus plots were shown to be helpful in determining the distance that an

eigenvalue can be moved using a particular feedback signal. This property was related to the magnitude of the residue of that eigenvalue. The control strategy would have to be one that forces the eigenvalue to move in the correct direction.

Some of the conclusions that can be drawn from this research are as follows:

- The speed deviation from synchronous of the generator on which the brake is acting proves to be a superior feedback signal for use in damping torsional oscillations of the turbine shaft. This signal is dominated by the spectrum of the mechanical modes of the shaft. The modes of the electrical network are seen to have small residues and are therefore weakly represented in the generator $\Delta\omega$.
- A straightforward, easily implemented control strategy provides excellent damping of the shaft torsional modes. This straight feedback control was shown to be "nearly optimal" through the use of root locus plots and time-domain simulations.
- The search for a truly optimal control law may not be worth the effort. The added complexity of control may make the algorithm lack robustness. Furthermore, should additional damping be required

it would be simpler to simply increase the brake size rather than attempt to make the brake only marginally more efficient.

- A high-pass filter acting on the feedback signal can provide more damping energy to the torsional modes at the expense of the electromechanical modes of the machine. The net result is improved damping of the transient torques in the short time frame that is considered for high-speed reclosing applications.
- The high-pass filter mentioned above may tend to reduce the damping of the electromechanical mode. This phenomenon may be of little concern given that the brake is only intended to operate for a few seconds. The brake can either be turned off at this time or the filter can be removed from the feedback circuit allowing the brake to damp the electromechanical modes. Both strategies were shown to be acceptable.
- The straight feedback control algorithm is robust with respect to a large range of operating conditions, fault types, generator power factors, and brake configurations. An explanation for this property is that since the feedback signal is dominated by the shaft modes, configurations and

anomalies in the electrical network do not significantly affect the control action. The shaft mass-spring system is linear and time-invariant which makes analysis relatively simple.

- For all cases tested, SCR's proved to be sufficient in solid-state switches for the dynamic brake. No need for more expensive GTO's was observed. The delay in commutation of the SCR's will be a maximum of 8 milliseconds. This delay does not severely affect the control action when damping shaft modes which are normally slow.
- A brake on the order of 12% of the rated generator MVA should be adequate in damping transient torques in conjunction with high-speed reclosing. Larger brakes may be more desirable if a secondary function of the brake is to damp electromechanical oscillations in the machine.
- Several brakes may be used at the same facility to damp different machines, however there is no need for multiple brakes to damp two identical machines which feed the same bus. Their shaft modes are also identical and they oscillate together when subjected to the same network disturbance.

- With modifications to the control algorithm, one larger brake may be used to damp oscillations in more than one non-identical machine feeding the same electrical bus. Problems may occur in this configuration when two non-identical machines have one or more nearly identical shaft modes. Analysis of shaft modal frequencies is simple and this situation should be easily recognizable should this design be considered by a utility.

Future work in optimal control and discrete-level GPC should focus on formulating the problem so as to minimize the discretization error for high-order systems. The Prony algorithm should be generalized to accommodate a feed-forward term, multiple eigenvalues, and a residue algorithm that can use data collected during the probing phase of the identification.

Finally, economic studies comparing the cost of dynamic braking to the cost of lost generation that may be avoided by the use of a braking resistor are needed. These studies should be completed before more detailed studies regarding the dynamics of the brake are pursued. Loss of generation due to stability problems resulting from the absence of a high-speed reclosing scheme is one form that may be avoided through the use of a dynamic brake. SSR relays are now commonplace in steam-turbine generation facilities. It may

be possible to reduce the sensitivity of these relays when a dynamic brake is in use. This would reduce the number of incidents of unnecessary trips at some facilities.

Along with showing the feasibility of dynamic braking, this dissertation gives enough background and analysis to obtain a good estimation of the cost of implementing dynamic braking at a generation facility. The cost of lost generation would have to be determined by the interested utility.

REFERENCES CITED

1. J. W. Butler and C. Concordia. "Analysis of Series Capacitor Application Problems." *AIEE Transactions*, 1937.

2. D. N. Walker, C. E. J. Bowler, R. L. Jackson and D. A. Hodges. "Results of Subsynchronous Resonance Test at Mohave." *IEEE Transactions on Power Apparatus and Systems*, Vol. PAS-94, No. 5, pp. 1878-1889, September/October 1975.

3. M. C. Hall and D. A. Hodges, "Experience with 500 KV Subsynchronous Resonance and Resulting Turbine Generator Shaft Damage at Mohave Generating Station," *IEEE PES Winter Meeting and Tesla Symposium*, 1976.

4. R. G. Farmer, A. L. Schwalb, and E. Katz. "Navajo Project Report on Subsynchronous Analysis and Solution." *IEEE Transactions on Power Apparatus and Systems*, Vol. PAS-96, pp. 1226-1231, 1977.

5. John S. Joyce, Tadeusz Kulig, and Dietrich Lambrecht, "Torsional Fatigue of Turbine-Generator Shafts Caused by Different Electrical System Faults and Switching Operations," *IEEE Transactions on Power Apparatus and Systems*, Vol. PAS-97, No. 5, pp. 1965-1973, Sept./Oct. 1978.

6. A. Abolins, D. Lambrecht, J. S. Joyce, and L. T. Rosenberg, "Effect of Clearing Short Circuits and Automatic Reclosing on Torsional Stress and Life Expenditure of Turbine-Generator Shafts," *IEEE Transactions on Power Apparatus and Systems*, Vol. PAS-95, No. 1, pp. 14-22, Jan./Feb. 1976.

7. M. C. Jackson, S. D. Umans, R. D. Dunlop, S. H. Horowitz, and A. C. Parikh. "Turbine-Generator Shaft Torques and Fatigue: Part I -- Simulation Methods and Fatigue Analysis," *IEEE Transactions on Power Apparatus and Systems*, Vol. PAS-98, No. 6, pp. 2299-2307, Nov./Dec. 1979.

8. Bibliography Task Force of the Subsynchronous Resonance Working Group of the Dynamic Systems Performance Subcommittee of the IEEE Power Systems Engineering Committee, "A Bibliography for the Study of Subsynchronous Resonance Between Rotating Machines and Power Systems," *IEEE Transactions on Power Apparatus and Systems*, Vol. PAS-95, No. 1, pp. 216-218, January/February 1976.

9. Bibliography Task Force of the Subsynchronous Resonance Working Group of the Dynamic Systems Performance Subcommittee of the IEEE Power Systems Engineering Committee, "First Supplement to A Bibliography for the Study of Subsynchronous Resonance Between Rotating Machines and Power Systems," *IEEE Transactions on Power Apparatus and Systems*, Vol. PAS-98, No. 6, pp. 1872-1875, November/December 1979.

10. Bibliography Task Force of the Subsynchronous Resonance Working Group of the Dynamic Systems Performance Subcommittee of the IEEE Power Systems Engineering Committee, "Second Supplement to A Bibliography for the Study of Subsynchronous Resonance Between Rotating Machines and Power Systems," *IEEE Transactions on Power Apparatus and Systems*, Vol. PAS-104, No. 2, pp. 321-327, February 1985.

11. Bibliography Task Force of the Subsynchronous Resonance Working Group of the Dynamic Systems Performance Subcommittee of the IEEE Power Systems Engineering Committee, "Third Supplement to A Bibliography for the Study of Subsynchronous Resonance Between Rotating Machines and Power Systems," *IEEE Transactions on Power Systems*, Vol. PWRS-6, No. 2, pp. 830-834, May 1991.

12. IEEE Subsynchronous Resonance Working Group of the System Dynamic Performance Subcommittee Power System Engineering Committee, "Terms, Definitions, and Symbols for Subsynchronous Oscillations," *IEEE Transactions on Power Apparatus and Systems*, Vol. PAS-104, No. 6, pp. 1326-1333, June 1985.

13. Colin E. J. Bowler, Understanding Subsynchronous Resonance, IEEE Power Engineering Society Winter Meeting and Tesla Symposium, IEEE Press, 1976.

14. Yao-Nan Yu, Electric Power System Dynamics, Academic Press, Orlando, FL, 1983.

15. R. M. Hamouda, M. R. Irvani, and R. Hackam, "Torsional Oscillations of Series Capacitor Compensated AC/DC Systems," *IEEE Transactions on Power Systems*, Vol. PWRS-4, No. 3, pp. 889-896, August 1989.

16. B. L. Agrawal, P. M. Anderson and J. E. VanNess, " Eigenvalue Analysis for SSR," IEEE Power Engineering Society Summer Meeting, Long Beach, CA, SSR Panel Session, July 9-14 1989.

17. A. H. M. A. Rahim and D. A. H. Alamgir, "A Closed-Loop Quasi-Optimal Dynamic Braking Resistor and Shunt Reactor Control Strategy for Transient Stability," *IEEE Transactions on Power Systems*, Vol. PWRS-3, No. 3, pp. 879-886, August 1988.

18. K. Nakamura and S. Muto, "Improvement of Power System Transient Stability by Optimum Bang-Bang Control of Series and Parallel Resistors," *Electrical Engineering in Japan*, Vol. 96, No. 2, pp. 47-54, 1976.

19. A. Sen and J. Meisel, "Transient Stability Augmentation with a Braking Resistor using Optimal Aiming Strategies," *Proceedings of the IEEE*, Vol. 125, No. 11, pp. 1249-1255, November 1978.

20. K. Yoshida, M. Fukunishi, and J. Aoi, "Development of System-Damping Resistors for Stabilizing Bulk Power Transmission," *Electrical Engineering in Japan*, Vol. 91, No. 3, pp. 79-90, 1971.

21. F. Ishiguro, S. Tanaka, M. Shimomura, T. Maeda, K. Matsushita and H. Sugimoto, "Coordinated Stabilizing Control of Exciter, Turbine and Braking Resistor," *IEEE Transactions on Power Systems*, Vol. PWRS-1, No. 3, pp. 7480, August 1986.

22. H. M. Ellis, J. E. Hardy, A. L. Blythe, and J. W. Skooglund, "Dynamic Stability of the Peace River Transmission System," *IEEE Transactions on Power Apparatus and Systems*, Vol. PAS-85, No. 6, pp. 586-600, June 1966.

23. M. L. Shelton, P. F. Winkelman, W. A. Mittelstadt and W. J. Bellerby, "Bonneville Power Administration 1400 MW Braking Resistor," *IEEE Transactions on Power Apparatus and Systems*, Vol. PAS-94, No. 3, pp. 602-611, March/April 1975.

24. Narain G. Hingorani, "A New Scheme for Subsynchronous Resonance Damping of Torsional Oscillations and Transient Torque - Part I," *IEEE Transactions on Power Apparatus and Systems*, Vol. PAS-100, No. 4, pp. 1852-1855, April 1981.

25. R. A. Hedin, K. B. Stump, and N. G. Hingorani, "A New Scheme for Subsynchronous Resonance Damping of Torsional Oscillations and Transient Torque - Part II, Performance," *IEEE Transactions on Power Apparatus and Systems*, Vol. PAS100, No. 4, pp. 1856-1863, April 1981.

26. A. M. El-Serafi and S. O. Fariad, "Effect of Field Discharge Resistors on Turbine-Generator Shaft Torsional Torques," IEEE Power Engineering Society 1989 Summer Meeting, Long Beach, CA, Paper No. 89 SM 754-3 EC, July 9-14, 1989.

27. O. Wasynczuk, "Damping Shaft Torsional Oscillations using a Dynamically Controlled Resistor Bank," *IEEE Transactions on Power Apparatus and Systems*, Vol. PAS-100, No. 7, pp. 3340-3349, July 1981.

28. O. Wasynczuk, "Damping Shaft Torsional Oscillations with Applications to High Speed Reclosure," *IEEE Transactions on Power Apparatus and Systems*, Vol. PAS-100, No. 3, pp. 1089-1095, March 1981.

29. IEEE Subsynchronous Resonance Working Group of the Dynamic Systems Performance Subcommittee of the IEEE Power Systems Engineering Committee, "Second Benchmark Model for Computer Simulation of Subsynchronous Resonance," *IEEE Transactions on Power Apparatus and Systems*, Vol. PAS-104, No. 5, pp. 1057-1066, May 1985.

30. IEEE Subsynchronous Resonance Working Group of the System Dynamic Performance Subcommittee Power System Engineering Committee, "First Benchmark Model for Computer Simulation of Subsynchronous Resonance," *IEEE Transactions on Power Apparatus and Systems*, Vol. PAS-96, No. 5, pp. 1565-1572, September/October 1977.

31. J. R. Marti, "Accurate Modeling of Frequency-Dependent Transmission Lines in Electromagnetic Transient Simulations," *IEEE Transactions on Power Apparatus and Systems*, Vol. PAS-101, No. 1, pp. 147-157, January 1982.

32. L. Dube and H. W. Dommel, "Simulation of Control Systems in an Electromagnetic Transients Program with TACS," *Proceedings of the 1977 Power Industry Computer Applications Conference (PICA-77)*, Toronto, Ont., Canada, IEEE Publication 77CH1131-2-PWR, pp. 266-271, 1977.

33. D. A. Pierre, Optimization Theory with Applications, Dover Publications, Inc., New York, 1986.

34. Hermann W. Dommel and W. Scott Meyer, "Computation of Electromagnetic Transients," *Proceedings of the IEEE*, Vol. 62, No. 7, pp. 983-993, July 1974.

35. Lee W. Johnson and R. Dean Riess, Numerical Analysis, Addison Wesley Publishing Co., Reading, Mass., 1982.

36. Roy M. Johnson, K. Marcotte, and Matt Donnelly, "A Feasibility Demonstration Experimental Facility Simulation of a PASC Consolidation/Inversion System for Faraday Connected MHD Generators," *Proceedings of the 28th Symposium on Engineering Aspects of Magnetohydrodynamics (SEAM)*, Chicago, IL, June 28-30, 1990.

37. Hermann W. Dommel, "Electromagnetic Transients Program Reference Manual (EMTP Theory Book)," Bonneville Power Administration, Portland, OR, Contract No. DE-AC79-81BP31364, August 1986.

38. B. L. Agrawal and R. G. Farmer, "Use of Frequency Scanning Techniques for Subsynchronous Resonance Analysis," *IEEE Transactions on Power Apparatus and Systems*, Vol. PAS-98, No. 2, pp. 341-349, March/April 1979.

39. C. Ray Wylie and Louis C. Barrett, Advanced Engineering Mathematics, McGraw-Hill Book Co., New York, 1982.

40. M. H. Banakar and B. T. Ooi, "Resonance in Long Distance Radial Transmission Lines with Static Var Compensation Part II -- Supersynchronous Limit," *IEEE Transactions on Power Apparatus and Systems*, Vol. PAS-103, No. 6, pp. 1233-1241, June 1984.

41. D. J. Trudnowski, "Decentralized Control Strategies for Damping Power-System Electromechanical Oscillations," Doctoral Dissertation in Electrical Engineering, Montana State University, Bozeman, MT, March 1991.

42. R. W. Hamming, Numerical Methods for Scientists and Engineers, Dover Publications, Inc., New York, 1973.

43. D. A. Pierre, D. J. Trudnowski, and J. F. Hauer, "Identifying Reduced Order Models for Large Nonlinear Systems with Arbitrary Initial Conditions and Multiple Outputs using Prony Signal Analysis," *Proceedings of the American Control Conference*, pp. 149-154, May 1990.

44. J. F. Hauer, C. J. Demeure, and L. L. Scharf, "Initial Results in Prony Analysis of Power System Response Signals," *IEEE Transactions on Power Systems*, Vol. PWRS-5, No. 1, pp. 80-89, February 1990.

45. J. R. Smith, "Experience with Spectral Estimation Techniques in Power Systems," IEEE Power Engineering Society 1991 Winter Meeting, New York, Presented at the IEEE Symposium on Inter-Area Oscillations, February 1991.

46. R. R. Hocking and R. N. Leslie, "Selection of the Best Subset in Regression Analysis," *Technometrics*, Vol. 9, No. 4, pp. 531-540, November 1967.

47. The MathWorks Inc., PRO-MATLAB User's Guide, The MathWorks Inc., South Natick, Mass., 1990.

48. D. W. Clarke, C. Mohtadi, and P. S. Tuffs, "Generalized Predictive Control - Part I. The Basic Algorithm, Part II. Extensions and Applications," *Automatica*, Vol. 23, No. 2, pp. 137-148, 1987.

49. Robert R. Bitmead, M. Gevers, and Vincent Wertz, Adaptive Optimal Control, Prentice-Hall, Englewood Cliffs, NJ, 1990.

50. K. Ogata, Discrete-Time Control Systems, Prentice-Hall, Englewood Cliffs, NJ, 1987.

51. Alan V. Oppenheim and Ronald W. Schafer, Digital Signal Processing, Prentice-Hall, Englewood Cliffs, NJ, 1975.

52. Richard H. Middleton and Graham C. Goodwin, Digital Control and Estimation, Prentice-Hall, Englewood Cliffs, NJ, 1990.

53. Peter Lancaster and Miron Tismenetsky, The Theory of Matrices, Academic Press, Orlando, FL, 1985.

54. R. D. Dunlop, S. H. Horowitz, A. C. Parikh, M. C. Jackson, and S. D. Umans, " Turbine-Generator Shaft Torques and Fatigue: Part II - Impact of System Disturbances and High Speed Reclosure," *IEEE Transactions on Power Apparatus and Systems*, Vol. PAS-98, No. 6, pp. 2308-2313, Nov./Dec. 1979.

55. C. Paul Dalpiaz, "Turbine-Generator Shaft Oscillation Monitoring with PC's," *IEEE Computer Applications in Power*, Vol. 2, No. 3, pp. 15-18, July 1989.

56. D. W. Olive, "New Techniques for the Calculation of Dynamic Stability," *IEEE Transactions on Power Apparatus and Systems*, Vol. PAS-85, No. 7, July 1966.

57. M. R. Iravani, "Torsional Oscillations of Unequally-Loaded Parallel Identical Turbine-Generators," *IEEE Transactions on Power Systems*, Vol. PWRS-4, No. 4, pp. 1514-1524, November 1989.

APPENDICES

APPENDIX A

IEEE SECOND SUBSYNCHRONOUS BENCHMARK DATA

This appendix contains the EMTP data file used to simulate the IEEE Second Subsynchronous Benchmark [29]. A dynamic brake is connected to the terminals of the generator to facilitate damping of shaft torsionals. The control subroutine described in Appendix C must be linked with the EMTP in order to provide control of the Type 60 sources and the TACS-controlled switches shown in this data file. More information on the control interface can be found in Chapter 2 and Appendix C. Figure 45 shows the benchmark in EMTP data format.

```
C ------------------------------------------------------------------------
C SubSynchronous Resonance Test Case as set up by Matt Donnelly Aug 1990
C This is a 4-mass SSR case
C The data comes from a case reported in the paper:
C
C IEEE Subsynchronous Resonance Task Force of the Dynamic System Performance
C Working Group, Power System Engineering Committee, "Second Benchmark Model
C for Computer Simulation of Subsynchronous Resonance," IEEE Transactions on
C Power Apparatus and Systems, Vol. PAS-104, May 1985.
C
C The SSR event is triggered by a fault (simulated by a breaker closing) and
C the subsequent opening of a breaker clearing the fault.
C This leads to an interaction between the resonant frequencies of the shaft
C and the subsynchronous resonant frequencies of the network which exist
C due to the presence of series capacitors.
C
C Turbine shaft damping factors or as specified in the paper under the
C heading "Torque Amplification Studies".
C
C A resistive dynamic brake is modeled to study damping of the torsinal
C modes.  The brake is switched by thyristors which are TACS controlled.
C
C The TACS thyristor control signals are meant to be controlled from an
C outside subroutine which is called from the EMTP module CSUPB.
C
C ------------------------------------------------------------------------
C
BEGIN NEW DATA CASE
C ........................  Miscelaneous data ..........................
C DeltaT<---TMax<---XOpt<---COpt<-Epsiln<-TolMat<-TStart
  .0001      2.0     60.     60.
C --IOut<--IPlot<-IDoubl<-KSSOut<-MaxOut<---IPun<-MemSav<---ICat<-NEnerg<-IPrSup
    1000       25       1       1       1       0                1
C --KChg<---Mult<---KChg<---Mult<---KChg<---Mult<---KChg<---Mult<---KChg<---Mult
C       5       5      20      20     100     100     500     500    2000    2000
C
C
```

Figure 45. EMTP Data File for IEEE Benchmark.

```
TACS HYBRID
C S_block
C Sources
C ------------------------------------
C The control subroutine calls for voltage at the generator terminals
C and generator velocity.  Voltages are picked up in array XTCS which
C carries TACS supplemental variables.  Generator velocity is picked up
C in array ETACS.  The following lines place the voltages into TACS
C supplemental variables.
C ------------------------------------
C 345678-1-2345678-2-2345678-3-2345678-4-2345678-5-2345678-6-2345678-7-2
90GENERA              60.0                                    -1.00    9999.
90GENERB              60.0                                    -1.00    9999.
90GENERC              60.0                                    -1.00    9999.
92GENVEL
C Supplemental Variables and Devices
98TEMPVA  = GENERA
98TEMPVB  = GENERB
98TEMPVC  = GENERC
98VSRCEA  = 0.0
C 98VSRCEA  = GENERA
C ------------------------------------
C The control subroutine passes back the values for the Type 60
C sources which are used in the brake legs.  These are passed back into
C array XTCS which contains TACS supplemental variables.  The following
C lines initialize the correct XTCS entries.
C ------------------------------------
98VSRCEB  = 0.0
98VSRCEC  = 0.0
98BRKOPN  = 0.0
C Outputs
33VSRCEA
C Initial Conditions
BLANK end of TACS
C
C ..........................  Circuit data  ..................................
C 3-phase coupled RL branch.
C Bus1->Bus2->Bus3->Bus4->><----R<----------L
51BUS_0ABUS_1A              3.50       75.00
52BUS_0BBUS_1B              3.50       75.00
53BUS_0CBUS_1C
51BUS_1ABUS_2A             46.50      525.00
52BUS_1BBUS_2B             16.75      184.75
53BUS_1CBUS_2C
51BUS_CABUS_2A             55.00      600.00
52BUS_CBBUS_2B             18.50      200.00
53BUS_CCBUS_2C
C Series RLC branch.
C Bus1->Bus2->Bus3->Bus4->><----R<----L<----C
  BUS_1ABUS_CA                        9091.
  BUS_1BBUS_CB                        9091.
  BUS_1CBUS_CC                        9091.
  GENERA_NGH_A              0.01                                          1
  GENERB_NGH_B              0.01
  GENERC_NGH_C              0.01
C
C Jumpers for thyristor connections
  _NGH_ATMP_A1              0.01
  TMP_A2BRAKEA_NGH_ATMP_A1
  _NGH_BTMP_B1_NGH_ATMP_A1
  TMP_B2BRAKEB_NGH_ATMP_A1
  _NGH_CTMP_C1_NGH_ATMP_A1
  TMP_C2BRAKEC_NGH_ATMP_A1
C
```

Figure 45. Continued.

```
C
C
C   ================ BEGIN DYNAMIC BRAKE  ========================
C 345678-1-2345678-2-2345678-3-2345678-4-2345678-5-2345678-6-2345678-7-2
C probing = 4 percent
C BRAKEAVSRCEA            20.000                                                1
C working = 16 percent is 5 ohms
C a disturbance caused by a 5 ohm brake is about 16% of the gen rated MVA
  BRAKEAVSRCEA             3.000                                                1
  BRAKEBVSRCEBBRAKEAVSRCEA
  BRAKECVSRCECBRAKEAVSRCEA
C
C
C Saturable transformer components.
C ----------->Bus3-><----><----I<--PhiBusSt><-Rmag<--------------------------->O
  TRANSFORMER                          TRAN A
C -------current<----------flux
           9999
C Bus1->Bus2-><----------><---Rk<---Lk<---Nk<---------------------------------->O
 1GENERAGENERC              0.001   0.1   22.
 2BUS_2A                     0.5  50.0 288.68
C <----------->Bus3-><---------------->BusSt>
  TRANSFORMER TRAN A                   TRAN B
C Bus1->Bus2->
 1GENERBGENERA
 2BUS_2B
C <----------->Bus3-><---------------->BusSt>
  TRANSFORMER TRAN A                   TRAN C
C Bus1->Bus2->
 1GENERCGENERB
 2BUS_2C
C
C Series RLC branch.
C Bus1->Bus2->Bus3->Bus4-><----R<----L<----C
BLANK End of circuit data
C
C ........................  Switch data  ....................................
C Bus-->Bus--><---Tclose<----Topen<-------Ie                                   O
  BUS_2A       .01661667 .09161667
  BUS_2B       .01661667 .09161667
  BUS_2C       .01661667 .09161667
  BUS_0AINFINA     -1.0   9999.                                                1
  BUS_0BINFINB     -1.0   9999.
  BUS_0CINFINC     -1.0   9999.
C  ======================== TACS CONTROLLED SWITCHES FOR BRAKE ===============
C     Type 11 Switches are TACS Controlled Switches.  These are SCR's.
C 345678-1-2345678-2-2345678-3-2345678-4-2345678-5-2345678-6-2345678-7-2
11TMP_A1BRAKEA                                                 BRKOPN          1
11TMP_A2_NGH_A                                                 BRKOPN
11TMP_B1BRAKEB                                                 BRKOPN
11TMP_B2_NGH_B                                                 BRKOPN
11TMP_C1BRAKEC                                                 BRKOPN
11TMP_C2_NGH_C                                                 BRKOPN
C
BLANK End of switch data
C
C ........................  Source data  ....................................
C Bus--><I<Amplitude<Frequency<--T0|Phi0<---0=Phi0         <----Tstart<----Tstop
14INFINA     389997.       60. -40.81293                        -1.
14INFINB     389997.       60.-160.81293                        -1.
14INFINC     389997.       60.  79.18707                        -1.
C
60VSRCEA 1                                                     -1.   9999.
60VSRCEB 1                                                     -1.   9999.
60VSRCEC 1                                                     -1.   9999.
C
```

Figure 45. Continued.

```
C
C
C Dynamic synchronous machine.
C Bus-->  <-----Volt<-----Freq<----Angle
59GENERA     17962.9       60.        0.0
C Bus-->  <-----Volt<--------><----Angle
  GENERB
  GENERC
C
C Machine parameter cards.
C -------><---EPSubA<---EPOmeg<---EPDgEl<--------><---NIOMax
TOLERANCES                                              20
C ---------------------><-----FM
PARAMETER FITTING             1.
C
C Electrical parameters of machine.
C <-<-<-NP<---SMOutP<---SMOutQ<-----RMVA<------RKV<---AGLine<-------S1<-------S2
 4 2 1   2        1.         1.      600.0       22.     -1800.      1907.      3050.
C Col: (1-2) NuMas, (3-4) KMac, (5-6) KExc.
C -------><------AD1<------AD2<------AQ1<------AQ2<-----AGLQ<------S1Q<------S2Q
                                                    -1.
C If S.M. is not saturable (AGLine >= 0), leave S1 - S2Q blank.
C
C Manufacturer supplied p.u. data.
C ------Ra<--------X1<-------Xd<--------Xq<------X'd<------X'q<------X"d<------X"q
     .0045        .14       1.65       1.59       .250       .460     .20000     .20000
C ----T'd0<-----T'q0<-----T"d0<-----T"q0<-------X0<-------Rn<-------Xn<-------Xc
       4.5        .55        .040        .09        .13
C
C Mass cards
C <------><----ExTrs<-----HIC0<------DSR<------DSM<------HSP<------DSD
 1                      .001383       34.4              4.39000
 2                      .176204     4383.2              97.9700
 3                .40   .310729     7729.6             50.12823
 4                .60   .049912     1241.6
C col: (1-2) ML
BLANK card teminates mass card.
C
C Machine output request.
C @@<-->---><---N1<---N2<---N3<---N4<---N5<---N6<---N7<---N8<---N9<--N10<--N11<--N12
  31
  41
C col: (3) Group, (4) All
BLANK card terminates output request.
C TACS input cards.
C ------------------------------------
C The following card enters the gen velocity into array ETACS to be picked up
C by the control subroutine.
C ------------------------------------
C Bus--><----><KI
74GENVEL        6
C col: (1-2) KK - either 71, 72 , 73 or 74
  FINISH
BLANK End of source data
C
C ..........................  Output Request ..................................
C Bus-->Bus-->Bus-->Bus-->Bus-->Bus-->Bus-->Bus-->Bus-->Bus-->Bus-->Bus-->Bus-->
  GENERA
BLANK End of output requests
C
C ..........................  Plot request  ...................................
C @@<--<-Ts<-Te<Ymi<YMaxBus-->Bus-->Bus-->Bus-->Header--------->Y axis--------->
C col: (3) Graph type, (4) Units on horizontal scale, (5-7) Units per inch,
BLANK End of Plot Request
BLANK End of All Cases
```

Figure 45. Continued.

APPENDIX B

SYSTEM DATA FOR MULTI-MACHINE SIMULATIONS

This appendix contains the EMTP data file used to simulate the multi-machine system described in Chapter 2. The EMTP node names correspond to the bus names in the one-line diagram of Figure 2. The brake is implemented at the terminals of the Colstrip #3 conglomerate machine. The generator velocity is transmitted to the array ETACS through the variable GENVEL. The EMTP must be linked with the control subroutine shown in Appendix C. This subroutine provides for the control of the Type 60 sources and TACS controlled switches shown in the data file. Figure 46 shows the data file for the multi-machine system.

```
C ------------------------------------------------------------------------------
C SubSynchronous Resonance Test Case adopted for EPRI RP2473-39 Oct 1989       |
C This is a 3 machine SSR case.                                                |
C The data comes from a Montana Power Company EMTP data file supplied          |
C by Ray Brush, Project Industry Advisor at MPC.                               |
C                                                                              |
C                                                                              |
C The SSR event is triggered by a fault (simulated by a breaker closing) and   |
C the subsequent opening of line clearing the fault.  The line is then         |
C reclosed into the original fault which extinuishes itself with not further   |
C circuit breaker operation.                                                   |
C This leads to an interaction between the resonant frequencies of the shaft   |
C and the subsynchronous resonant frequencies of the network which exist       |
C due to the presence of series capacitors.                                    |
C                                                                              |
C A resistive dynamic brake is modeled to study damping of the torsinal        |
C modes.  The brake is switched by thyristors which are TACS controlled.       |
C                                                                              |
C The TACS thyristor control signals are meant to be controlled from an        |
C outside subroutine which is called from the EMTP module CSUPB.               |
C                                                                              |
C ------------------------------------------------------------------------------
C
BEGIN NEW DATA CASE
 .000100    3.00     60.      60.
    1000      50       1        1       1       0              1
C
TACS HYBRID
C S_block
C Sources
C 345678-1-2345678-2-2345678-3-2345678-4-2345678-5-2345678-6-2345678-7-2

C -------------------------------------
C The control subroutine calls for voltage at the generator terminals
C and generator velocity.  Voltages are picked up in array XTCS which
C carries TACS supplemental variables.  Generator velocity is picked up
C in array ETACS.  The following lines place the voltages into TACS
C supplemental variables.
C -------------------------------------
90CS261A              60.0                                    -1.00    9999.
90CS261B              60.0                                    -1.00    9999.
90CS261C              60.0                                    -1.00    9999.
92GENVEL
C Supplemental Variables and Devices
98TEMPVA  = CS261A
98TEMPVB  = CS261B
98TEMPVC  = CS261C
98VSRCEA  = 0.0
C 98VSRCEA  = CS261A
C
```

Figure 46. EMTP Data File for Multi-Machine System.

```
C ---------------------------------------
C The control subroutine passes back the values for the Type 60
C sources which are used in the brake legs.  These are passed back into
C array XTCS which contains TACS supplemental variables.  The following
C lines initialize the correct XTCS entries.
C ---------------------------------------
98VSRCEB  = 0.0
98VSRCEC  = 0.0
98BRKOPN  = 0.0
C Outputs
33VSRCEA
C Initial Conditions
BLANK end of TACS
C        1         2         3         4         5         6         7         8
C 345678901234567890123456789012345678901234567890123456789012345678901234567890
C  ========================TRANSFORMER DATA=====================================
C        1         2         3         4         5         6         7         8
C ---------------------------------------
C This block contains transformer data.  A trasnformer is employed at the
C generator terminals and at every 230 kV to 500 kV interface bus.
C ---------------------------------------
C 345678901234567890123456789012345678901234567890123456789012345678901234567890
51CS500A                  .40196 136281.867
52CS230A                  .10039 59831.1654 .11677 26274.2463
53CS341ACS341B            -.0685 14801.5902 -.0398 6499.64371 .01729 1608.93290
51CS500B                  .40196 136281.867
52CS230B                  .10039 59831.1654 .11677 26274.2463
53CS341BCS341C            -.0685 14801.5902 -.0398 6499.64371 .01729 1608.93290
51CS500C                  .40196 136281.867
52CS230C                  .10039 59831.1654 .11677 26274.2463
53CS341CCS341A            -.0685 14801.5902 -.0398 6499.64371 .01729 1608.93290
51BV500A                  .30543 131311.152
52BV230A                  .06864 57649.8716 .08938 25316.0989
53BV341ABV341B            -.0502 14262.1651 -.0296 6262.72945 .01277 1550.237553
51BV500B                  .30543 131311.152
52BV230B                  .06864 57649.8716 .08938 25316.0989
53BV341BBV341C            -.0502 14262.1651 -.0296 6262.72945 .01277 1550.237553
51BV500C                  .30543 131311.152
52BV230C                  .06864 57649.8716 .08938 25316.0989
53BV341CBV341A            -.0502 14262.1651 -.0296 6262.72945 .01277 1550.237553
C XFRMR.DATA ==================================================================
51CS230A                  .03101 11398.5604
52CS221ACS221B            -.0049 1791.69765 .00077 281.771773
51CS230B                  .03101 11398.5604
52CS221BCS221C            -.0049 1791.69765 .00077 281.771773
51CS230C                  .03101 11398.5604
52CS221CCS221A            -.0049 1791.69765 .00077 281.771773
51CS230A                  .03101 11398.5604
52CS222ACS222B            -.0049 1791.69765 .00077 281.771773
51CS230B                  .03101 11398.5604
52CS222BCS222C            -.0049 1791.69765 .00077 281.771773
51CS230C                  .03101 11398.5604
52CS222CCS222A            -.0049 1791.69765 .00077 281.771773
51CS500A                  .08423 41874.9137
52CS261ACS261B            -.0071 3507.66603 .00059 293.943793
51CS500B                  .08423 41874.9137
52CS261BCS261C            -.0071 3507.66603 .00059 293.943793
51CS500C                  .08423 41874.9137
52CS261CCS261A            -.0071 3507.66603 .00059 293.943793
51GA500A                  .08399 46050.4691
52GA230A                  -.0368 20170.8879 .01613 8841.80996
51GA500B                  .08399 46050.4691
52GA230B                  -.0368 20170.8879 .01613 8841.80996
51GA500C                  .08399 46050.4691
52GA230C                  -.0368 20170.8879 .01613 8841.80996
51HS500A                  .08399 46050.4691
52HS230A                  -.0368 20170.8879 .01613 8841.80996
51HS500B                  .08399 46050.4691
52HS230B                  -.0368 20170.8879 .01613 8841.80996
51HS500C                  .08399 46050.4691
52HS230C                  -.0368 20170.8879 .01613 8841.80996
```

Figure 46. Continued.

```
C  ========================SERIES CAPACITOR DATA=============================
C       1         2         3         4         5         6         7         8
C 34567890123456789012345678901234567890123456789012345678901234567890123456789
C
   BCSW1ACB341A                        50916.                                  3
   BCSW1BCB341B                        50916.                                  3
   BCSW1CCB341C                        50916.                                  3
   BCSW2ACB342A                        50916.                                  3
   BCSW2BCB342B                        50916.                                  3
   BCSW2CCB342C                        50916.                                  3
   GBSW1ABG751A                        24887.                                  3
   GBSW1BBG751B                        24887.                                  3
   GBSW1CBG751C                        24887.                                  3
   GBSW2ABG752A                        24887.                                  3
   GBSW2BBG752B                        24887.                                  3
   GBSW2CBG752C                        24887.                                  3
   GTSW1AGT001A                        34680.                                  3
   GTSW1BGT001B                        34680.                                  3
   GTSW1CGT001C                        34680.                                  3
   GTSW2AGT002A                        34680.                                  3
   GTSW2BGT002B                        34680.                                  3
   GTSW2CGT002C                        34680.                                  3
C  ================================JUMPERS=====================================
C       1         2         3         4         5         6         7         8
C 34567890123456789012345678901234567890123456789012345678901234567890123456789
   CB001ACBFF1A                  0.01
C  CB001BCBFF1BCB001ACBFF1A
C  CB001CCBFF1CCB001ACBFF1A
C  CB002ACBFF2ACB001ACBFF1A
C  CB002BCBFF2BCB001ACBFF1A
C  CB002CCBFF2CCB001ACBFF1A
C  CB341ABCFF1ACB001ACBFF1A
C  CB341BBCFF1BCB001ACBFF1A
C  CB341CBCFF1CCB001ACBFF1A
C  CB342ABCFF2ACB001ACBFF1A
C  CB342BBCFF2BCB001ACBFF1A
C  CB342CBCFF2CCB001ACBFF1A
   BG001ABGFF1ACB001ACBFF1A
   BG001BBGFF1BCB001ACBFF1A
   BG001CBGFF1CCB001ACBFF1A
C  BG002ABGFF2ACB001ACBFF1A
C  BG002BBGFF2BCB001ACBFF1A
C  BG002CBGFF2CCB001ACBFF1A
C  BG751AGBFF1ACB001ACBFF1A
C  BG751BGBFF1BCB001ACBFF1A
C  BG751CGBFF1CCB001ACBFF1A
C  BG752AGBFF2ACB001ACBFF1A
C  BG752BGBFF2BCB001ACBFF1A
C  BG752CGBFF2CCB001ACBFF1A
C  GT001AGTFF1ACB001ACBFF1A
C  GT001BGTFF1BCB001ACBFF1A
C  GT001CGTFF1CCB001ACBFF1A
C  GT002AGTFF2ACB001ACBFF1A
C  GT002BGTFF2BCB001ACBFF1A
C  GT002CGTFF2CCB001ACBFF1A
C  GT391ATGFF1ACB001ACBFF1A
C  GT391BTGFF1BCB001ACBFF1A
C  GT391CTGFF1CCB001ACBFF1A
C  GT392ATGFF2ACB001ACBFF1A
C  GT392BTGFF2BCB001ACBFF1A
C  GT392CTGFF2CCB001ACBFF1A
```

Figure 46. Continued.

```
C INSERT JUMPERS HERE AS NEEDED=================================================
C    these jumpers are for the brake
  CS261A_NGH_A              0.01                                                 1
  CS261B_NGH_BCS261A_NGH_A
  CS261C_NGH_CCS261A_NGH_A
C Jumpers for thyristor connections
  _NGH_ATMP_A1              0.01
  TMP_A2BRAKEA_NGH_ATMP_A1
  _NGH_BTMP_B1_NGH_ATMP_A1
  TMP_B2BRAKEB_NGH_ATMP_A1
  _NGH_CTMP_C1_NGH_ATMP_A1
  TMP_C2BRAKEC_NGH_ATMP_A1

C   ================ BEGIN DYNAMIC BRAKE  ==========================
C 345678-1-2345678-2-2345678-3-2345678-4-2345678-5-2345678-6-2345678-7-2
C probing = 4 percent
  BRAKEAVSRCEA            10.000                                               1
C a disturbance caused by a 5 ohm brake is about 9% of the large gen MVA
C BRAKEAVSRCEA             5.000                                               1
C BRAKEAVSRCEA             3.500                                               1
C BRAKEAVSRCEA             1.700                                               1
C BRAKEAVSRCEA             0.850                                               1
C BRAKEAVSRCEA             0.425                                               1
C BRAKEAVSRCEA             0.212                                               1
  BRAKEBVSRCEBBRAKEAVSRCEA
  BRAKECVSRCECBRAKEAVSRCEA
C  ========================STRAY CAPACITANCE DATA=============================
C       1         2         3         4         5         6         7         8
C 34567890123456789012345678901234567890123456789012345678901234567890123456789
  CS221A                              37.699
  CS221B                              37.699
  CS221C                              37.699
  CS222A                              37.699
  CS222B                              37.699
  CS222C                              37.699
  CS341A                              37.699
  CS341B                              37.699
  CS341C                              37.699
  BV341A                              37.699
  BV341B                              37.699
  BV341C                              37.699
C       1         2         3         4         5         6         7         8
C 34567890123456789012345678901234567890123456789012345678901234567890123456789
C AUX-LOAD=================AUX-LOAD DATA============================
C AUX-LOAD CS1
  CS221A                  13.5535.8729
  CS221B                  13.5535.8729
  CS221C                  13.5535.8729
C AUX-LOAD CS2
  CS222A                  13.5535.8729
  CS222B                  13.5535.8729
  CS222C                  13.5535.8729
C AUX-LOAD CS3&4
  CS261A                  4.2118.94766
  CS261B                  4.2118.94766
  CS261C                  4.2118.94766
C
C   ==================END OF AUX-LOAD DATA=========================
```

Figure 46. Continued.

```
C     ==================BEGIN LINE DATA============================
C LINE-MODEL          FD-LINE
C ENGLISH
C   0    .5   1.217 4           .0355  -90.25    102.    102.
C   0    .5   1.217 4           .0355  -49.75    102.    102.
C   0    .5   1.217 4           .0355   53.00     97.     97.
C   0    .5   1.217 4           .0355   87.00     97.     97.
C   1    .5    .111 4          1.140   -92.00     58.     58.     18.             4
C   2    .5    .111 4          1.140   -70.00     88.     88.     18.             4
C   3    .5    .111 4          1.140   -48.00     58.     58.     18.             4
C   4    .5    .111 4          1.140    51.00     58.     58.     18.             4
C   5    .5    .111 4          1.140    70.00     86.     86.     18.             4
C   6    .5    .111 4          1.140    89.00     58.     58.     18.             4
C LINE LENGTH =  1.8363E+02  KM
C TRANSFORMATION MATRIX AT F =  6.0000E+01  HZ
C
-1CB001ACB341A                1.                    -2 6
      17      4.359066318965257238 46E+02
  2.338503266862541992D+02  4.607025887907407764D+03 -1.120704261724998764D+04
  7.576834382353307092D+03  2.371811402242927302D+00  1.626077136742044360D+03
  1.553934907365646995D+04  1.239955896651661647D+03  1.855115543686415003D+04
  1.303277879477250099D+04  6.041075105998212530D+04  3.565511897423155751D+05
  1.051367575432140584D+06  3.173782052948331169D+06  9.772944967024798039D+06
  1.788800464233595878D+07  9.697832386580994166D+07
  3.215552750799266935D-03  1.366422002065763447D+00  1.481937981804738791D+00
  1.502368897665527586D+00  1.739261577341605358D+00  1.813361892790934515D+01
  8.883134776932094567D+01  9.894953912820452757D+01  1.699077331332729806D+02
  3.231483173792362109D+02  2.360165964307623142D+03  1.401695415313843205D+04
  4.373782152485587267D+04  1.391197319580966760D+05  4.543061779895553482D+05
  1.720826673075218219D+06  9.501318499961066293D+06
      20      6.710203508862291394 60E-04
  2.011900277981229317D-05  5.251917054175893524D-04  6.143188938689774620D-04
  4.588898860084572031D-03  3.673213967943864382D-02  1.310920694691021342D-01
  5.079103839811955623D-01  2.273122721543585301D+00  2.322591614930783699D+00
  3.344846128277546848D+00  1.787365926589398724D+01  1.793874642721145953D+02
  4.565945987609417287D+02  9.838432007534183725D+02  2.605599258416033251D+03
  3.133956389415313197D+03  8.071949154778653065D+04  6.865223171533790417D+06
 -7.007366106724821962D+06  5.403756702878579199D+04
  1.985910919608001356D-02  1.579274337661374733D+00  1.854493286967705545D+00
  6.893476457704126426D+00  2.713384818840752821D+01  4.766789109899327759D+01
  8.554248425508355247D+01  1.059222595596668022D+02  1.791866081532796144D+02
  1.927858339948064241D+02  8.203738463800586800D+02  3.048684192543276993D+03
  5.355560189399535489D+03  6.919590712767171567D+03  1.067565497313505011D+04
  1.313151681067512368D+04  2.573539378358522890D+04  3.187140841388348736D+04
  3.190298029200530436D+04  4.320249960627566361D+04
-2CB001BCB341B                1.                    -2 6
      17      3.619127053714712971 55E+02
  2.179095507925209141D+02  1.917622208210564708D+03 -5.491042173376289242D+02
 -3.398942756219749484D+02  1.953576204285552720D+02  4.782172719259605298D+01
  4.311368937771456302D+02  3.746789506457803896D+02 -9.699771043113183566D+01
  1.169167130888102086D+02  2.289318258532243426D+02  4.178014062019370499D+03
  3.076163302584957250D+03  1.148294637484817904D+05  3.152667199158905656D+06
  7.731944862554415129D+06  4.253656963687165827D+07
  3.058240977417195513D-03  1.353025611085977992D+00  1.885315614318739091D+00
  1.985593179875473319D+00  2.087500541855408176D+00  2.965369900935183600D+00
  8.075819525738295424D+00  9.881227064003834215D+00  1.040632849003995930D+01
  1.742496285891184282D+01  2.914809137316892373D+01  4.919127056615716143D+02
  5.066481626583442832D+02  2.412061118132854244D+04  3.334005532842211396D+05
  1.672657578545732918D+06  9.311039332295559580D+06
      21      6.272202720071619677 64E-04
  2.428401412499489389D-05  1.215739715150534003D-03  1.248684470309135779D-03
  1.605775757898926574D-03  3.091474673101401256D-03  1.558653377089461774D-02
  2.575111574861040347D-02  8.306539628916730263D-02  9.918909329150904230D-01
  1.984514141022057226D-01  1.140396655863642383D+01  2.968556269168396042D+02
  1.756463180569881843D+03  7.914873814780635939D+03  5.261418445948879253D+04
  1.758079464863565772D+05  2.475768142174146175D+10 -4.961721168453832817D+10
  2.485929476269118595D+10 -3.129715794945099551D+05  3.100683656069762187D+05
  1.985702309233852454D-02  2.091957570410926837D+00  2.196592455357775531D+00
  2.812289257637698214D+00  5.412674814600893058D+00  5.539074440068783645D+01
  8.943993577573018605D+01  1.437732943629891551D+02  2.064826302775020501D+02
  2.115611873451258376D+02  1.220525766209303868D+03  1.187063330236078514D+04
  2.485146854825878563D+04  4.080934151466981621D+04  6.972219484653677682D+04
  1.022549043303515391D+05  1.749675104472769490D+05  1.751408335977126917D+05
  1.753143284423927362D+05  1.020979665995474104D+06  1.021991050405007307D+06
-3CB001CCB341C                1.                    -2 6
```

Figure 46. Continued.

```
     16      2.364667458333852678 72E+02
  2.027334571071493201D+02  8.188775839955864200D+02  2.339891066132751014D+02
 -4.261828212195938104D+01  3.737882708082099992D+01 -1.867793860247369014D+00
  3.987016512302339493D+02  2.942140682150029463D+02  1.476408928092131447D+03
 -1.118659993072341024D+03  9.648992611492295879D+01  1.382893775040682272D+02
  1.241039152699909014D+02  1.101964541538011328D+02  5.748316031904185479D+03
  6.372966149471395765D+05
  2.751287812218837048D-03  1.149531578482481858D+00  1.473823560810080535D+00
  1.762820485028454620D+00  2.200321601762747492D+00  2.667804972883472403D+00
  5.585368779717997167D+00  8.848647667537052675D+00  1.172149987881583177D+01
  1.191691385218775134D+01  1.635609444711203286D+01  2.735670121005287614D+01
  4.322607015176157486D+01  7.073677505506140584D+01  6.346552264856925603D+03
  7.053081233617870748D+05
     20      6.128433779420870643 11E-04
  3.080512402523813596D-05  1.187814274898724994D-03  1.319151786310325975D-03
  5.928215484760702525D-03  1.133716335016841915D-02  1.032822350520959300D-02
  7.651007103122165571D-03  5.007326771328374140D-02  1.637897730066717704D-01
  4.469076600420847356D+01  7.764151417225381735D+01  8.124332637937782380D+02
  6.270882413135950287D+03  8.136136516624922297D+04  3.143650743615337487D+05
  1.775833190748597437D+06  5.164538609007590055D+09 -5.215268340932500839D+09
  2.991171886495864809D+09 -2.942620920100842357D+09
  1.985375577827807984D-02  1.718237645576082051D+00  1.930397336473244574D+00
  4.321401186917370629D+00  8.271820713928397906D+00  1.514763302613922735D+01
  4.546088536397406177D+01  2.967974570692586909D+02  4.753434228112728022D+02
  4.064178391307669415D+03  1.394147069533916851D+04  3.598193110631682157D+04
  1.281839930469732426D+05  5.055833293516242120D+05  8.820378216485530429D+05
  1.671127411059296457D+06  3.177446977397485229D+06  3.180594562449460616D+06
  3.765736550438711012D+06  3.769466896266714612D+06
-4CB002ACB342A                1.                    -2 6
     14      2.382728735252447052 06E+02
  2.012029085139368760D+02  8.224126852081407293D+02  2.124265274271990016D+02
 -2.971838590731365581D+01  2.980361380791350445D+01  1.644562341240904058D+01
  2.868440713463574383D+02  3.522735794724300547D+03 -2.811397689378306382D+03
  1.096664729303038754D+02  1.412312295716831336D+02  1.276920309263619586D+02
  5.965165239448656962D+03  2.680277963981326553D+06
  2.760968718467001588D-03  1.148962038095385385D+00  1.465027927550343501D+00
  1.758765335951147174D+00  2.183241811585384495D+00  2.708251528617456105D+00
  5.027453672664701112D+00  1.040630265918836517D+01  1.057230684137963750D+01
  1.659022551673712886D+01  2.755372978813364426D+01  4.511224222335009149D+01
  3.340954803595282669D+03  1.506314582944249385D+06
     20      6.136399707237529644 42E-04
  3.046123937847916840D-05  1.130952220779668429D-03  1.150634353936737518D-03
  4.652944886837621138D-03  1.026912042971909133D-02  7.672462534509525843D-03
  4.877633796802588895D-03  1.030491957936744167D-02  4.160595796268227488D-02
  9.789017185654686592D+00  8.735861157293759227D+01  5.685083790639082650D+02
  1.248077575604981394D+04  2.352343064240948434D+04  1.659643641747026777D+05
  1.769984156268122344D+06  1.682064013554501645D+08 -1.718800117293104865D+08
  1.660712411310175173D+08 -1.643702492217016034D+08
  1.985392811538086964D-02  1.770113730243480871D+00  1.851751819557516970D+00
  3.702076801442149734D+00  8.156274882642042368D+00  1.221420412055928106D+01
  1.577318496620633881D+01  6.624188776830366088D+01  2.692780348685650083D+02
  1.935636807574446323D+03  8.458359826413313840D+03  2.634243609539448289D+04
  1.495164289074515218D+05  1.895701731498906083D+05  3.768020592728455304D+05
  7.089576085699869000D+05  1.023923031788554887D+06  1.024937331901871279D+06
  1.510901670224446512D+06  1.512398372308236489D+06
-5CB002BCB342B                1.                    -2 6
     14      2.268673966692551644 54E+02
  2.000998550656040926D+02  9.287237775891225766D+02  2.687548332637988535D+01
  2.909588034131549827D+01  2.459106692702308639D+01  1.869617504002738695D+01
  4.175369564657338373D+02  8.240861765980306899D+02 -2.059329414117720560D+02
  1.128799668081186720D+02  1.414391635949617303D+02  1.409902253086494142D+02
  1.461044607122781429D+03  6.265540827703812192D+04
  2.725846462765486010D-03  1.172909652828836080D+00  1.436074580027391467D+00
  1.770966350693486152D+00  2.195580893940022871D+00  2.742435856814943118D+00
  5.826964296030853641D+00  1.020082754588044494D+01  1.144508245895899323D+01
  1.707290117035850585D+01  2.918439403705802659D+01  5.012680599812697491D+01
  8.508105300887960425D+02  3.637251187057040534D+04
```

Figure 46. Continued.

```
      24      6.12584515416046012878E-04
   3.13834672503565557 55D-05  1.21847082030618022 2D-03  1.27599704034136641 1D-03
   4.39612525260541040 6D-03  1.10023229066858003 7D-02  4.27114958664099990 1D-03
   1.01927856415217417 6D-02  7.43664856543006206 0D-03  2.21286907332610933 7D+01
   4.92725278003988744 8D+01  5.82144472110559064 5D+02  3.64906258853903278 8D+03
   2.51140390197981605 5D+04  6.28408194342948845 6D+04  4.36552784222745012 8D+04
   1.71587346417111813 9D+05  3.30955080643293513 3D+05  2.18029695850018753 8D+05
   7.11981743014082312 6D+05 -1.07690768189049820 6D+05  4.36110204783720627 4D+08
  -4.38282530732259281 0D+08  4.97144499957101168 1D+07 -4.90028999298871271 3D+07
   1.98534659285649842 8D-02  1.84295511427760411 2D+00  1.96820131957430982 7D+00
   3.37079799757101683 5D+00  8.40114508067265486 3D+00  1.31830387539434577 0D+01
   1.57265786909957532 3D+01  2.31920591129607354 1D+01  2.12154416087697342 2D+03
   9.33062526793435199 6D+03  2.70092043993539341 5D+04  8.09252443415057841 8D+04
   2.36524522432559726 4D+05  4.49634059974043179 0D+05  5.55522181947270000 8D+05
   8.54202310688339610 4D+05  1.35392975188795483 0D+06  1.75023949370793072 7D+06
   3.08879720664807752 5D+06  4.22822739387311658 4D+06  7.09639304998658027 0D+06
   7.10342275051218108 3D+06  1.34862879509743675 6D+07  1.34996474936081487 7D+07
-6CB002CCB342C                  1.                    -2 6
      14      2.22691865734314387026E+02
   1.98526466062685226 9D+02  9.11187021129366485 2D+02  4.64826278994838002 5D+01
   1.95977809398916571 5D+01  3.23734737810623398 6D+01  1.03029410890314476 7D+00
   4.20739620295714871 6D+02  8.36974154726616546 9D+02 -2.13952711986191463 5D+02
   1.18851093433784326 3D+02  1.52695252038768043 0D+02  3.10604800180015232 1D+02
   3.30910168523839854 5D+03  2.41745456361416097 9D+05
   2.71525685176467852 2D-03  1.17338369252990337 7D+00  1.44419025582318447 1D+00
   1.77458436687779438 9D+00  2.21310541929287579 7D+00  2.70043416120835994 0D+00
   5.89428989925193047 6D+00  1.03831390092253605 9D+01  1.16344456844091646 0D+01
   1.77880257416185796 3D+01  3.09158097616041560 6D+01  9.85296571675728998 2D+01
   1.93481775856649289 8D+03  1.41608114719262706 8D+05
      23      6.12631723286972805107E-04
   3.15973956555636251 2D-05  1.76757443055642130 0D-03  4.75117807845350284 8D-04
   4.78852626753410509 3D-03  4.67637449810567602 4D-03  1.45874747427404366 6D-02
   8.48341028339455395 7D-03  4.81381869495992276 2D+00  6.09915382726655606 0D+01
   4.42493925232001025 4D+02  2.47049279562355548 0D+03  1.33631667350371221 8D+04
   2.28363075851000194 2D+04  3.84301669267115758 0D+04  7.97430814373094199 3D+04
   5.98912096798768427 1D+05 -3.03141870982989909 0D+05  5.41981661004542183 9D+05
   3.67775848105029999 7D+04  1.30831806163654644 0D+08 -1.31886257398069107 9D+08
   1.74032121609796056 9D+06 -1.71775100288579301 6D+06
   1.98533587216411454 8D-02  1.72970022429842310 0D+00  1.73164654825558281 3D+00
   3.70335806185395877 1D+00  7.22546812239271985 0D+00  1.12445727217408113 5D+01
   1.34033869365823206 1D+01  9.30875459321701583 8D+02  5.81450172454880578 2D+03
   2.03665124083728624 1D+04  5.38347560238010246 4D+04  1.30276253965548698 0D+05
   2.23784958972622098 4D+05  3.43933662816123956 9D+05  4.80135756078268888 8D+05
   9.05987644239858258 5D+05  9.84197938380368010 3D+05  1.94695453745972691 1D+06
   2.74516833127728448 0D+06  4.24208642128072341 4D+06  4.24628864020169724 2D+06
   5.28841054044476905 8D+07  5.29364925003905063 5D+07
C   Q MATRIX BY ROWS (IMAGINARY PART = 0)
  0.44364168 -0.54250481 -0.31965924  0.51440260 -0.40757985 -0.12395691
  0.00000000  0.00000000  0.00000000  0.00000000  0.00000000  0.00000000
  0.34003824 -0.32366413 -0.03778065  0.01099281  0.76017469  0.35250691
  0.00000000  0.00000000  0.00000000  0.00000000  0.00000000  0.00000000
  0.43251837 -0.29410167  0.54988139 -0.53854693 -0.24036744 -0.19732722
  0.00000000  0.00000000  0.00000000  0.00000000  0.00000000  0.00000000
  0.42289065  0.29655495 -0.64921677 -0.43042328  0.07468529 -0.31444056
  0.00000000  0.00000000  0.00000000  0.00000000  0.00000000  0.00000000
  0.34832059  0.35902679  0.05622246 -0.00653088 -0.36512374  0.75456892
  0.00000000  0.00000000  0.00000000  0.00000000  0.00000000  0.00000000
  0.43388185  0.51378486  0.40262051  0.48850481  0.21781819 -0.36967658
  0.00000000  0.00000000  0.00000000  0.00000000  0.00000000  0.00000000

C LINE-MODEL          FD-LINE
C ENGLISH
C   0    .5    1.217 4           .0355  -90.25     102.     102.
C   0    .5    1.217 4           .0355  -49.75     102.     102.
C   0    .5    1.217 4           .0355   53.00      97.      97.
C   0    .5    1.217 4           .0355   87.00      97.      97.
C   1    .5     .111 4          1.140  -92.00      58.      58.      18.              4
C   2    .5     .111 4          1.140  -70.00      88.      88.      18.              4
C   3    .5     .111 4          1.140  -48.00      58.      58.      18.              4
C   4    .5     .111 4          1.140   51.00      58.      58.      18.              4
C   5    .5     .111 4          1.140   70.00      86.      86.      18.              4
C   6    .5     .111 4          1.140   89.00      58.      58.      18.              4
C LINE LENGTH =  2.1469E+02  KM
```

Figure 46. Continued.

```
C TRANSFORMATION MATRIX AT F =  6.0000E+01  HZ
C
-1BG001ATN151A                    1.                    -2 6
      17      4.35906631896525723846E+02
  2.3385032668625419 92D+02  4.6070258879074077 64D+03 -1.1207042617249987 64D+04
  7.5768343823533070 92D+03  2.3718114022429273 02D+00  1.6260771367420443 60D+03
  1.5539349073656469 95D+04  1.2399558966516616 47D+03  1.8551155436864150 03D+04
  1.3032778794772500 99D+04  6.0410751059982125 30D+04  3.5655118974231557 51D+05
  1.0513675754321405 84D+06  3.1737820529483311 69D+06  9.7729449670247980 39D+06
  1.7888004642335958 78D+07  9.6978323865809941 66D+07
  3.2155527507992669 35D-03  1.3664220020657634 47D+00  1.4819379818047387 91D+00
  1.5023688976655275 86D+00  1.7392615773416053 58D+00  1.8133618927909345 15D+01
  8.8831347769320945 67D+01  9.8949539128204527 57D+01  1.6990773313327298 06D+02
  3.2314831737923621 09D+02  2.3601659643076231 42D+03  1.4016954153138432 05D+04
  4.3737821524855872 67D+04  1.3911973195809667 60D+05  4.5430617798955534 82D+05
  1.7208266730752182 19D+06  9.5013184999610662 93D+06
      19      7.89369387577934085941E-04
  2.3518019213336261 60D-05  4.5014320384263909 43D-04  6.2561140528187573 81D-04
  2.4276499847747295 75D-03  2.2241491970944394 28D-02  1.0105142605248593 20D-01
  3.7851831441905102 46D-01  1.9838452732113971 70D+00  1.3844763972659118 73D+00
  7.6668803243661332 04D+00  6.7433841284545231 08D+01  2.9437934829382889 75D+02
  7.8700134111383280 300D+02  1.6660201840622355 86D+03  2.7148471904449880 87D+03
  6.3068328695473152 95D+04  5.5789941680991228 20D+06 -5.6752563628556514 16D+06
  2.7652643615682683 50D+04
  1.9857406812056140 40D-02  1.4475399923159784 63D+00  2.0140171045963504 16D+00
  3.9042266838456544 11D+00  1.7670014569153567 50D+01  3.9321803924929162 65D+01
  7.0198259517781304 24D+01  9.6255571501958774 76D+01  1.3792086427709611 13D+02
  2.0606457103881388 09D+02  1.5018199836513458 65D+03  4.0501754521541824 94D+03
  5.5986489657543899 06D+03  8.3821750509455264 36D+03  1.0680325562977463 51D+04
  2.1126784099922143 92D+04  2.6019897560497282 03D+04  2.6045672920778013 12D+04
  3.9066992458949052 89D+04
-2BG001BTN151B                    1.                    -2 6
      17      3.61912705371471297155E+02
  2.1790955079252091 41D+02  1.9176222082105647 08D+03 -5.4910421733762892 42D+02
 -3.3989427562197494 84D+02  1.9535762042855527 20D+02  4.7821727192596052 98D+01
  4.3113689377714563 02D+02  3.7467895064578038 96D+02 -9.6997710431131835 66D+01
  1.1691671308881020 86D+02  2.2893182585322434 26D+02  4.1780140620193704 99D+03
  3.0761633025849572 50D+03  1.1482946374848179 04D+05  3.1526671991589056 56D+06
  7.7319448625544151 29D+06  4.2536569636871658 27D+07
  3.0582409774171955 13D-03  1.3530256110859779 92D+00  1.8853156143187390 91D+00
  1.9855931798754733 19D+00  2.0875005418554081 76D+00  2.9653699009351836 00D+00
  8.0758195257382954 24D+00  9.8812270640038342 15D+00  1.0406328490039959 30D+01
  1.7424962858911842 82D+01  2.9148091373168923 73D+01  4.9191270566157161 43D+02
  5.0664816265834428 32D+02  2.4120611181328542 44D+04  3.3340055328422113 96D+05
  1.6726575785457329 18D+06  9.3110393322955595 80D+06
      21      7.35013517912762580917E-04
  2.8385672461362782 86D-05  1.2166788101728208 75D-03  1.5738938336146373 98D-03
  1.9186562235526623 86D-03  3.9006579009019129 40D-03  1.8223214038815544 69D-02
  3.0119602224094879 03D-02  9.7326512019320639 28D-02  1.0676750774168987 93D+00
  3.7686627311905231 82D-01  1.3335030358838543 93D+01  3.3814671036411205 31D+02
  2.4813704312164915 68D+03  1.1476850054708915 88D+04  6.6015376884870998 77D+04
  1.6008004019907559 27D+05  1.3905174041225450 99D+10 -2.7916417154582228 18D+10
  1.4011003315723285 91D+10 -7.5843892578141310 88D+04  7.5234807954213361 88D+04
  1.9854968074883896 14D-02  1.8087237069752704 07D+00  2.3471010161583228 95D+00
  2.8733930803199939 64D+00  5.8441883130088346 79D+00  5.5389427491725786 72D+01
  8.9437766328509418 66D+01  1.4376635911776740 43D+02  1.9863150552785525 70D+02
  2.8209373680822839 25D+02  1.2195777893628819 87D+03  1.1405972795669423 25D+04
  2.6242322906870612 77D+04  4.2143120397908972 34D+04  6.7552058366382239 91D+04
  9.5988503318474418 85D+04  1.6014134481222553 22D+05  1.6029998113463142 73D+05
  1.6045877460248169 52D+05  1.7370553198720102 96D+06  1.7387760501936100 48D+06
-3BG001CTN151C                    1.                    -2 6
      16      2.36466745833385267872E+02
  2.0273345710714932 01D+02  8.1887758399558642 00D+02  2.3398910661327510 14D+02
 -4.2618282121959381 04D+01  3.7378827080820999 92D+01 -1.8677938602473690 14D+00
  3.9870165123023394 93D+02  2.9421406821500294 63D+02  1.4764089280921314 47D+03
 -1.1186599930723410 24D+03  9.6489926114922958 79D+01  1.3828937750406822 72D+02
  1.2410391526999090 14D+02  1.1019645415380113 28D+02  5.7483160319041854 79D+03
  6.3729661494713957 65D+05
  2.7512878122188370 48D-03  1.1495315784824818 58D+00  1.4738235608100805 35D+00
  1.7628204850284546 20D+00  2.2003216017627474 92D+00  2.6678049728834724 03D+00
  5.5853687797179971 67D+00  8.8486476675370526 75D+00  1.1721499878815831 77D+01
  1.1916913852187751 34D+01  1.6356094447112032 86D+01  2.7356701210052876 14D+01
  4.3226070151761574 86D+01  7.0736775055061405 84D+01  6.3465522648569256 03D+03
  7.0530812336178707 48D+05
```

Figure 46. Continued.

```
      16      7.165563657492282959 55E-04
  3.600626236887048324D-05  2.126810610944591278D-03  5.530886125329801599D-03
  8.093652849739074034D-03  9.371560477745685593D-03  6.496196967750670570D+00
  2.283577877140079408D+02  3.620175170437186907D+02  4.487117900469629490D+03
  3.612706575490800969D+04  3.178730512568672202D+05  2.316379135212652443D+06
  2.724707146389467835D+09 -2.750842222224150717D+09  1.611546844769302368D+09
 -1.588087232201403707D+09
  1.985114854356833823D-02  1.618314093609028920D+00  4.196835461633274478D+00
  6.159694092226879469D+00  7.254154077105924081D+00  1.239858763305356604D+03
  1.080854065239597844D+04  3.347858264822641559D+04  9.679533829627119303D+04
  3.094504321569743843D+05  7.967793675458243524D+05  1.535311772793581418D+06
  2.607347086712459219D+06  2.609929929722531931D+06  3.182820925602462084D+06
  3.185973834097805666D+06
-4BG002ATN152A                1.                    -2 6
      14      2.382728735252447052 06E+02
  2.012029085139368760D+02  8.224126852081407293D+02  2.124265274271990016D+02
 -2.971838590731365581D+01  2.980361380791350445D+01  1.644562341240904058D+01
  2.868440713463574383D+02  3.522735794724300547D+03 -2.811397689378306382D+03
  1.096664729303038754D+02  1.412312295716831336D+02  1.276920309263619586D+02
  5.965165239448656962D+03  2.680277963981326553D+06
  2.760968718467001588D-03  1.148962038095385385D+00  1.465027927550343501D+00
  1.758765335951147174D+00  2.183241811585384495D+00  2.708251528617456105D+00
  5.027453672664701112D+00  1.040630265918836517D+01  1.057230684137963750D+01
  1.659022551673712886D+01  2.755372978813364426D+01  4.511224222335009149D+01
  3.340954803595282669D+03  1.506314582944249385D+06
      19      7.176157843102952372 48E-04
  3.560441461646778799D-05  2.006371792020794664D-03  3.400297068322265530D-03
  8.605635024716794300D-03  9.011783948007955330D-03  6.301616075797549237D-03
  4.523605883732900474D-02  1.236869735405286302D+00  8.195701356099135859D+00
  3.904939859814423286D+01  4.118653731843671792D+02  3.716713233711550572D+03
  2.515132978148222628D+04  1.860479531048385215D+05  1.250779542345901689D+06
  1.250482821617042776D+08 -1.271758170235558897D+08  6.931534074409944564D+07
 -6.865396184265389852D+07
  1.985135000515751789D-02  1.693775018558264567D+00  2.880980948905442207D+00
  7.192428250100501685D+00  7.764901229321995446D+00  1.082373111031509061D+01
  7.818297217246722930D+01  1.049119371776877529D+03  3.284401744382081176D+03
  4.130343553490189038D+03  2.037523235604570709D+04  7.459567566694840025D+04
  1.763499453585742194D+05  3.519625502376136137D+05  5.878903619093909365D+05
  8.401441976089045784D+05  8.409764460576461133D+05  1.479790996965424740D+06
  1.481256880756792089D+06
-5BG002BTN152B                1.                    -2 6
      14      2.268673966692551644 54E+02
  2.000998550656040926D+02  9.287237775891225766D+02  2.687548332637988535D+01
  2.909588034131549827D+01  2.459106692702308639D+01  1.869617504002738695D+01
  4.175369564657338373D+02  8.240861765980306899D+02 -2.059329414117720560D+02
  1.128799668081186720D+02  1.414391635949617303D+02  1.409902253086494142D+02
  1.461044607122781429D+03  6.265540827703812192D+04
  2.725846462765486010D-03  1.172909652828836080D+00  1.436074580027391467D+00
  1.770966350693486152D+00  2.195580893940022871D+00  2.742435856814943118D+00
  5.826964296030853641D+00  1.020082754588044494D+01  1.144508245895899323D+01
  1.707290117035850585D+01  2.918439403705802659D+01  5.012680599812697491D+01
  8.508105300887960425D+02  3.637251187057040534D+04
      24      7.162261464101256645 86E-04
  3.668210303443587347D-05  2.142199045915825191D-03  4.882162107648864327D-03
  8.603219696419861506D-03  9.454993576091990379D-03  2.570312526798858466D+00
  4.748376894205520760D+01  4.366836906171794226D+02  1.348957000671694431D+03
  2.049675185444157023D+03  8.457698763291426530D+03  1.338978453369773501D+04
  4.817743271471302069D+04  5.670602631231045234D+04  1.272160878161802611D+05
  3.243790990070531188D+05  3.845687328637833925D+05 -1.115004222965506269D+05
  1.160905306246272828D+08 -1.156782544014404770D+08  3.733475372837983519D+08
 -3.758415495743961111D+08  8.030245902909705788D+07 -7.907600279647796601D+07
  1.985080971073484475D-02  1.610905209536139221D+00  3.670993554972808215D+00
  6.450224272571836504D+00  7.241980419208585928D+00  4.862055882523386430D+02
  4.464182829413816194D+03  2.008174649878132323D+04  5.772720421515192265D+04
  8.711020857833591435D+04  1.593403746124463796D+05  2.409690391360748436D+05
  3.737930619195899271D+05  5.082052913700518839D+05  7.041507176436980808D+05
  1.174867413849422359D+06  1.586806187791461009D+06  2.117108132182733505D+06
  4.026823453164174862D+06  4.030812432177289389D+06  5.800126742095700349D+06
  5.805872358737881295D+06  8.831932526581201702D+06  8.840681455831153318D+06
-6BG002CTN152C                1.                    -2 6
```

Figure 46. Continued.

```
      14      2.22691865734314387026E+02
  1.98526466060626852269D+02  9.11187021129366485 2D+02  4.64826278994838002 5D+01
  1.95977809398916571 5D+01  3.23734737810623398 6D+01  1.03029410890314476 7D+00
  4.20739620295714871 6D+02  8.36974154726616546 9D+02 -2.13952711986191463 5D+02
  1.18851093433784326 3D+02  1.52695252038768043 0D+02  3.10604800180015232 1D+02
  3.30910168523839854 5D+03  2.41745456361416097 9D+05
  2.71525685176467852 2D-03  1.17338369252990337 7D+00  1.44419025582318447 1D+00
  1.77458436687779438 9D+00  2.21310541929287579 7D+00  2.70043416120835994 0D+00
  5.89428989925193047 6D+00  1.03831390092253605 9D+01  1.16344456844091646 0D+01
  1.77880257416185796 3D+01  3.09158097616041560 6D+01  9.85296571675728998 2D+01
  1.93481775856649289 8D+03  1.41608114719262706 8D+05
      25      7.16277452086275655155E-04
  3.69319936443325976 7D-05  2.55517667251471740 3D-03  4.19106757057084841 5D-03
  6.88336786060835860 2D-03  1.12593241270413622 6D-02  2.23855478250039469 1D+00
  4.61451044520449853 4D+01  3.61568203233922894 0D+02  8.61827484998041796 9D+02
  1.79192283336377067 8D+03  3.84203759508070311 3D+03  8.07594832191398177 2D+03
  1.97951700065357367 7D+04  4.99668396928047841 4D+04  1.75445334769811124 7D+04
  8.49872402704182732 1D+04  2.87184968247993281 7D+05 -1.61603719877848208 9D+05
  1.24884444183705221 8D+05  5.34444067388858748 0D+05 -2.51543939004262891 1D+05
  2.12776581972801577 3D+08 -2.13940956151403233 4D+08  3.05948490453865723 7D+07
 -3.01511161841932414 1D+07
  1.98506843866006793 7D-02  1.93504112874046890 8D+00  3.18418332424726502 3D+00
  5.24940261589534196 1D+00  8.61428698326019826 0D+00  4.26799169301957064 7D+02
  4.33556476045830129 4D+03  1.63820362084767532 5D+04  3.73408754748476330 9D+04
  6.48508473567693254 2D+04  8.29453313532508509 5D+04  1.38225003458487648 5D+05
  1.92244929691206569 3D+05  3.12322077394449978 0D+05  3.59206822473715314 0D+05
  5.34405976657908933 7D+05  6.81995970967564091 6D+05  7.32722336631283367 8D+05
  1.10315391498667968 0D+06  1.64447379206810536 6D+06  2.12750925043791241 5D+06
  3.55929127927577804 1D+06  3.56281712002338678 6D+06  6.25299704813293030 0D+06
  6.25919127896628680 2D+06
C   Q MATRIX BY ROWS (IMAGINARY PART = 0)
  0.44364168 -0.54250481 -0.31965924  0.51440260 -0.40757985 -0.12395691
  0.00000000  0.00000000  0.00000000  0.00000000  0.00000000  0.00000000
  0.34003824 -0.32366413 -0.03778065  0.01099281  0.76017469  0.35250691
  0.00000000  0.00000000  0.00000000  0.00000000  0.00000000  0.00000000
  0.43251837 -0.29410167  0.54988139 -0.53854693 -0.24036744 -0.19732722
  0.00000000  0.00000000  0.00000000  0.00000000  0.00000000  0.00000000
  0.42289065  0.29655495 -0.64921677 -0.43042328  0.07468529 -0.31444056
  0.00000000  0.00000000  0.00000000  0.00000000  0.00000000  0.00000000
  0.34832059  0.35902679  0.05622246 -0.00653088 -0.36512374  0.75456892
  0.00000000  0.00000000  0.00000000  0.00000000  0.00000000  0.00000000
  0.43388185  0.51378486  0.40262051  0.48850481  0.21781819 -0.36967658
  0.00000000  0.00000000  0.00000000  0.00000000  0.00000000  0.00000000

C LINE-MODEL          FD-LINE
C ENGLISH
C   0    .5    2.400 4           .0250    -7.00   140.25   140.25
C   0    .5    2.400 4           .0250     7.00   140.25   140.25
C   1    .5   .04967 4           1.603   -15.00    52.25    52.25      18.              3
C   2    .5   .04967 4           1.603   -25.00    83.25    83.25      18.              3
C   3    .5   .04967 4           1.603   -15.00   114.25   114.25      18.              3
C   4    .5   .04967 4           1.603    15.00    52.25    52.25      18.              3
C   5    .5   .04967 4           1.603    25.00    83.25    83.25      18.              3
C   6    .5   .04967 4           1.603    15.00   114.25   114.25      18.              3
C LINE LENGTH =  1.6270E+02  KM
C TRANSFORMATION MATRIX AT F =  6.0000E+01  HZ
C
-1TN151ABG751A                1.                    -2 6
      17      6.22346036394520879753E+02
  1.99855129225614511 8D+02  1.57134677022961514 6D+03 -1.70870154479912972 1D+03
  7.96027328843028243 5D+02  5.71642801025934970 1D+01  1.75418004250790636 4D+03
  9.01225687743302069 1D+03  4.36585853932664371 D+04  1.80188750474649073 1D+04
  5.98399460677932875 1D+04  2.22821905947156828 5D+05  4.07132065794561232 9D+05
  3.19414371040473162 4D+06  6.11581861772686836 8D+06  1.14285444448723204 0D+07
  3.15944266314474451 4D+07  1.95827717261948503 6D+08
  3.64253839697159276 5D-03  1.24516650162617206 8D+00  1.33402952950784359 2D+00
  1.35452631767229847 4D+00  1.88072793634330126 5D+00  2.08500592097440784 5D+01
  1.05041211961673212 7D+02  2.76389908105326348 7D+02  4.07521618261106603 1D+02
  1.06916256056727690 3D+03  7.70332023198599552 0D+03  1.52304870241528062 7D+04
  6.16461618385635856 6D+04  2.45298761879355861 3D+05  4.94641580555115127 9D+05
  1.41057088807729628 8D+06  8.94181052729782369 0D+06
```

Figure 46. Continued.

```
      20      6.0853786479810319611 8E-04
  1.049726308933693033D-05  3.246715218532977664D-04  5.293898010052091110D-04
  2.572672642788628229D-03  1.112330355269013039D-02  5.751698996574868862D-02
  2.332271855995639263D-01  8.582180038231629060D-01  4.641496548239720132D+00
  2.919793433104464708D+00  1.852538714357278016D+01  8.564579368954899508D+01
  3.426504835149501531D+02  8.576410845344026370D+02  1.462553011592528435D+03
  3.512440463148572007D+03  2.685064160435767508D+04  1.537983073130476335D+07
 -1.544959863664037012D+07  3.662908269493468288D+04
  1.986392573563205196D-02  2.052429058457878375D+00  3.346209272163513770D+00
  8.112551884066862229D+00  1.747569183878789767D+01  4.462227980411529948D+01
  8.853444951737301594D+01  1.550375375137585046D+02  2.164666078978139687D+02
  2.893223658233031088D+02  4.707022729734484301D+02  1.880244041083157981D+03
  4.680996184303707878D+03  6.381616473833702798D+03  9.237414649422191360D+03
  1.271692109814614628D+04  2.315540894972390788D+04  3.235257776419865422D+04
  3.238462628959902349D+04  4.854947471768705691D+04
-2TN151BBG751B                1.                    -2 6
      12      3.1297774412143564859 4E+02
  1.653268819615301375D+02  1.006149278061805816D+03  4.296003175421227294D+01
  2.449905265356602335D+02 -4.019954496863743927D+02  1.303875441368934379D+00
  1.189956792050327348D+02  8.825288927025238053D+02 -5.485074294833235484D+02
  2.143312612183241413D+03  2.453301326694599265D+04  6.370937884452725644D+06
  2.924452766520347377D-03  1.254306104345097150D+00  1.770473727482938187D+00
  2.115282168323128320D+00  2.134285725776589315D+00  2.562069147085389131D+00
  4.334934003769711053D+00  1.097352735181817063D+01  1.110907234614896377D+01
  3.125395297778056118D+02  7.176968452045063032D+03  1.879980274339852389D+06
      21      5.4475704899506344745 3E-04
  1.800261744011191716D-05  4.795714178837854905D-04  1.374044058423752455D-03
  9.456893491125060530D-04  1.346794611970190026D-03  1.863890695344662564D-03
  2.289390105358818719D-02  1.196921739279616977D-01  3.495900123971575624D-01
  1.712768012657519934D+00  8.529956854224216706D-01  3.218865357717073161D+00
  9.948736496957322295D+01  4.292377971814960702D+02  4.119395636245416313D+03
  2.124130421746338698D+04  3.816090208653164427D+04  3.194188566145100049D+05
  1.138617374112553418D+09 -1.148933306117312789D+09  9.932456538208378246D+06
  1.986016895546076962D-02  1.611998573152559566D+00  2.313559726178101572D+00
  3.190971201274661717D+00  4.549361472323718569D+00  1.282073426629702229D+01
  1.566424895883776784D+02  1.988579896509128631D+02  2.941160571611377819D+02
  7.046665869155578719D+02  7.466085788618416359D+02  1.357992739284225308D+03
  9.821870395273039549D+03  2.050039361592455998D+04  7.055809205259632108D+04
  1.274585541961093677D+05  1.721496045776232459D+05  3.603116730055085573D+05
  7.093530847702630126D+05  7.100557712925174710D+05  7.904782447363616520D+05
-3TN151CBG751C                1.                    -2 6
      12      2.7324304276277306513 5E+02
  1.561748364951333023D+02  8.025073458911930175D+03 -1.218803945122922642D+04
  4.954737226896735365D+03  2.112491767424330247D+01  1.977312938812674830D+02
  2.858446661588330500D+02 -2.900494459181575602D+01  7.618760366377432369D+01
  7.783872568416446747D+01  8.417318183784606299D+04  6.019338145536675234D+06
  2.858341495169046203D-03  1.545573584591995786D+00  1.647513935051179074D+00
  1.713622406060108905D+00  2.626969405164170324D+00  5.297031594685054023D+00
  1.003264570504244713D+01  1.070182651418540698D+01  1.783766831197359082D+01
  3.104375830413941584D+01  5.495861134116000721D+04  3.946176189740385278D+06
      23      5.4398866709726186713 9E-04
  1.897810022478309382D-05  1.067007004662705468D-03  1.560621043463281522D-03
  1.363949557552913522D-03  2.146181072115603029D-03  7.228640952632055911D-04
  6.351961005954498521D-04  9.167329438232446745D-03  6.518622715777153825D-02
  3.190268489037920152D-01  1.240247168191010274D+00  1.606988326673156942D+00
  9.188970496906596175D+00  9.881508796223038571D+00  1.958875056980897540D+02
  8.150646804373583620D+02  6.517854458996745393D+03  6.535409416026362760D+04
  3.494150753234249169D+04  7.322713687570751499D+05  6.420503895895764232D+08
 -6.449485288572827876D+08  2.058021172000622610D+06
  1.985968053392854005D-02  1.790017210279721993D+00  2.625552055837476362D+00
  4.548845881516825895D+00  7.271385319282651971D+00  9.787134683503283084D+00
  1.758723405790738781D+01  2.548377638978908415D+02  4.438085065537282929D+02
  1.016930341581537192D+03  1.054354569063928295D+03  1.334731608302741535D+03
  3.728518891663099510D+03  4.200727377811051838D+03  1.903283291764120349D+04
  3.804078789606581358D+04  1.135837708798764870D+05  2.396219483364610060D+05
  2.741276553441619544D+05  6.191593533967411349D+05  1.073687464489984850D+06
  1.074751061345498689D+06  1.447044867750565463D+06
-4TN152ABG752A                1.                    -2 6
```

Figure 46. Continued.

```
     13      2.20177781503156975162E+02
  1.53342994949195674169D+02  1.02326066262942616 4D+03  1.70151190216473018 8D+02
 -1.13374248063053934 7D+03  6.93064463037600461 3D+02  1.89241587798652712 8D+01
  6.19062380509695387 3D+02 -1.41705324493408532 8D+02  6.24164948708950140 2D+01
  8.06318764437976884 8D+01  7.04185379546573262 4D+01  6.89094099931015460 2D+01
  1.27970387869301378 0D+04
  2.68913704235750397 9D-03  1.32489994214266429 4D+00  1.92115159251146641 6D+00
  2.04570050540091941 1D+00  2.08899055812894951 5D+00  2.84098089942945747 4D+00
  8.09205913150287092 8D+00  8.98576041648824075 4D+00  1.26417348124666626 4D+01
  2.06783175672952079 8D+01  3.20288904913738177 2D+01  5.63045441607613099 7D+01
  9.21969357908486222 0D+03
     23       5.42722536070877845126E-04
  2.16539474552958916 7D-05  1.18040827824021285 7D-03  1.75847634399539366 7D-03
  3.52925061395640242 6D-03  2.90610731330743864 5D-03  1.92573427869399425 1D-03
  1.34389486184920996 4D-03  2.88750658452767887 7D-02  1.66328762210330109 0D-01
  5.10980672780648084 7D-01  2.44838986338041443 6D-01  1.24282687786030061 6D+01
  6.60231758218323450 1D+00  1.38897949926327463 3D+02  1.09069590117740983 7D+03
  8.46852165261376717 4D+03  6.56534219949904054 4D+04  2.08398802430960229 7D+05
  4.12542076240632908 6D+05  1.13417074131736159 3D+06  1.56162024388456039 0D+06
  7.45899788763205520 8D+07 -6.25641838935410957 8D+07
  1.98583405661094483 1D-02  1.75538142646271802 5D+00  2.62278913024777843 3D+00
  5.26422159649859866 5D+00  8.57349507071259364 6D+00  1.15717454533599220 0D+01
  1.64265847286588164 7D+01  3.52077444856213908 5D+02  4.98336794576321942 4D+02
  7.47099193953779007 4D+02  7.59324876441583896 3D+02  2.31785039793662178 9D+03
  4.92611562969620183 6D+03  1.29970058388526927 0D+04  5.12978553900188935 6D+04
  2.01337719886235412 6D+05  7.93699076308188261 5D+05  2.43001768528210208 8D+06
  4.70497601132454886 1D+06  7.85540603692569898 0D+06  1.38387353119645125 7D+07
  4.03970225593684148 0D+07  4.32771721325852172 4D+07
-5TN152BBG752B                1.                    -2 6
     12       2.33212776567026324415E+02
  1.52994144607350353 5D+02  1.00086910116997758 0D+04 -9.59275380329424638 1D+03
  3.25657357948660198 6D+02  3.40689297509954247 5D+01  4.19059374811755091 6D+02
  2.33144786117335023 3D+01  6.33853971671989189 2D+01  8.03446900522340925 5D+01
  6.83017160578480204 7D+01  7.36873923638511485 0D+02  1.39050951311003646 0D+04
  2.74335550163608981 9D-03  1.54764936319969101 4D+00  1.59928734193603050 4D+00
  1.86726913696326360 4D+00  2.85092411570617787 5D+00  7.30660423126926317 2D+00
  8.89552582115001766 5D+00  1.20382056671023307 5D+01  1.97166473503638504 1D+01
  3.05524734065464014 2D+01  5.21188284742291728 0D+02  9.84149979616832934 0D+03
     24       5.42736309301992278183E-04
  2.08285382898121627 3D-05  1.26648576766905620 0D-03  1.56127121428274137 9D-03
  3.77422846165391227 8D-03  2.97322146061617184 5D-03  1.41013004836055218 8D-03
  2.21340345769780720 0D-02  1.43898901515769454 1D-01  1.15320438582444792 5D+00
  1.69117056531801543 4D+00  6.13174514967878503 4D+00  1.06549616247370408 9D+02
  2.93469117111426784 9D+01  3.98446650446636488 1D+03  6.21205621348320812 6D+03
  6.70788201998346412 4D+04  5.89849672903440397 9D+05  6.88067693645929510 2D+05
  6.94515710160505071 3D+08 -6.90193820925778165 5D+08  3.99267335906774566 7D+12
 -4.82891446664919934 1D+12  4.61023513327758166 5D+12 -3.77399970292312005 6D+12
  1.98587539281477780 7D-02  1.91985699125910158 6D+00  2.38089370898847646 5D+00
  5.74530608432434097 8D+00  9.05834299598702208 4D+00  1.75906578670428142 0D+01
  2.75754101798044324 3D+02  8.32668780836933549 9D+02  8.70356085265599176 6D+02
  1.29782857848465107 5D+03  2.36071384953771269 0D+03  1.00294874207565048 9D+04
  1.18471128595752507 0D+04  9.46148919383117536 2D+04  2.88144689421366965 7D+05
  7.53078181923196578 3D+05  2.55430358814272913 2D+06  4.23527477116433810 4D+06
  9.89666223540570144 5D+06  9.90897679131246521 1D+06  3.59411491600246662 3D+07
  3.59767525311120962 7D+07  3.63090612585057588 3D+07  3.63450290840214900 7D+07
-6TN152CBG752C                1.                    -2 6
     12       2.38428075051592937683E+02
  1.56295492620238448 5D+02  1.24229494260161370 7D+04 -2.67637682572960948 2D+04
  1.51041453843498366 0D+04  3.38153301563239505 6D+01  5.94057357169452444 6D+02
 -1.38428937538933006 1D+02  6.66816923582811327 3D+01  7.71448307314911048 1D+01
  7.21807692158066824 8D+01  8.87548640419394772 0D+02  1.83125604332081020 4D+04
  2.74920691867872773 2D-03  1.57872650105727366 2D+00  1.66209836251578366 2D+00
  1.69843396612050384 6D+00  2.85513549257065024 6D+00  7.60808243873209344 4D+00
  8.42096339361865675 6D+00  1.20869773635966573 1D+01  1.90981492052733954 3D+01
  3.11796445381588887 0D+01  6.14322401191096119 5D+02  1.26461032435620188 6D+04
```

Figure 46. Continued.

```
      23      5.427535622335882305l8E-04
   2.085955599229596916D-05  1.338996142032353745D-03  1.977702913359153357D-03
   4.757015436042039570D-03  1.852812318499691044D-03  6.757763689435925984D-04
   8.591341266752282324D-03  3.620576256203986501D-02  1.445271703749602038D+00
   1.303574105743703637D+00  3.379102363055385624D-01  8.376346211240381123D+01
   1.440334418039532274D+02  1.399486812621064786D+03  1.228562424222564164D+04
   7.530692085646290070D+04  1.340665641285117075D+06 -1.525898807320570427D+04
   6.350697090973523096D+06 -6.839386898120301217D+08  6.766638950154676884D+08
   7.974715475144418422D+06 -8.465247393758189864D+06
   1.985873839454865624D-02  1.862812870140722527D+00  2.760834251493200220D+00
   6.641642052392319417D+00  1.036629439931317753D+01  1.533055705715490791D+01
   1.946973111004724650D+02  4.080195400158612102D+02  9.406065271133197996D+02
   9.632018925989714120D+02  9.988364625640331411D+02  7.304897238792896815D+03
   2.488221493613995926D+04  6.061971691176961940D+04  2.500944480219643119D+05
   7.100776475486042473D+05  2.359797367365973594D+06  3.387074323434089252D+06
   8.179870195075289346D+06  1.524743638261611620D+07  1.526254052225408982D+07
   2.263243269911192451D+07  2.265485243022319302D+07
C    Q MATRIX BY ROWS (IMAGINARY PART = 0)
  0.50087070 -0.46167319 -0.49313081  0.24515321  0.47310880 -0.30648209
  0.00000000  0.00000000  0.00000000  0.00000000  0.00000000  0.00000000
  0.34049665 -0.02109095 -0.44756805 -0.44697417 -0.25127029  0.58002629
  0.00000000  0.00000000  0.00000000  0.00000000  0.00000000  0.00000000
  0.35677436  0.53295208 -0.18697741  0.48533423 -0.44765855 -0.26281078
  0.00000000  0.00000000  0.00000000  0.00000000  0.00000000  0.00000000
  0.50087517 -0.46168710  0.49313768 -0.24513653 -0.47333592 -0.30604273
  0.00000000  0.00000000  0.00000000  0.00000000  0.00000000  0.00000000
  0.34049490 -0.02108988  0.44755453  0.44693392  0.25174401  0.57993411
  0.00000000  0.00000000  0.00000000  0.00000000  0.00000000  0.00000000
  0.35677883  0.53297823  0.18698441 -0.48531000  0.44741519 -0.26322140
  0.00000000  0.00000000  0.00000000  0.00000000  0.00000000  0.00000000

C LINE-MODEL          FD-LINE
C ENGLISH
C   0    .5    2.400 4           .0250    -7.00   140.25   140.25
C   0    .5    2.400 4           .0250     7.00   140.25   140.25
C   1    .5   .04967 4           1.603   -15.00    52.25    52.25      18.              3
C   2    .5   .04967 4           1.603   -25.00    83.25    83.25      18.              3
C   3    .5   .04967 4           1.603   -15.00   114.25   114.25      18.              3
C   4    .5   .04967 4           1.603    15.00    52.25    52.25      18.              3
C   5    .5   .04967 4           1.603    25.00    83.25    83.25      18.              3
C   6    .5   .04967 4           1.603    15.00   114.25   114.25      18.              3
C LINE LENGTH =  2.5154E+02  KM
C TRANSFORMATION MATRIX AT F =  6.0000E+01  HZ
C
-1GT001AGT391A                  1.                      -2 6
      17      6.22346036394520879753E+02
  1.998551292256145118D+02  1.571346770229615146D+03 -1.708701544799129721D+03
  7.960273288430282435D+02  5.716428010259349701D+01  1.754180042507906364D+03
  9.012256877433020691D+03  4.365858539932664371D+04  1.801887504746490731D+04
  5.983994606779328751D+04  2.228219059471568289D+05  4.071320657945612329D+05
  3.194143710404731624D+06  6.115818617726868368D+06  1.142854444487232040D+07
  3.159442663144744514D+07  1.958277172619485036D+08
  3.642538396971592765D-03  1.245166501626172068D+00  1.334029529507843592D+00
  1.354526317672298474D+00  1.880727936343301265D+00  2.085005920974407845D+01
  1.050412119616732127D+02  2.763899081053263487D+02  4.075216182611066031D+02
  1.106916256056727690D+03  7.703320231985995520D+03  1.523048702415280627D+04
  6.164616183856358566D+04  2.452987618793558613D+05  4.946415805551151279D+05
  1.410570888077296288D+06  8.941810527297823690D+06
      20      9.591828042291443591616-04
  1.622389006637656498D-05  2.161925607784703852D-04  2.844485765432061393D-04
  1.621592759115266077D-03  8.117305980332966504D-03  2.745650994227643660D-02
  1.407246503214002430D-01  5.827001161636710808D-01  2.254827786129737666D+00
  1.053181508240430775D+01  9.584318996460890361D+00  1.424536892776863950D+01
  6.003090979687323436D+01  5.231341825349134922D+02  7.792937746126549143D+02
  2.030909266766466345D+03  1.275233746602577025D+04  9.739360766438018065D+06
 -9.770702127622512635D+06  1.515827811691109309D+04
  1.986105941787055709D-02  1.381740472126613495D+00  1.819331998670494194D+00
  5.171507082780827713D+00  1.286882083731184201D+01  2.169424162355176078D+01
  5.436994790605101002D+01  1.081505631362237185D+02  1.885753194571055715D+02
  2.486778696887722440D+02  3.951409553438248210D+02  4.474643508010343922D+02
  1.366804845899864659D+03  3.739280967169870848D+03  5.430903102242293926D+03
  7.692744615701141811D+03  1.414977825460381791D+04  2.059481936928183040D+04
  2.061522063673208049D+04  3.460881497732154912D+04
-2GT001BGT391B                  1.                      -2 6
```

Figure 46. Continued.

```
      12      3.12977744121435648594E+02
  1.65326881961530l375D+02  1.00614927806l805816D+03  4.29600317542l227294D+01
  2.44990526535660233 5D+02 -4.01995449686374392 D+02  1.30387544136893437 9D+00
  1.18995679205032734 8D+02  8.82528892702523 853D+02 -5.48507429483323548 D+02
  2.14331261218324141 3D+03  2.45330132669459926 5D+04  6.37093788445272564 4D+06
  2.92445276652034737 7D-03  1.25430610434509715 0D+00  1.77047372748293818 7D+00
  2.11528216832312832 0D+00  2.13428572577658931 5D+00  2.56206914708538913 1D+00
  4.33493400376971105 3D+00  1.09735273518181706 3D+01  1.11090723461489637 7D+01
  3.12539529777805611 8D+02  7.17696845204506303 2D+03  1.87998027433985238 9D+06
      21      8.42999570573233378778E-04
  2.78179216690808152 2D-05  1.03512622191003457 4D-03  1.39944936072287784 8D-03
  1.43131958958489193 7D-03  3.15095135779645309 0D-03  1.64160042040587873 3D-03
  1.17474086021438634 0D-02  4.09976929782067635 0D-02  1.45141515209784178 3D-01
  9.42378226605067578 8D-01  8.88207923914932195 9D-01  5.31700263681234089 3D-01
  2.37161144630108080 6D+01  2.40108952330221509 2D+02  8.61832752913169752 0D+04
 -7.70577042946419096 6D+04  4.42354079997390445 0D+04  3.63854294587472853 9D+05
  2.01821473562575139 1D+08 -2.02827005717829063 5D+08  5.88050487743697158 3D+05
  1.98552525959308978 3D-02  1.75730199664589181 7D+00  2.35808022752814000 5D+00
  2.46633860476849392 5D+00  5.40196032018264471 5D+00  1.13791604275743134 5D+01
  8.18038663181297369 7D+01  1.39808221642424467 0D+02  2.42702503508552499 8D+02
  3.79592005658842317 9D+02  3.96977808373970049 2D+02  4.64695939318771394 3D+02
  2.49174857068305766 5D+03  1.17299686091837834 3D+04  5.68492658065448649 7D+04
  5.70122778505625892 6D+04  1.34681478207098698 5D+05  2.65723901572113012 7D+05
  4.34767502543956623 4D+05  4.35198184063373453 7D+05  6.20196279717607874 8D+05
-3GT001CGT391C                 1.                    -2 6
      12      2.73243042762773065135E+02
  1.56174836495133302 3D+02  8.02507345891193017 5D+03 -1.21880394512292264 2D+04
  4.95473722689673536 5D+03  2.11249176742433024 7D+01  1.97731293881267483 0D+02
  2.85844666158833050 0D+02 -2.90049445918157560 2D+01  7.61876036637743236 9D+01
  7.78387256841644674 7D+01  8.41731818378460629 9D+04  6.01933814553667523 4D+06
  2.85834149516904620 3D-03  1.54557358459199578 6D+00  1.64751393505117907 4D+00
  1.71362240606010890 5D+00  2.62696940516417032 4D+00  5.29703159468505402 3D+00
  1.00326457050424471 3D+01  1.07018265141854069 8D+01  1.78376683119735908 2D+01
  3.10437583041394158 4D+01  5.49586113411600072 1D+04  3.94617618974038527 8D+06
      24      8.41552877364927206030E-04
  2.93244778983569187 9D-05  1.08691836287240096 8D-03  1.18665341819688675 8D-03
  1.51315974575341537 9D-03  2.49760435171137665 9D-03  2.12931740306126479 4D-03
  1.30158042444195303 6D-03  1.86280116263298639 9D-03  1.22357007329175876 9D-02
  1.93431375086189744 6D-02  5.74632187959094632 7D-02  2.20026467269591179 1D-01
  3.00588196058393969 4D+00  3.08669517172262608 5D+00  1.77874652354036835 7D+00
  1.30540205537149762 4D+03 -8.65465220968641077 1D+02  7.19176020071834534 5D+03
  1.02365445555269423 0D+04  7.93613599409564103 6D+04  8.38622530926587074 6D+05
  1.56171471116544604 3D+08 -1.57533426872140612 5D+08  4.26095431138093634 2D+05
  1.98544976911323111 3D-02  1.84156740729638676 6D+00  2.03291968915469201 1D+00
  2.58781784224343958 1D+00  4.28531342037407858 6D+00  7.26873284458912793 9D+00
  8.94209647724151990 3D+00  1.28313131952184880 1D+01  1.77210915498766006 2D+02
  2.62424655348849341 9D+02  3.89468259598560955 2D+02  7.36826284301941115 0D+02
  1.23436710678203121 5D+03  1.34384062737714856 4D+03  1.55113102089817795 1D+03
  1.47730448502612766 8D+04  1.48135952841283860 8D+04  9.07546938240026866 0D+04
  1.07484501376474998 3D+05  2.27880305775846380 1D+05  4.52122232405903669 1D+05
  6.73230002233265462 6D+05  6.73896905160881404 3D+05  1.14235718579342754 7D+06
-4GT002AGT392A                 1.                    -2 6
      13      2.20177781503156975162E+02
  1.53342994919567416 9D+02  1.02326066262942616 4D+03  1.70151190216473018 8D+02
 -1.13374248063053934 7D+03  6.93064463037600461 3D+02  1.89241587798652712 8D+01
  6.19062380509695387 3D+02 -1.41705324493408532 8D+02  6.24164948708950140 2D+01
  8.06318764437976884 8D+01  7.04185379546573262 4D+01  6.89094099931015460 2D+01
  1.27970387869301378 0D+04
  2.68913704235750397 9D-03  1.32489994214266429 4D+00  1.92115159251146641 6D+00
  2.04570050540091941 1D+00  2.08899055812894951 5D+00  2.84090899429457474 0D+00
  8.09205913150287092 8D+00  8.98576041648824075 4D+00  1.26417348124666626 4D+01
  2.06783175672952079 8D+01  3.20288904913738177 2D+01  5.63045441607613099 7D+01
  9.21969357908486222 2D+03
```

Figure 46. Continued.

```
      23      8.3905020136149728506 7E-04
  3.345672249978830877D-05  1.824931134321452087D-03  2.714235953525537780D-03
  5.446100361995422079D-03  4.482048568296678791D-03  2.968685285509357950D-03
  2.072081972291936122D-03  4.549723947598739021D-02  2.570558948046472725D-01
  4.013448422814709995D-01  8.285052595038885637D-01  1.917607954095914025D+01
  7.685394650151693652D+00  2.358359705055646103D+02  1.531932070132484228D+03
  1.397295661749917281D+04  3.852670645304363916D+04  6.798580223552355892D+04
  2.707494589161305339D+05  8.934332430498463655D+05  6.496003671930655109D+05
  1.503002208944438142D+07 -9.591236279726429144D+06
  1.985242668761175687D-02  1.755059325921745239D+00  2.622307866298561163D+00
  5.263255262530036283D+00  8.572698389638721439D+00  1.157121703462194051D+01
  1.642621606070900420D+01  3.588903731997720712D+02  4.982914009148966841D+02
  7.592550729535527836D+02  8.065514073878039341D+02  2.314450104152379140D+03
  3.764247589439823628D+03  1.426378626076299497D+04  4.722974046128395730D+04
  2.148611254165751488D+05  5.931672033538679243D+05  1.104231538120967540D+06
  2.240837701663324318D+06  5.058486311470985413D+06  6.555050609153178171D+06
  2.141246496559439925D+07  2.684626833391015185D+07
-5GT002BGT392B                      1.                      -2 6
      12      2.3321277656702632441 5E+02
  1.529941446073503535D+02  1.000869101169977580D+04 -9.592753803294246381D+03
  3.256573579486601986D+02  3.406892975099542475D+01  4.190593748117550916D+02
  2.331447861173350233D+01  6.338539716719891892D+01  8.034469005223409255D+01
  6.830171605784802047D+01  7.368739236385114850D+02  1.390509513110036460D+04
  2.743355501636089819D-03  1.547649363199691014D+00  1.599287341936030504D+00
  1.867269136963263604D+00  2.850924115706177875D+00  7.306604231269263172D+00
  8.895525821150017665D+00  1.203820566710233075D+01  1.971664730536385041D+01
  3.055247340654640142D+01  5.211882847422917280D+02  9.841499796168329340D+03
      24      8.3908478878890142892 2E-04
  3.218213508666184969D-05  1.079629751700157469D-03  1.223490919382833330D-03
  4.744324735791581159D-03  4.237269439211929301D-03  3.044384970926175310D-03
  3.578010362636582938D-03  6.751686668260689465D-02  3.839495369209688716D-01
  2.085314483542033359D+00  8.419199419823845953D-01  4.519256079672459236D+01
  2.284563817070413227D+01  3.903042020672668571D+02  1.183532818828718359D+04
  1.844929484395894269D+04  2.422510413268591656D+05  4.027326150456589021D+05
  4.644893596037459443D+06 -1.861251261715965375D+06  2.066479115604374847D+11
 -2.185619058718700562D+11  1.884689312279777565D+11 -1.765583962888977242D+11
  1.985306555618748109D-02  1.668137350915711303D+00  1.907957805073028701D+00
  3.693150736478408636D+00  6.622695155104903364D+00  9.548695782010181432D+00
  2.244358548348068183D+01  4.195191586159912731D+02  6.017262717226218740D+02
  8.151941083822414527D+02  1.288127870174403000D+03  4.390254808716459479D+03
  8.860416451238182617D+03  1.921399460074315630D+04  1.435915318579269770D+05
  4.314419136789233016D+05  1.202974074580392393D+06  2.308263336519368284D+06
  5.453187348532194854D+06  7.661634055870635319D+06  1.810150218633255409D+07
  1.811943356901345914D+07  1.870564109430891508D+07  1.872417093814734416D+07
-6GT002CGT392C                      1.                      -2 6
      12      2.3842807505159293768 3E+02
  1.562954926202384485D+02  1.242294942601613707D+04 -2.676376825729609482D+04
  1.510414538434983660D+04  3.381533015632395056D+01  5.940573571694524446D+02
 -1.384289375389330061D+02  6.668169235828113273D+01  7.714483073149110481D+01
  7.218076921580668248D+01  8.875486404193947720D+02  1.831256043320810204D+04
  2.749206918678727732D-03  1.578726501057273662D+00  1.662098362515783662D+00
  1.698433966120503846D+00  2.855135492570650246D+00  7.608082438732093444D+00
  8.420963393618656756D+00  1.208697736359665731D+01  1.909814920527339543D+01
  3.117964453815888870D+01  6.143224011910961195D+02  1.264610324356201886D+04
      25      8.3912435576265075488 0E-04
  3.223002174036391186D-05  1.426841444457575733D-03  1.373839888408177743D-03
  1.997204523683885897D-03  3.190627042229111454D-03  6.690601383681067942D-03
  2.009031536793877892D-03  5.715671809551795771D-02  1.787386264527622663D-01
  1.539087591827702856D+00  9.294762606854175990D+00  7.235994351552861481D+01
  6.130339867502484594D+02  4.550800145955444350D+03  1.432371471893910439D+04
  3.527671421963016019D+04  1.092482796993357733D+05  3.203849733427758692D+05
  1.567652330494054077D+05  5.054251989596674917D+06 -3.425473663962425082D+06
  1.257762985838904905D+10 -1.284572843286217380D+10  9.076603897420798063D+09
 -8.810775347468850136D+09
  1.985304154821940399D-02  1.969821600297402886D+00  2.015729947176768400D+00
  2.855331574297062858D+00  4.565270037140504722D+00  9.567014509488023677D+00
  1.159447782832099061D+01  3.280519063206397945D+02  5.072291051411820177D+02
  1.085109652758968821D+03  1.661772731604049113D+03  6.465427139752371090D+03
  2.718357146135007861D+04  9.884320020190892319D+04  2.832813881377051439D+05
  5.669708150173612667D+05  8.677958856099859404D+05  1.415944092302752979D+06
  1.644334837264334783D+06  3.657412766549189982D+06  4.228762662739145919D+06
  1.039243419366760901D+07  1.040272895885309111D+07  1.127533887431346043D+07
  1.128650824656394962D+07
```

Figure 46. Continued.

```
C   Q MATRIX BY ROWS (IMAGINARY PART = 0)
  0.50087070 -0.46167319 -0.49313081  0.24515321  0.47310880 -0.30648209
  0.00000000  0.00000000  0.00000000  0.00000000  0.00000000  0.00000000
  0.34049665 -0.02109095 -0.44756805 -0.44697417 -0.25127029  0.58002629
  0.00000000  0.00000000  0.00000000  0.00000000  0.00000000  0.00000000
  0.35677436  0.53295208 -0.18697741  0.48533423 -0.44765855 -0.26281078
  0.00000000  0.00000000  0.00000000  0.00000000  0.00000000  0.00000000
  0.50087517 -0.46168710  0.49313768 -0.24513653 -0.47333592 -0.30604273
  0.00000000  0.00000000  0.00000000  0.00000000  0.00000000  0.00000000
  0.34049490 -0.02108988  0.44755453  0.44693392  0.25174401  0.57993411
  0.00000000  0.00000000  0.00000000  0.00000000  0.00000000  0.00000000
  0.35677883  0.53297823  0.18698441 -0.48531000  0.44741519 -0.26322140
  0.00000000  0.00000000  0.00000000  0.00000000  0.00000000  0.00000000

C  ========================EQUIVALENTS FOR EXTERNAL SYSTEM====================
C        1         2         3         4         5         6         7         8
C 345678901234567890123456789012345678901234567890123456789012345678901234567890
C
C
-1CS230ABV230A             .368102.80883.3763131.44
-2CS230BBV230B             .08191.753035.6271131.44
-3CS230CBV230C
C                          !     !     !     !     !
-1BV230AGA230A             .184051.40446.752683.5
-2BV230BGA230B             .04095.3765211.25483.5
-3BV230CGA230C
C                          !     !     !     !     !
-1HS230AGA230A             .184051.40446.7526135.0
-2HS230BGA230B             .04095.3765211.254135.0
-3HS230CGA230C
C 51CS230A                   .00529 5.0202100
C 52CS230B                   .04232 21.511785
C 53CS230C
C                          !     !     !     !     !
C 51BV230A                   2.6609 32.083850
C 52BV230B                   2.4202 45.665925
C 53BV230C
51HS230A                   26.857 246.13841
52HS230B                   24.366 381.87981
53HS230C
C                          !     !     !     !     !
51GA230A                   4.3748 41.833320
52GA230B                   3.7533 50.699360
53GA230C
51TF500AHS500A             17.134 116.2794
52TF500BHS500B             1.6922 32.5802
53TF500CHS500C
51TF500ADW500A             28.557 193.7991
52TF500BDW500B             2.8204 54.3003
53TF500CDW500C
51TF500ABE500A             32.91  218.60
52TF500BBE500B             3.25   61.25
53TF500CBE500C
51BE500A                         176.25
52BE500B                          55.75
53BE500C
51DW500A                          44.38
52DW500B                          34.25
53DW500C
C   ==================END OF EXTERNAL EQUIVALENTS ================
```

Figure 46. Continued.

```
C     ==================BEGIN THEVENIN IMPEDANCES ================
C 345678-1-2345678-2-2345678-3-2345678-4-2345678-5-2345678-6-2345678-7-2345678-8
  BTHEVABE500A                    55.75
  BTHEVBBE500BBTHEVABE500A
  BTHEVCBE500CBTHEVABE500A
  DTHEVADW500A                    34.25
  DTHEVBDW500BDTHEVADW500A
  DTHEVCDW500CDTHEVADW500A
  HTHEVAHS230A             .3703 32.639
  HTHEVBHS230BHTHEVAHS230A
  HTHEVCHS230CHTHEVAHS230A
  GTHEVAGA230A            3.703 44.066
  GTHEVBGA230BGTHEVAGA230A
  GTHEVCGA230CGTHEVAGA230A
  BVTHVABV230A            2.486 43.219
  BVTHVBBV230BBVTHVABV230A
  BVTHVCBV230CBVTHVABV230A

C  ====================LINE CHARGING DATA FOR TF-HS,DW,BE==================
  TF500A                              974.86
  TF500B                              974.86
  TF500C                              974.86
  HS500A                              189.28
  HS500B                              189.28
  HS500C                              189.28
  DW500A                              315.46
  DW500B                              315.46
  DW500C                              315.46
  BE500A                              470.12
  BE500B                              470.12
  BE500C                              470.12
C  =========================END OF BRANCH DATA=================================
C
BLANK CARD TO END BRANCH DATA
C  =========================BEGIN SWITCH DATA==================================
C   =============CIRCUIT BREAKERS=======================================
C  ==============================COLSTRIP - BROADVIEW==================
C Bus-->Bus--><---Tclose<-----Topen<-------Ie                                  O
  CB001ACS500A -.020    12.0                                                   1
  CB001BCS500B -.020    12.0                                                   1
  CB001CCS500C -.020    12.0                                                   0
  CB002ACS500A -.020    12.0                                                   1
  CB002BCS500B -.020    12.0                                                   1
  CB002CCS500C -.020    12.0                                                   0
  BV500ABCSW1A -.020    12.0                                                   0
  BV500BBCSW1B -.020    12.0                                                   0
  BV500CBCSW1C -.020    12.0                                                   0
  BV500ABCSW2A -.020    12.0                                                   0
  BV500BBCSW2B -.020    12.0                                                   0
  BV500CBCSW2C -.020    12.0                                                   0
C  ============================BROADVIEW - GARRISON=======================
  BG001ABV500A -.020    0.298                                                  1
  BG001BBV500B -.020    0.298                                                  0
  BG001CBV500C -.020    0.298                                                  0
C BG001ABV500A -.020    12.00                                                  1
C BG001BBV500B -.020    12.00                                                  0
C BG001CBV500C -.020    12.00                                                  0
  BV500ABG001A 1.112    12.0                                                   0
  BV500BBG001B 1.112    12.0                                                   0
  BV500CBG001C 1.112    12.0                                                   0
  BG002ABV500A -.020    12.0                                                   0
  BG002BBV500B -.020    12.0                                                   0
  BG002CBV500C -.020    12.0                                                   0
  GA500AGBSW1A -.020    0.298                                                  0
  GA500BGBSW1B -.020    0.298                                                  0
  GA500CGBSW1C -.020    0.298                                                  0
C GA500AGBSW1A -.020    12.00                                                  0
C GA500BGBSW1B -.020    12.00                                                  0
C GA500CGBSW1C -.020    12.00                                                  0
  GBSW1AGA500A 1.112    12.0                                                   0
  GBSW1BGA500B 1.112    12.0                                                   0
  GBSW1CGA500C 1.112    12.0                                                   0
  GA500AGBSW2A -.020    12.0                                                   0
  GA500BGBSW2B -.020    12.0                                                   0
  GA500CGBSW2C -.020    12.0                                                   0
```

Figure 46. Continued.

```
C  ============================GARRISON - TAFT=============================
  GT391ATF500A -.020     12.0                                                1
  GT391BTF500B -.020     12.0                                                0
  GT391CTF500C -.020     12.0                                                0
  GT392ATF500A -.020     12.0                                                0
  GT392BTF500B -.020     12.0                                                0
  GT392CTF500C -.020     12.0                                                0
  GA500AGTSW1A -.020     12.0                                                0
  GA500BGTSW1B -.020     12.0                                                0
  GA500CGTSW1C -.020     12.0                                                0
  GA500AGTSW2A -.020     12.0                                                0
  GA500BGTSW2B -.020     12.0                                                0
  GA500CGTSW2C -.020     12.0                                                0

C  ========================= FAULT SWITCHES ===================================
  BGFF1A        .220     1.16
  BGFF1B        .220     1.16
  BGFF1C        .220     1.16

C

C  ======================== TACS CONTROLLED SWITCHES FOR BRAKE ===============
C     Type 11 Switches are TACS Controlled Switches.  These are SCR's.
C 345678-1-2345678-2-2345678-3-2345678-4-2345678-5-2345678-6-2345678-7-2
11TMP_A1BRAKEA                                                    BRKOPN          1
11TMP_A2_NGH_A                                                    BRKOPN
11TMP_B1BRAKEB                                                    BRKOPN
11TMP_B2_NGH_B                                                    BRKOPN
11TMP_C1BRAKEC                                                    BRKOPN
11TMP_C2_NGH_C                                                    BRKOPN
C  ========================END SWITCH DATA=====================================
BLANK CARD TO END SWITCH DATA
C  ========================BEGIN SOURCE DATA==================================
C        1         2         3         4         5         6         7         8
C 345678901234.... thevenins ....45678901234567890123456789012345678901234567890
14DTHEVA  455000.   60.       -20.00                          -1.
14DTHEVB  455000.   60.       -140.0                          -1.
14DTHEVC  455000.   60.        100.0                          -1.
14BTHEVA  455000.   60.       -32.53                          -1.
14BTHEVB  455000.   60.       -152.53                         -1.
14BTHEVC  455000.   60.        87.47                          -1.
14HS230A  165348.   60.       -10.0                           -1.
14HS230B  165348.   60.       -130.0                          -1.
14HS230C  165348.   60.       110.00                          -1.
14BVTHVA  177372.   60.       16.00                           -1.
14BVTHVB  177372.   60.       -104.00                         -1.
14BVTHVC  177372.   60.       136.00                          -1.
C CS230A  197184.   60.       26.17                           -1.
C CS230B  197184.   60.       -93.83                          -1.
C CS230C  197184.   60.       146.17                          -1.
14GTHEVA  180175.   60.         7.0                           -1.
14GTHEVB  180175.   60.       -113.0                          -1.
14GTHEVC  180175.   60.       127.00                          -1.
C
C ..............Voltage Contr. Source data for brake ............................
60VSRCEA 1                                                          -1.   9999.
60VSRCEB 1                                                          -1.   9999.
60VSRCEC 1                                                          -1.   9999.
C Dynamic synchronous machines.
C Bus-->  <-----Volt<-----Freq<----Angle
59CS221A  17941.37    60.0      -1.90
  CS221B
  CS221C
TOLERANCES          1.0E-12
PARAMETER FITTING       1.0
 3 3 0   2                     377.0     22.0      -971.3     1150.0     1788.4
                                                   -971.3     1150.0     1788.4
0.0052    0.175     1.72      1.71      0.277     0.373     0.253     0.253
5.50      1.80      0.03      0.07      0.110     2187.0    271.0
01        0.550     0.040101  0.000     0.000     43.05367
02        0.450     0.191576  0.000     0.000     51.00225
03        0.000     0.116460  0.000     0.000     00.00000
BLANK card terminates mass cards
BLANK card terminates output requests
  FINISH
```

Figure 46. Continued.

```
C Dynamic synchronous machine.
C Bus-->  <-----Volt<-----Freq<----Angle
59CS222A  17937.78    60.0       -1.90
  CS222B
  CS222C
TOLERANCES          1.0E-12
PARAMETER FITTING       1.0
 3 3 0   2                      377.0      22.0       -971.3      1150.0      1788.4
                                                      -971.3      1150.0      1788.4
0.0052     0.175      1.72       1.71       0.277      0.373      0.253      0.253
5.50       1.80       0.03       0.07       0.110      2187.0     271.0
01         0.550      0.040101   0.000      0.000      43.05367
02         0.450      0.191576   0.000      0.000      51.00225
03         0.000      0.116460   0.000      0.000      00.00000

C        1         2         3         4         5         6         7         8
C 345678901234567890123456789012345678901234567890123456789012345678901234567890
BLANK card terminates mass cards
  31
  41
BLANK card terminates output requests
  FINISH
C   SCOURCE DATA FOR COLSTRIP UNIT THREE AND FOUR (PARALLEL)
C Dynamic synchronous machine.
C Bus-->  <-----Volt<-----Freq<----Angle
59CS261A  21727.79    60.0       -1.90
  CS261B
  CS261C
PARAMETER FITTING       1.0
 6 5 6   2                      1638.0     26.0       -5800.      6200.0     11200.0
                                                      -5800.      6200.0     11200.0
0.00132    0.1284     1.2356     1.2221     0.2197     0.3482     0.1776     0.1742
4.777      0.531      0.041      0.067      0.0861     2329.0     640.0
01         0.272      0.063598   941.4      201.50     53.50      0.000
02         0.275      0.119634   1171.      809.6      73.34      0.000
03         0.2265     0.598438   963.2      809.6      73.34      0.000
04         0.2265     0.605408   963.2      724.2      110.5      0.000
05         0.000      0.504274   0.000      144.4      58.34      0.000
06         0.000      0.024816   1056.4     0.000      0.000      0.000
C        1         2         3         4         5         6         7         8
C 345678901234567890123456789012345678901234567890123456789012345678901234567890
BLANK card terminates mass cards
  31
  41
BLANK card terminates output request.
C TACS input cards.
C ------------------------------------
C The following card enters the gen velocity into array ETACS to be picked up
C by the control subroutine.
C ------------------------------------
C Bus--><---><KI
74GENVEL       11
C col: (1-2) KK - either 71, 72 , 73 or 74
  FINISH
BLANK CARD TO END MACHINE DATA
  CS500A
BLANK CARD TO END NODE-VOLTAGE OUTPUT SPECIFICATION
BLANK CARD TO END BATCH MODE CONTROL CARDS
BEGIN NEW DATA CASE
BLANK
```

Figure 46. Continued.

APPENDIX C

EMTP INTERFACE AND CONTROLLER CODE

This appendix contains the information necessary to interface the dynamic brake to the EMTP digital simulation package. Figure 47 shows the FORTRAN source code used to obtain the control values at each simulation time step. The subroutine INJECT, shown in Figure 47, is called from the modified EMTP subroutine CSUP. CSUP is is shown in Figure 48. The procedure to implement the brake in the EMTP would be to first modify CSUP by adding the subroutine call statement. Then CSUP and INJECT would be compiled and linked with the original EMTP library. The data files in Appendices A and B could then be simulated following the procedures spelled out in an EMTP User's Manual supplied with the EMTP code.

```
C ************************************************************************
C                                                                       ***
C     Controller subroutine to be called from CSUPB in EMTP.            ***
C   The called variables are:                                           ***
C                                                                       ***
C     ISTEP - the step number in the time domain simulation             ***
C     DELTAT - the step size
C     Va - the "A" phase terminal voltage for the gen being controlled
C     Vb - the "B" phase terminal voltage for the gen being controlled
C     Vc - the "C" phase terminal voltage for the gen being controlled
C
C   The returned variables are:                                         ***
C                                                                       ***
C     VBa - the set point "A" phase voltage for the Type 60 source      ***
C     VBa - the set point "A" phase voltage for the Type 60 source      ***
C     VBa - the set point "A" phase voltage for the Type 60 source      ***
C     brake - the thyristor gate signal for the TACS switches           ***
C                                                                       ***
C ************************************************************************
C ************************************************************************
      SUBROUTINE INJECT(ISTEP,DELTAT,Va,Vb,Vc,VBa,VBb,VBc,brake)
*CALL IMPLIDP                                                          GPC  B
      IMPLICIT DOUBLE PRECISION (A-H, O-Z)                             IMPLIDP
*END  IMPLIDP                                                          .......
      DIMENSION Yold(-2:0),Ynew(-2:0)
*CALL SYNCOMB
C     THIS DECK CONTAINS S.M. STORAGE USED BY TACS MODULES.            SYNCOMB
      COMMON  /SMTACS/   ETAC(20)                                      SYNCOMB
      COMMON  /SMTACS/   ISMTAC(20), NTOTAC, LBSTAC                    SYNCOMB
*END  SYNCOMB                                                          .......
      DATA samplefreq /200.D0/

C Decide whether this is a sample point or not.  This is useful
C   for digital controller implementation.  If controller is continuous
C   then comment out the IF statement.

      TIMEX=ISTEP*DELTAT*10000.D0
      samplerate=1.D0/samplefreq*10000.D0
      itime=IDNINT(TIMEX)
      irate=IDNINT(samplerate)
      itimemodulo=MOD(itime,irate)
c     IF (itimemodulo .NE. 0) GO TO 777
```

Figure 47. Controller subroutine INJECT.

```
C Update the filter coefficients.
C     DELTAVGEN is the current generator delta omega.

         Yold(-2)=Yold(-1)
         Yold(-1)=Yold(0)
       deltavgen=etac(1)-376.991118431D0
         Yold(0)=deltavgen
         Ynew(-2)=Ynew(-1)
         Ynew(-1)=Ynew(0)

C Implement the filter. This is a high-pass digital filter
C     with sample rate = 10,000 and cutoff = 2 hertz.

         Ynew(0)=1.D0*Yold(0)-1.99999967967526D0*Yold(-1)
      &+0.99999967967526D0*Yold(-2)+1.99835970522999D0*Ynew(-1)
      &-0.99836034570430D0*Ynew(-2)

C The control action U is the gain times the filtered signal.

      U= 9.d0*Ynew(0)

C The following lines implement a "dead-zone"scheme.  If the filtered
C     signal stays below .2 for three time steps in a row the control
C     action is always zero.

C     Ysav=0.d0
C     DO I=-2,1,0
C       IF(Ynew(I) .GT. 0.2D0) Ysav=1.D0
C     END DO
C     if(Ysav.EQ.0.D0) U=0.d0

C Uncomment this to run the uncontrolled case.

c        U= 0.D0

C The brake is on when "brake"=1.  The IF statements are for implemeting
C     bang-bang control.  These can be commented out for classical control.

      brake=0.D0
      IF (U .LT. 0.1D0) U=0.D0
C     IF (U .GT. 1.D0)  U=1.D0
      IF (U .GT. 0.D0)  brake=1.D0

C These set the voltage to the Type 60 sources.

      VBa=Va*(1.D0-DSQRT(U))
      VBb=Vb*(1.D0-DSQRT(U))
      VBc=Vc*(1.D0-DSQRT(U))


c     write(*,*) ' hit point',istep,deltavgen,u

777   RETURN                                                    GPC  B
      END                                                       GPC  B
```

Figure 47. Continued.

Figure 48 shows some of the EMTP subroutine CSUP. Much of the subroutine has been deleted for brevity. The CALL statement for the controller subroutine shown in Figure 47 can be found at the end of CSUP -- just before the RETURN statement.

```
      SUBROUTINE CSUP( L )                                      CSUPB      1
*CALL IMPLIDP                                                   CSUPB      2
      IMPLICIT DOUBLE PRECISION (A-H, O-Z)                      IMPLIDP    1
*END  IMPLIDP                                                   ........   0
```

Figure 48. Modifications to EMTP Subroutine CSUP.

```
.
.
.
Common block declarations of Subroutine CSUP deleted

.
.
.

*CALL TACSARB                                                          CSUPB      5
C     000000            DEFINITION OF TABLE NAMES                 000000TACSARB   1
      DIMENSION ISBLK (1), INSUP (1), JOUT  (1), ICOLCS(1), ILNTAB(1)  TACSARB   2
      DIMENSION KSUS  (1), IUTY  (1), IVARB (1)                        TACSARB   3
      DIMENSION RSBLK (1), UD1   (1), XTCS  (1), ATCS  (1), XAR   (1)  TACSARB   4
      DIMENSION PARSUP(1), AWKCS (1)                                   TACSARB   5
C     EQUIVALENCING OF SCALARS WHICH ARE TO BE CARRIED BETWEEN MODULES. TACSARB   6
      EQUIVALENCE (KONSCE, SPTACS(  1)), (KONCUR, SPTACS(  2))         TACSARB   7
      EQUIVALENCE (KONTOT, SPTACS(  3)), (KOFSCE, SPTACS(  4))         TACSARB   8
      EQUIVALENCE (KCOLCS, SPTACS(  5)), (KSPVAR, SPTACS(  6))         TACSARB   9
      EQUIVALENCE (KATCS , SPTACS(  7)), (KONSUP, SPTACS(  8))         TACSARB  10
      EQUIVALENCE (KPRSUP, SPTACS(  9)), (KIVARB, SPTACS( 10))         TACSARB  11
      EQUIVALENCE (KALIU , SPTACS( 11)), (KJOUT , SPTACS( 12))         TACSARB  12
      EQUIVALENCE (KIUTY , SPTACS( 13)), (KUD1  , SPTACS( 14))         TACSARB  13
      EQUIVALENCE (KAWKCS, SPTACS( 15)), (KXAR  , SPTACS( 16))         TACSARB  14
      EQUIVALENCE (KXTCS , SPTACS( 17)), (KLNTAB, SPTACS( 18))         TACSARB  15
      EQUIVALENCE (KISBLK, SPTACS( 19)), (KRSBLK, SPTACS( 20))         TACSARB  16
      EQUIVALENCE (KKSUS , SPTACS( 21)), (KALKSU, SPTACS( 22))         TACSARB  17
      EQUIVALENCE (KINSUP, SPTACS( 23))                                TACSARB  18
      EQUIVALENCE ( SPTACS(1), ISBLK (1), KSUS  (1), IUTY  (1) )       TACSARB  19
      EQUIVALENCE ( SPTACS(1), ILNTAB(1), ICOLCS(1), JOUT  (1) )       TACSARB  20
      EQUIVALENCE ( SPTACS(1), INSUP (1), IVARB (1), PARSUP(1) )       TACSARB  21
      EQUIVALENCE ( SPTACS(1), RSBLK (1), UD1   (1), XTCS  (1) )       TACSARB  22
      EQUIVALENCE ( SPTACS(1), ATCS  (1), XAR   (1), AWKCS (1) )       TACSARB  23
      EQUIVALENCE   ( NUK   , LSTAT(51) ),      ( IA    , LSTAT(52) )  TACSARB  24
      EQUIVALENCE   ( NSU   , LSTAT(53) ),      ( NIU   , LSTAT(54) )  TACSARB  25
      EQUIVALENCE   ( NSUP  , LSTAT(55) ),      ( KARG  , LSTAT(56) )  TACSARB  26
      EQUIVALENCE   ( KPAR  , LSTAT(57) ),      ( KXIC  , LSTAT(58) )  TACSARB  27
      EQUIVALENCE   ( IOUTCS, LSTAT(59) ),      ( NSUDV , LSTAT(60) )  TACSARB  28
*END  TACSARB                                                          ........   0
      DIMENSION ARG( 50), ACC( 20), AMX( 20)                           CSUPB      6
      DIMENSION IOP( 50), IFL( 20), IDN( 20)                           CSUPB      7
C     000  B = THE ARGUMENT AND LATER THE VALUE OF THE FUNCTION,       CSUPB      8
C     000      BEFORE IT IS AFFECTED BY THE ALGEBRAIC OPERATION        CSUPB      9
C     000      WHICH WILL UPDATE 'A' .                                 CSUPB     10
C     000  A = INTERMEDIATE VALUES OF THE SUPPLEMENTAL                 CSUPB     11
C     000      VARIABLE OR DEVICE .                                    CSUPB     12


.
.
.
Much of Subroutine CSUP deleted

.
.
.


C     --- MIN/MAX TRACKING, CONTROLLED ACCUMULATOR OR COUHTER ---      CSUPB    654
  664 NDX4 = KXTCS + IVARB( N1 + 3 )                                   CSUPB    655
      IF ( NDX4 .EQ. KXTCS )  GO TO 6641                               CSUPB    656
      IF ( XTCS( NDX4) .LE. FLZERO )  GO TO 6641                       CSUPB    657
      A = PARSUP( NN + 2 )                                             CSUPB    658
      GO TO 6643                                                       CSUPB    659
 6641 NDX5 = KXTCS + IVARB( N1 + 4 )                                   CSUPB    660
```

Figure 48. Continued.

```
      IF ( NDX5 .EQ. KXTCS )  GO TO 6642                                CSUPB     661
      IF ( XTCS( NDX5) .LE. FLZERO )  GO TO 6642                        CSUPB     662
      A = PARSUP(NN)                                                    CSUPB     663
      GO TO 11                                                          CSUPB     664
 6642 IF ( N2 .EQ. 16 ) GO TO 665                                       CSUPB     665
      A = PARSUP(NN)                                                    CSUPB     666
      RDEV1 = PARSUP( NN + 1 )                                          CSUPB     667
      IF ( RDEV1 .EQ. -1.0  .AND.  B .LT. A )  A = B                    CSUPB     668
      IF ( RDEV1 .EQ. +1.0  .AND.  B .GT. A )  A = B                    CSUPB     669
      GO TO 6643                                                        CSUPB     670
  665 A = PARSUP(NN) + B                                                CSUPB     671
 6643 PARSUP(NN) = A                                                    CSUPB     672
      GO TO 11                                                          CSUPB     673
  666 IVARB(N1+4) = IVARB(N1+4) + 1                                     CSUPB     674
      K = IVARB( N1 + 3 )                                               CSUPB     675
      IF ( IVARB(N1+4) .GT. K ) IVARB(N1+4) = 1                         CSUPB     676
      NDX1 = NN + IVARB( N1 + 4 )                                       CSUPB     677
      PARSUP(NDX1) = B * B                                              CSUPB     678
      DO 6666 JI = 1, K                                                 CSUPB     679
 6666 A = A + PARSUP( NN + JI )                                         CSUPB     680
      A = SQRTZ( A * PARSUP(NN) )                                       CSUPB     681
      GO TO 11                                                          CSUPB     682
  667 J = IVARB( N1 + 1 )                                               CSUPB     683
      K = IVARB( N1 + 2 )                                               CSUPB     684
      B = 0.0                                                           CSUPB     685
      DO 1166 MJ = J, K                                                 CSUPB     686
      N = KKSUS + MJ                                                    CSUPB     687
      IF ( KSUS(N)  .EQ.  9 ) GO TO 1166                                CSUPB     688
      M = KALKSU + MJ                                                   CSUPB     689
      BB = XTCS( KXTCS + KSUS(M) ) * KSUS(N)                            CSUPB     690
      NJ = MJ                                                           CSUPB     691
 1144 NJ = NJ - 1                                                       CSUPB     692
      N = N - 1                                                         CSUPB     693
      M = M - 1                                                         CSUPB     694
      IF ( NJ  .LT.  J ) GO TO 1155                                     CSUPB     695
      IF ( KSUS(N)  .NE.  9 ) GO TO 1155                                CSUPB     696
      BB = BB * XTCS( KXTCS + KSUS(M) )                                 CSUPB     697
      GO TO 1144                                                        CSUPB     698
 1155 B = B + BB                                                        CSUPB     699
 1166 CONTINUE                                                          CSUPB     700
      A = B * PARSUP( NN + 3 )                                          CSUPB     701
      AA = A * PARSUP( NN )                                             CSUPB     702
      IF ( AA .GE. PARSUP(NN+1) ) GO TO 6677                            CSUPB     703
      A = PARSUP(NN+1) / PARSUP(NN)                                     CSUPB     704
      GO TO 11                                                          CSUPB     705
 6677 IF ( AA .LE. PARSUP(NN+2) ) GO TO 11                              CSUPB     706
      A = PARSUP(NN+2) / PARSUP(NN)                                     CSUPB     707
   11 NDX1 = NNN + I                                                    CSUPB     708
      XTCS(NDX1) = A                                                    CSUPB     709
   10 I = INSUP(KINSUP+I)                                               CSUPB     710
      IF ( I .GT. 0 ) GO TO 1234                                        CSUPB     711

C***********************************************************************
C Call the controller subroutine to compute the control action.
C    XTCS holds the voltages specified by the TACS Supplemental Variables.
C    Generator Delta Omega is brought in through the common block ETACS.
C***********************************************************************

      call inject(ISTEP,DELTAT,xtcs(nnn+1),xtcs(nnn+2),xtcs(nnn+3),     MKD21491    1
     &xtcs(nnn+4),xtcs(nnn+5),xtcs(nnn+6),xtcs(nnn+7))                  MKD21491    2
 9999 RETURN                                                            CSUPB     712
      END                                                               CSUPB     713
```

Figure 48. Continued.

APPENDIX D

ADAMS PREDICTOR-CORRECTOR TO IMPLEMENT A PASC SYSTEM

This appendix contains the source code to implement a fourth-order Adams Predictor-Corrector on an experimental PASC system. Much of the program is specific to the PASC system. This is particularly true with the INPUT subroutine which initializes the "A" and "B" matrices for the state-space formulation $\dot{x} = Ax + Bu$. The generic implementation of the integration algorithm can be easily gleaned from the information contained herein. Figure 49 shows the entire program while Figure 50 shows an example of a file that can be used to execute the program for typical PASC data.

```
C*********************************************************************
C**                                    ***
C**   Program A_MOULTON is a 4-step, predictor-corrector integration *
C**     routine using the fourth order ADAMS-BASHFORTH predictor    ***
C**     and the fourth order ADAMS-MOULTON corrector.  Function     ***
C**     calls are made to APRED and ACORR to advance to the next    ***
C**     integration step.  Since the global truncation error        ***
C**     inherent in this scheme is on the order of h^4, a step      ***
C**     size of smaller than 10e-02 should not be taken with        ***
C**     single precision math.                                      ***
C**                                                                   ***
C**   Multi-step methods require more than one starting value to    ***
C**     proceed.  Usually, a Runge-Kutta method would be used to    ***
C**     get the first three steps.  In some cases, however, it can ***
C**     be assumed that the system has been at rest for some time   ***
C**     and the conditions at the first four steps are known (first **
C**     three steps and the initial condition).                     ***
C**                                    ***
C*********************************************************************

      PROGRAM A_MOULTON

C
C - Subroutines called,
C     >>INPUT   - allows inputs to the routine.(step size, etc.)
C     >>INITIAL - develops the four initial states required for the
C                 algorithm.  One state is initial condition, and
C                 the rest are usually found with three steps of
C                 Runge-Kutta.
C     >>STATE   - evaluates f  =y' = di/dt  for use in the function
C                 calls.     n   n
C     >>OUTPUT  - sets up and records the output data.
C
C - Functions called,
C     >>APRED
C     >>ACORR
C

C - Declare variables

      IMPLICIT REAL*8 (A-H),(O-Z)
      REAL*8 TNOW,TFIN,h,hOVER24,PERIOD,DCVOLTS,Linv,LinvR,Cur
      INTEGER N_prnt_var
      CHARACTER*20 FILENAME
```

Figure 49. Adams Predictor-Corrector for Experimental PASC System.

```
C
C - Dimension arrays
C
      DIMENSION Ynplus1(100),Yn(100),Fnplus1(100),Fn(100),Fn_1(100),
     &          Fn_2(100),Fn_3(100)
      DIMENSION Cur(100)

C
C - Common buffer caries some integration variables that should be
C     defined in input
C
      COMMON/INTVARS/ TNOW,TFIN,TNRMLIZD,h,hOVER24
      COMMON/INTVARS2/ N_st_eqs,N_btw_out,N_prnt_var(50)
      COMMON/STVARS/ PERIOD,Vs,Linv(50,50),LinvR(50,50)
      COMMON/PARAMS/ a,RS1(50),RS2p(50),RS2s(50),Rl,SUPPLY(50)
      COMMON/PARAMS1/ Lm,Ls
      COMMON/PARAMS2/ RS1closed,RS2popen

C
C - Subroutine INPUT establishes integration parameters such as step
C     size and any input variables used.
C
      h=0.D0
      CALL INPUT

C
C - Subroutine INITIAL steps the integration through its first three
C     steps using a single step method such as Runge-Kutta.  It may
C     also be possible to assume that the system has been at rest
C     for some time and use an assumed value for the first three
C     steps.
C
      CALL INITIAL(Yn,Fn_1,Fn_2,Fn_3)

C
C - Initialize TNOW
C
      TNOW = 0.D0

C
C - Call OUTPUT to initialize the output file
C
      WRITE(*,*) ' Input the name of the OUTPUT file. <fid.ext>'
      READ(*,101) FILENAME
      OPEN(UNIT=1,FILE=FILENAME,STATUS='NEW')
 101  FORMAT(A20)

C
C - Subroutine STATE evaluates the function at the current step.  It
C      returns a value for Fn(I) from the values of Yn(1 thru N_st_eqs).
C      This particular call evaluates Fn using the corrected Yn for use
C      in predicting the value of Ynplus1.
C
C - Beginning of integration loop.
C
 777  CALL STATE(Fn,Yn)
```

Figure 49. Continued.

```
C
C - Subroutine OUTPUT provides a format for storage of the desired
C     output at integration step n.
C

      Tprnt = TNOW/(N_btw_out*h) - NINT(TNOW/(N_btw_out*h))
      IF(ABS(Tprnt) .LE. 1.0D-08) CALL OUTPUT(Yn,Fn)

C
C - Function APRED predicts the value of Ynplus1 using an explicit
C     algorithm.
C

      DO I=1,N_st_eqs
        Ynplus1(I) = APRED(Yn(I),Fn(I),Fn_1(I),Fn_2(I),Fn_3(I))
      END DO

C
C - Subroutine STATE evaluates the function at the current step.  It
C      returns a value for Fn(I) from the values of Yn(1 thru N_st_eqs).
C      This particular call evaluates Fnplus1 using the predicted
C      Ynplus1 for use in correcting the value of Ynplus1.
C

      CALL STATE(Fnplus1,Ynplus1)

C
C - Function ACORR corrects the value of Ynplus1 using an implicit
C     algorithm.
C

      DO I=1,N_st_eqs
        Ynplus1(I) = ACORR(Yn(I),Fnplus1(I),Fn(I),Fn_1(I),Fn_2(I))
      END DO

C
C - Move to the next integration step.
C

      DO I=1,N_st_eqs
        Fn_3(I) = Fn_2(I)
        Fn_2(I) = Fn_1(I)
        Fn_1(I) = Fn(I)
        Yn(I)   = Ynplus1(I)
      END DO
        TNOW    = TNOW + h



C
C - End of integration loop
C

      IF(TNOW .LE. TFIN) GO TO 777


      STOP 'INTEGRATION COMPLETED'
      END
```

Figure 49. Continued.

```
C*********************************************************************
C**                                                                 ***
C**   APRED is a fourth order ADAMS-BASHFORTH predictor to be used ***
C**     with a fourth order ADAMS-MOULTON corrector AMOULT.         ***
C**     The predictor is of the form                                ***
C**                                                                   ***
C**       y   =y  + h/24*(55f -59f   +37f   -9f   )              ***
C**        n+1  n            n    n-1    n-2   n-3               ***
C**                                                                   ***
C**   f -f    are defined by f =y'(x ,y )                           ***
C**    n  n-3                 n     n  n                           ***
C**                                                                   ***
C**       and are passed into APRED from the main program.      ***
C**                                                                   ***
C**   This fourth order Predictor, when used with an appropriate    ***
C**     fourth order Corrector has a global truncation error on     ***
C**     the order of h^4, so a step size smaller than 10e-02        ***
C**     will be affected largely by machine error and not by        ***
C**     error in integration.                                       ***
C**                                                                 ***
C**                                                                   ***
C**                                        ***
C*********************************************************************

      REAL FUNCTION APRED(Yn,Fn,Fn_1,Fn_2,Fn_3)

      IMPLICIT REAL*8 (A-H),(O-Z)

      COMMON/INTVARS/ TNOW,TFIN,TNRMLIZD,h,hOVER24
      COMMON/INTVARS2/ N_st_eqs,N_btw_out,N_prnt_var(50)


      APRED = Yn + hOVER24*(55.*Fn - 59.*Fn_1 + 37.*Fn_2 - 9.*Fn_3)

      RETURN

      END



C*********************************************************************
C**                                        ***
C**   ACORR is a fourth order ADAMS-MOULTON corrector to be used   ***
C**     with a fourth order ADAMS-BASHFORTH predictor APRED.       ***
C**     The corrector is of the form                               ***
C**                                                                   ***
C**       y   =y  + h/24*(9f   +19f -5f   +f    )              ***
C**        n+1  n           n+1    n   n-1  n-2                ***
C**                                                                   ***
C**   f -f    are defined by f =y'(x ,y )                           ***
C**    n  n-2                 n     n  n                           ***
C**                                                                   ***
C**       and are passed into ACORR from the main program.      ***
C**                                                                   ***
C**   This fourth order Corrector, when used with an appropriate    ***
C**     fourth order Predictor has a global truncation error on     ***
C**     the order of h^4, so a step size smaller than 10e-02        ***
C**     will be affected largely by machine error and not by        ***
C**     error in integration.                                       ***
C**                                                                 ***
C**                                                                   ***
C**                                        ***
C*********************************************************************
```

Figure 49. Continued.

```
      REAL FUNCTION ACORR(Yn,Fnplus1,Fn,Fn_1,Fn_2)

      IMPLICIT REAL*8 (A-H),(O-Z)

      COMMON/INTVARS/ TNOW,TFIN,TNRMLIZD,h,hOVER24
      COMMON/INTVARS2/ N_st_eqs,N_btw_out;N_prnt_var(50)


      ACORR = Yn + hOVER24*(9.*Fnplus1 + 19.*Fn - 5.*Fn_1 + Fn_2)

      RETURN

      END



C*************************************************************************
C**                                        ***
C** Subroutine INPUT is used to define the user parameters of the    ***
C**   integration.  The value for step size should be defined and  ***
C**   the number of state variables declared.  The common variable ***
C**   hOVER24 should also be initialized.  Also,                   ***
C**   certain changeable inputs can be initialized here and used   ***
C**   throughout the code such as in STATE.                        ***
C**                                        ***
C*************************************************************************

      SUBROUTINE INPUT

      IMPLICIT REAL*8 (A-H),(O-Z)
      REAL*8 Lp,Ls,Lm,L,Linv,LinvR

      INTEGER N_prnt_var,SaveTruncTNRML

      DIMENSION L(50,50),R(50,50)

      COMMON/INTVARS/ TNOW,TFIN,TNRMLIZD,h,hOVER24
      COMMON/INTVARS2/ N_st_eqs,N_btw_out,N_prnt_var(50)
      COMMON/STVARS/ PERIOD,Vs,Linv(50,50),LinvR(50,50)
      COMMON/PARAMS/ a,RS1(50),RS2p(50),RS2s(50),Rl,SUPPLY(50)
      COMMON/PARAMS1/ Lm,Ls
      COMMON/PARAMS2/ RS1closed,RS2popen

C
C - If this is the first time through, initialize the integration
C     parameters.  Otherwise update the L and R matrices.
C
      IF(h .NE. 0.D0) GO TO 7
C
C - Integration parameters
C

      WRITE(*,*) ' Input the number of state equations. <??>'
      READ(*,*) N_st_eqs

      WRITE(*,*) ' Input the finish time. <?.??>'
      READ(*,*) TFIN

      WRITE(*,*) ' Input the step size. <?.??>'
      READ(*,*) h
      hOVER24 = h/24.D0
```

Figure 49. Continued.

```
      WRITE(*,*) ' Input the number of steps between calls to OUTPUT.
     & <??>'
      READ(*,*) N_btw_out

      WRITE(*,*) ' Input the number of output variables. <??>'
      READ(*,*) N_prnt_var(1)

      WRITE(*,*) ' Input the output variables. <??,??,??,...>'
      READ(*,*) (N_prnt_var(I), I=2,N_prnt_var(1)+1)

C
C - User parameters
C
      WRITE(*,*) ' Input the turns ratio. (Prim:Sec=a:1) <?.??>'
      READ(*,*) a

      WRITE(*,*) ' Input the primary inductance in Henrys. <?.??>'
      READ(*,*) Lp

      WRITE(*,*) ' Input the secondary inductance in Henrys. <?.??>'
      READ(*,*) Ls

      WRITE(*,*) ' Input the magnetizing inductance in Henrys. <?.??>'
      READ(*,*) Lm

      WRITE(*,*) ' Input the core loss resistance in Ohms. <?.??>'
      READ(*,*) Rc

      WRITE(*,*) ' Input the source resistance in Ohms. <?.??>'
      READ(*,*) RS1closed

      WRITE(*,*) ' Input the open source GTO forward resistance
     &in Ohms. <?.??>'
      READ(*,*) RS1open

      WRITE(*,*) ' Input the primary shorting (snubbing)
     &resistance in Ohms. <?.??>'
      READ(*,*) RS2pclosed

      WRITE(*,*) ' Input the primary open shorting (snubbing)
     &GTO resistance in Ohms. <?.??>'
      READ(*,*) RS2popen

      WRITE(*,*) ' Input the secondary shorting (snubbing)
     &resistance in Ohms. <?.??>'
      READ(*,*) RS2sclosed

      WRITE(*,*) ' Input the secondary open shorting (snubbing)
     &GTO resistance in Ohms. <?.??>'
      READ(*,*) RS2sopen

      WRITE(*,*) ' Input the load resistance in Ohms. <?.??>'
      READ(*,*) Rl

      WRITE(*,*) ' Input the period. <?.??>'
      READ(*,*) PERIOD

      WRITE(*,*) ' Input the DC supply voltage. <?.??>.'
      READ(*,*) Vs
      IF(Vs .LT. 0.0) Vs = (-1.)*Vs
```

Figure 49. Continued.

```
C
C - Initialize the matrix of inductances for the 1-core.
C

      DO I=1,50
        DO J=1,50
          R(I,J) = 0.D0
          L(I,J) = 0.D0
          LINV(I,J) = 0.D0
          LINVR(I,J) = 0.D0
        END DO
      END DO

      SaveTruncTNRML = 1

C
C - Vary the Resistance values depending on whether or not the
C -   appropriate supplies are "switched in".  This is supposed
C -   to simulate diodes.  Example: RS1=1.E+06 means that GTO1
C -   is open.  This only needs to be done if this is the first
C -   time through, or a switch point has been reached.
C

 7    IF(SaveTruncTNRML .EQ. IDINT(TNRMLIZD)) GO TO 77

      DO I=1,22,3

        IF(SUPPLY(I) .EQ. 0.D0) RS1((I+2)/3) = RS1open
        IF(SUPPLY(I) .NE. 0.D0) RS1((I+2)/3) = RS1closed

        IF(SUPPLY(I) .NE. 0.D0) RS2p((I+2)/3) = RS2popen
        IF(SUPPLY(I) .EQ. 0.D0) RS2p((I+2)/3) = RS2pclosed

        IF(SUPPLY(I) .NE. 0.D0) RS2s((I+2)/3) = RS2sopen
        IF(SUPPLY(I) .EQ. 0.D0) RS2s((I+2)/3) = RS2sclosed

      END DO

C
C - Develop the matrix of inductances for the 1-core.
C

      L(1,1) = Lp/a**2
      L(1,2) = Lm/a**2
      L(2,2) = Lm/Rc
      L(3,2) = -Lm*(1.D0/RS2s(1)+1.D0/Rl)/a**2
      L(3,3) = Ls*(1.D0/RS2s(1)+1.D0/Rl)/a**2
      L(3,5) = -Lm/(Rl*a**2)
      L(3,6) = Ls/Rl
      L(3,8) = -Lm/(Rl*a**2)
      L(3,9) = Ls/Rl
      L(3,11) = -Lm/(Rl*a**2)
      L(3,12) = Ls/Rl
      L(3,14) = -Lm/(Rl*a**2)
      L(3,15) = Ls/Rl
      L(3,17) = -Lm/(Rl*a**2)
      L(3,18) = Ls/Rl
      L(3,20) = -Lm/(Rl*a**2)
      L(3,21) = Ls/Rl
      L(3,23) = -Lm/(Rl*a**2)
      L(3,24) = Ls/Rl
```

Figure 49. Continued.

```
L(4,4) = Lp/a**2
L(4,5) = Lm/a**2
L(5,5) = Lm/Rc
L(6,2) = -Lm/(Rl*a**2)
L(6,3) = Ls/Rl
L(6,5) = -Lm*(1.D0/RS2s(2)+1.D0/Rl)/a**2
L(6,6) = Ls*(1.D0/RS2s(2)+1.D0/Rl)/a**2
L(6,8) = -Lm/(Rl*a**2)
L(6,9) = Ls/Rl
L(6,11) = -Lm/(Rl*a**2)
L(6,12) = Ls/Rl
L(6,14) = -Lm/(Rl*a**2)
L(6,15) = Ls/Rl
L(6,17) = -Lm/(Rl*a**2)
L(6,18) = Ls/Rl
L(6,20) = -Lm/(Rl*a**2)
L(6,21) = Ls/Rl
L(6,23) = -Lm/(Rl*a**2)
L(6,24) = Ls/Rl

L(7,7) = Lp/a**2
L(7,8) = Lm/a**2
L(8,8) = Lm/Rc
L(9,2) = -Lm/(Rl*a**2)
L(9,3) = Ls/Rl
L(9,5) = -Lm/(Rl*a**2)
L(9,6) = Ls/Rl
L(9,8) = -Lm*(1.D0/RS2s(3)+1.D0/Rl)/a**2
L(9,9) = Ls*(1.D0/RS2s(3)+1.D0/Rl)/a**2
L(9,11) = -Lm/(Rl*a**2)
L(9,12) = Ls/Rl
L(9,14) = -Lm/(Rl*a**2)
L(9,15) = Ls/Rl
L(9,17) = -Lm/(Rl*a**2)
L(9,18) = Ls/Rl
L(9,20) = -Lm/(Rl*a**2)
L(9,21) = Ls/Rl
L(9,23) = -Lm/(Rl*a**2)
L(9,24) = Ls/Rl

L(10,10) = Lp/a**2
L(10,11) = Lm/a**2
L(11,11) = Lm/Rc
L(12,2) = -Lm/(Rl*a**2)
L(12,3) = Ls/Rl
L(12,5) = -Lm/(Rl*a**2)
L(12,6) = Ls/Rl
L(12,8) = -Lm/(Rl*a**2)
L(12,9) = Ls/Rl
L(12,11) = -Lm*(1.D0/RS2s(4)+1.D0/Rl)/a**2
L(12,12) = Ls*(1.D0/RS2s(4)+1.D0/Rl)/a**2
L(12,14) = -Lm/(Rl*a**2)
L(12,15) = Ls/Rl
L(12,17) = -Lm/(Rl*a**2)
L(12,18) = Ls/Rl
L(12,20) = -Lm/(Rl*a**2)
L(12,21) = Ls/Rl
L(12,23) = -Lm/(Rl*a**2)
L(12,24) = Ls/Rl
```

Figure 49. Continued.

```
L(13,13) = Lp/a**2
L(13,14) = Lm/a**2
L(14,14) = Lm/Rc
L(15,2) = -Lm/(Rl*a**2)
L(15,3) = Ls/Rl
L(15,5) = -Lm/(Rl*a**2)
L(15,6) = Ls/Rl
L(15,8) = -Lm/(Rl*a**2)
L(15,9) = Ls/Rl
L(15,11) = -Lm/(Rl*a**2)
L(15,12) = Ls/Rl
L(15,14) = -Lm*(1.D0/RS2s(5)+1.D0/Rl)/a**2
L(15,15) = Ls*(1.D0/RS2s(5)+1.D0/Rl)/a**2
L(15,17) = -Lm/(Rl*a**2)
L(15,18) = Ls/Rl
L(15,20) = -Lm/(Rl*a**2)
L(15,21) = Ls/Rl
L(15,23) = -Lm/(Rl*a**2)
L(15,24) = Ls/Rl

L(16,16) = Lp/a**2
L(16,17) = Lm/a**2
L(17,17) = Lm/Rc
L(18,2) = -Lm/(Rl*a**2)
L(18,3) = Ls/Rl
L(18,5) = -Lm/(Rl*a**2)
L(18,6) = Ls/Rl
L(18,8) = -Lm/(Rl*a**2)
L(18,9) = Ls/Rl
L(18,11) = -Lm/(Rl*a**2)
L(18,12) = Ls/Rl
L(18,14) = -Lm/(Rl*a**2)
L(18,15) = Ls/Rl
L(18,17) = -Lm*(1.D0/RS2s(6)+1.D0/Rl)/a**2
L(18,18) = Ls*(1.D0/RS2s(6)+1.D0/Rl)/a**2
L(18,20) = -Lm/(Rl*a**2)
L(18,21) = Ls/Rl
L(18,23) = -Lm/(Rl*a**2)
L(18,24) = Ls/Rl

L(19,19) = Lp/a**2
L(19,20) = Lm/a**2
L(20,20) = Lm/Rc
L(21,2) = -Lm/(Rl*a**2)
L(21,3) = Ls/Rl
L(21,5) = -Lm/(Rl*a**2)
L(21,6) = Ls/Rl
L(21,8) = -Lm/(Rl*a**2)
L(21,9) = Ls/Rl
L(21,11) = -Lm/(Rl*a**2)
L(21,12) = Ls/Rl
L(21,14) = -Lm/(Rl*a**2)
L(21,15) = Ls/Rl
L(21,17) = -Lm/(Rl*a**2)
L(21,18) = Ls/Rl
L(21,20) = -Lm*(1.D0/RS2s(7)+1.D0/Rl)/a**2
L(21,21) = Ls*(1.D0/RS2s(7)+1.D0/Rl)/a**2
L(21,23) = -Lm/(Rl*a**2)
L(21,24) = Ls/Rl
```

Figure 49. Continued.

```
      L(22,22) = Lp/a**2
      L(22,23) = Lm/a**2
      L(23,23) = Lm/Rc
      L(24,2) = -Lm/(Rl*a**2)
      L(24,3) = Ls/Rl
      L(24,5) = -Lm/(Rl*a**2)
      L(24,6) = Ls/Rl
      L(24,8) = -Lm/(Rl*a**2)
      L(24,9) = Ls/Rl
      L(24,11) = -Lm/(Rl*a**2)
      L(24,12) = Ls/Rl
      L(24,14) = -Lm/(Rl*a**2)
      L(24,15) = Ls/Rl
      L(24,17) = -Lm/(Rl*a**2)
      L(24,18) = Ls/Rl
      L(24,20) = -Lm/(Rl*a**2)
      L(24,21) = Ls/Rl
      L(24,23) = -Lm*(1.D0/RS2s(8)+1.D0/Rl)/a**2
      L(24,24) = Ls*(1.D0/RS2s(8)+1.D0/Rl)/a**2

C - Invert L

      CALL FULPIVOT(L,24,LINV)

C - Develop the matrix of resistance coefficients for the 8-core.

      R(1,1) = -RS2p(1)*RS1(1)/(a**2*(RS1(1)+RS2p(1)))
        R(2,1) = 1.D0
      R(2,2) = -1.D0
      R(2,3) = -1.D0
      R(3,3) = -1.D0

      R(4,4) = -RS2p(2)*RS1(2)/(a**2*(RS1(2)+RS2p(2)))
        R(5,4) = 1.D0
      R(5,5) = -1.D0
      R(5,6) = -1.D0
      R(6,6) = -1.D0

      R(7,7) = -RS2p(3)*RS1(3)/(a**2*(RS1(3)+RS2p(3)))
        R(8,7) = 1.D0
      R(8,8) = -1.D0
      R(8,9) = -1.D0
      R(9,9) = -1.D0

      R(10,10) = -RS2p(4)*RS1(4)/(a**2*(RS1(4)+RS2p(4)))
        R(11,10) = 1.D0
      R(11,11) = -1.D0
      R(11,12) = -1.D0
      R(12,12) = -1.D0

      R(13,13) = -RS2p(5)*RS1(5)/(a**2*(RS1(5)+RS2p(5)))
        R(14,13) = 1.D0
      R(14,14) = -1.D0
      R(14,15) = -1.D0
      R(15,15) = -1.D0

      R(16,16) = -RS2p(6)*RS1(6)/(a**2*(RS1(6)+RS2p(6)))
        R(17,16) = 1.D0
      R(17,17) = -1.D0
      R(17,18) = -1.D0
      R(18,18) = -1.D0
```

Figure 49. Continued.

```
      R(19,19) = -RS2p(7)*RS1(7)/(a**2*(RS1(7)+RS2p(7)))
        R(20,19) = 1.D0
      R(20,20) = -1.D0
      R(20,21) = -1.D0
      R(21,21) = -1.D0

      R(22,22) = -RS2p(8)*RS1(8)/(a**2*(RS1(8)+RS2p(8)))
        R(23,22) = 1.D0
      R(23,23) = -1.D0
      R(23,24) = -1.D0
      R(24,24) = -1.D0

C - Multiply Linv and R

      CALL EMPROD(LINV,R,24,24,24,LINVR)

 77   SaveTruncTNRML = IDINT(TNRMLIZD)

      RETURN
      END


C*********************************************************************
C
C     MATRXPAK is a small set of routines that do the grinding
C     involved in numerical matrix calculations.  They are
C     equivalent to addition/subtraction, multiplication and
C     division for scalars.  Multiplication has two algorithms:
C     The garden variety procedure of forming repeated inner
C     (dot) vector products, and an algorithm by Lynn Cannon that
C     is suited to parallel processing in an array machine that
C     is nearest-neighbor connected, e.g., ILLIAC IV.  The inversion
C     routine does full pivoting of the array so that effects of
C     numerical ill-conditioning are minimized.  All routines show
C     dimensioning for 6 x 6 arrays but are useable for any size
C     problem without modification, since subroutine dimensioning
C     indicates only how indexing is to be performed.
C
C     The routines are not in way proprietary.  Feel free to
C     transport them anywhere.
C
C*********************************************************************

C***********************************************
C     Subroutine EMPROD multiplies matrices
C     using classical notions of inner products
C***********************************************

      SUBROUTINE EMPROD(A,B,N,M,L,C)

      REAL*8 A,B,C
      DIMENSION A(50,50),B(50,50),C(50,50)

      DO I=1,N
          DO J=1,L
          C(I,J)=0.
          DO K=1,M
              C(I,J) = C(I,J) + A(I,K)*B(K,J)
          END DO
          END DO
      END DO
      RETURN
      END
```

Figure 49. Continued.

```
C*****************************************************************
C     FULPIVOT inverts matrices using a Gauss-Jordan procedure
C     with full-pivoting.
C
C     AA = Matrix to be inverted
C     B  = Inverse of AA
C     N  = Size of matrices AA and B
C
C*****************************************************************

      SUBROUTINE FULPIVOT(AA,N,B)

      REAL*8 AA,A,B

      DIMENSION AA(50,50),A(50,50),B(50,50),JK(50)

C If AA is only 1 x 1 (a scalar), invert and return.
C
      IF (N .EQ. 1) THEN
          IF (AA(1,1) .NE. 0.0) THEN
              B(1,1) = 1.0 / AA(1,1)
          ELSE
              WRITE(7,100)
100           FORMAT(/' >>>>>  Determinant is zero.',
     &                         '  No inversion.  <<<<'/)
          END IF
          RETURN
      END IF

C  Copy AA into a working array.  At the same time, construct an
C  identity matrix, B, into which row operations on A will be
C  copied, thus forming the inverse.  Also clear the JK array
C  (which is used to mark those rows that have been processed)
C  to indicate that no rows have been processed.
C
      DO I=1,N
          DO J=1,N
              A(I,J) = AA(I,J)
              B(I,J) = 0.0
          END DO
      END DO

      DO I=1,N
          B(I,I) = 1.0
          JK(I)  = 0
      END DO

C  Execute the reduction loop N times
C
      DO K=1,N

C  Find the pivot element.  It is the largest element in the array
C  that is in the rows and columns that have not been processed.
C  The check for non-processed rows is for JK = 0.
C
          COMP = 0.0
```

Figure 49. Continued.

```
            DO J=1,N
                IF (JK(J) .EQ. 0) THEN
                    DO I=1,N
                        IF (JK(I) .EQ. 0) THEN
                            IF (ABS( A(I,J) ) .GT. COMP) THEN
                                COMP = ABS( A(I,J) )
                                II = I
                                JJ = J
                            END IF
                        END IF
                    END DO
                END IF
            END DO
            JK(JJ) = 1

C       COMP=0.
C       DO 4 J=1,N
C       IF(JK(J))4,5,4
C     5 DO 14 I=1,N
C       IF(JK(I))14,15,14
C    15 IF(COMP-ABS(A(I,J)))6,14,14
C     6 COMP=ABS(A(I,J))
C       II=I
C       JJ=J
C    14 CONTINUE
C     4 CONTINUE
C       JK(JJ)=1

C   Interchange rows if necessary.  Make the same interchanges on A and B.
C
            IF (II .NE. JJ) THEN
                DO J=1,N
                    TEMP    = A(II,J)
                    A(II,J) = A(JJ,J)
                    A(JJ,J) = TEMP
                    TEMP    = B(II,J)
                        B(II,J) = B(JJ,J)
                    B(JJ,J) = TEMP
                END DO
            END IF

C   Normalize the pivot row.
C
            IF ( A(JJ,JJ) .EQ. 0.0) THEN
                WRITE(7,100)
                RETURN
            END IF

            TEMP = 1.0 / A(JJ,JJ)
            DO J=1,N
                A(JJ,J) = TEMP * A(JJ,J)
                B(JJ,J) = TEMP * B(JJ,J)
            END DO
            A(JJ,JJ) = 1.0
```

Figure 49. Continued.

```
C  Perform the row operations.  Record them in both A and B.
C
          DO I=1,N
              IF (I .NE. JJ) THEN
                  TEMP = A(I,JJ)
                  DO J=1,N
                      A(I,J) = A(I,J) - TEMP*A(JJ,J)
                      B(I,J) = B(I,J) - TEMP*B(JJ,J)
                  END DO
              END IF
          END DO

      END DO
      RETURN
      END

C*************************************************************************
C**                                    ***
C** Subroutine INITIAL is used to find the values of the system at   ***
C**   the first three integation steps.  Usually, a Runge-Kutta     ***
C**   routine would be used to find these values, but it may be     ***
C**   possible to assume values for these states if the system can ***
C**   be assumed to be at rest for some time before the integration***
C**   is to start.                                                  ***
C**                                                                   ***
C**   Yn_3 is known (initial condition)                             ***
C**   Fn_3, Fn_2, Fn_1, and Yn need to be found by initial.         ***
C**                                                                   ***
C*************************************************************************

      SUBROUTINE INITIAL(Yn,Fn_1,Fn_2,Fn_3)

      IMPLICIT REAL*8 (A-H),(O-Z)

      DIMENSION Yn(100),Fn_1(100),Fn_2(100),Fn_3(100)

      DO I=1,100
        Yn(I)   = 0.0
        Fn_1(I) = 0.0
        Fn_2(I) = 0.0
        Fn_3(I) = 0.0
        END DO

      RETURN
      END



C*************************************************************************
C**                                    ***
C**       Subroutine STATE is a user-written subroutine              ***
C**     that describes the state equations for continuous          ***
C**     modeling of a system.  In this case, the system is         ***
C**     the 8-core PASC transformer with series connected          ***
C**     secondaries.  The state equations are of the form             ***
C**                                                                   ***
C**           Lx = Rx + u                                  ***
C**     where L is the matrix of inductances, R is the matrix      ***
C**     of resistances and u is a vector of driving functions.     ***
C**                                    ***                            ***
C**                                                                   ***
C*************************************************************************
```

Figure 49. Continued.

```
      SUBROUTINE STATE(DD,SS)

C - Declare variables that aren't implicit and dimension arrays

      IMPLICIT REAL*8 (A-H),(O-Z)
      REAL*8 LINV,LINVR,PERIOD,Vs

      INTEGER LOCK(20)

      DIMENSION DD(100),SS(100)

C - Common buffer STVARS is a buffer from input that contains
C -   some state equation parameters
C     INTVARS is the integration variables buffer

      COMMON/INTVARS/ TNOW,TFIN,TNRMLIZD,h,hOVER24
      COMMON/INTVARS2/ N_st_eqs,N_btw_out,N_prnt_var(50)
      COMMON/STVARS/ PERIOD,Vs,Linv(50,50),LinvR(50,50)
      COMMON/PARAMS/ a,RS1(50),RS2p(50),RS2s(50),Rl,SUPPLY(50)
      COMMON/PARAMS2/ RS1closed,RS2popen


C - Determine which DC supplies are energized by finding out
C -   where you are in time relative to one period.

      DO I=1,50
        SUPPLY(I) = 0.D0
      END DO

      TNRMLIZD = DMOD(TNOW,PERIOD)*32.D0/PERIOD

          IF((TNRMLIZD .GE. FLOAT(1)) .AND.
     &          (TNRMLIZD .LT. FLOAT(9))) THEN
        SUPPLY(1) = Vs/a*RS2popen/(RS1closed+RS2popen)
      END IF
          IF((TNRMLIZD .GE. FLOAT(2)) .AND.
     &          (TNRMLIZD .LT. FLOAT(10))) THEN
        SUPPLY(4) = Vs/a*RS2popen/(RS1closed+RS2popen)
      END IF
          IF((TNRMLIZD .GE. FLOAT(3)) .AND.
     &          (TNRMLIZD .LT. FLOAT(11))) THEN
        SUPPLY(7) = Vs/a*RS2popen/(RS1closed+RS2popen)
      END IF
          IF((TNRMLIZD .GE. FLOAT(4)) .AND.
     &          (TNRMLIZD .LT. FLOAT(12))) THEN
        SUPPLY(10) = Vs/a*RS2popen/(RS1closed+RS2popen)
      END IF
          IF((TNRMLIZD .GE. FLOAT(5)) .AND.
     &          (TNRMLIZD .LT. FLOAT(13))) THEN
        SUPPLY(13) = Vs/a*RS2popen/(RS1closed+RS2popen)
      END IF
          IF((TNRMLIZD .GE. FLOAT(6)) .AND.
     &          (TNRMLIZD .LT. FLOAT(14))) THEN
        SUPPLY(16) = Vs/a*RS2popen/(RS1closed+RS2popen)
      END IF
          IF((TNRMLIZD .GE. FLOAT(7)) .AND.
     &          (TNRMLIZD .LT. FLOAT(15))) THEN
        SUPPLY(19) = Vs/a*RS2popen/(RS1closed+RS2popen)
      END IF
          IF((TNRMLIZD .GE. FLOAT(8)) .AND.
     &          (TNRMLIZD .LT. FLOAT(16))) THEN
        SUPPLY(22) = Vs/a*RS2popen/(RS1closed+RS2popen)
      END IF
```

Figure 49. Continued.

```
          IF((TNRMLIZD .GE. FLOAT(17)) .AND.
     &          (TNRMLIZD .LT. FLOAT(25))) THEN
            SUPPLY(1) = -Vs/a*RS2popen/(RS1closed+RS2popen)
          END IF
            IF((TNRMLIZD .GE. FLOAT(18)) .AND.
     &          (TNRMLIZD .LT. FLOAT(26))) THEN
            SUPPLY(4) = -Vs/a*RS2popen/(RS1closed+RS2popen)
          END IF
            IF((TNRMLIZD .GE. FLOAT(19)) .AND.
     &          (TNRMLIZD .LT. FLOAT(27))) THEN
            SUPPLY(7) = -Vs/a*RS2popen/(RS1closed+RS2popen)
          END IF
            IF((TNRMLIZD .GE. FLOAT(20)) .AND.
     &          (TNRMLIZD .LT. FLOAT(28))) THEN
            SUPPLY(10) = -Vs/a*RS2popen/(RS1closed+RS2popen)
          END IF
            IF((TNRMLIZD .GE. FLOAT(21)) .AND.
     &          (TNRMLIZD .LT. FLOAT(29))) THEN
            SUPPLY(13) = -Vs/a*RS2popen/(RS1closed+RS2popen)
          END IF
            IF((TNRMLIZD .GE. FLOAT(22)) .AND.
     &          (TNRMLIZD .LT. FLOAT(30))) THEN
            SUPPLY(16) = -Vs/a*RS2popen/(RS1closed+RS2popen)
          END IF
            IF((TNRMLIZD .GE. FLOAT(23)) .AND.
     &          (TNRMLIZD .LT. FLOAT(31))) THEN
            SUPPLY(19) = -Vs/a*RS2popen/(RS1closed+RS2popen)
          END IF
            IF((TNRMLIZD .GE. FLOAT(24)) .AND.
     &          (TNRMLIZD .LT. FLOAT(32))) THEN
            SUPPLY(22) = -Vs/a*RS2popen/(RS1closed+RS2popen)
          END IF

C
C - Call input to update the LINV and LINVR matrices due to time-
C -   varying resistances.
C
      CALL INPUT

C - Write the state equations.
C -   DD(i) is the vector of time derivatives of current  x
C -   SS(i) is the vector of currents  x
C -   SS(1) is the first positive primary (P0)
C -   LINV is the inverse of the inductance matrix
C -   LINVR is the above multiplied by the resistance matrix
C -   SUPPLY is the vector of DC supply voltages
C -

      DO 11 I = 1,24
        DD(I) = 0.D0
        DO 10 J = 1,24
          DD(I) = DD(I) + LINVR(I,J)*SS(J) + LINV(I,J)*SUPPLY(J)
 10   CONTINUE
 11   CONTINUE


C - Return to MAIN

      RETURN

      END
```

Figure 49. Continued.

```
C*********************************************************************
C**                                                    ***
C** Subroutine OUTPUT is used to format the integration output.     ***
C**                                                    ***
C*********************************************************************

      SUBROUTINE OUTPUT(Yn,Fn)

      IMPLICIT REAL*8 (A-H),(O-Z)
      REAL*8 Lm,Ls,Isec

      INTEGER N_prnt_var,N_plot

      DIMENSION Yn(100),Fn(100)

      COMMON/INTVARS/ TNOW,TFIN,TNRMLIZD,h,hOVER24
      COMMON/INTVARS2/ N_st_eqs,N_btw_out,N_prnt_var(50)
      COMMON/PARAMS/ a,RS1(50),RS2p(50),RS2s(50),Rl,SUPPLY(50)
      COMMON/PARAMS1/ Lm,Ls


C
C - This is TEKPLOT format
C

      IF(TNOW .EQ. 0.0) THEN
        WRITE(1,*) 'US Dept. of Energy PASC Project'
        WRITE(1,*) ' '

C
C - Adjust for addition of Isec to output plots
C

        N_plot = N_prnt_var(1) + 1
        WRITE(1,102) N_plot
      END IF

C
C - Secondary current is same as 1st primary unless RS2s(1) is
C -   shorting.  Then use current in last primary.
C

      Isec = 0.D0
      IF (RS2s(1) .GE. 1.D3) THEN
        Isec = Yn(3)
      ELSE
        Isec = Yn(24)
      END IF

      WRITE(1,101) TNOW,Isec,(Yn(N_prnt_var(I)), I=2,N_prnt_var(1)+1)
 101  FORMAT(1X,F9.5,8(2X,',',F9.5))
 102  FORMAT(1X,I2)

      RETURN
      END
```

Figure 49. Continued.

Figure 50 shows a file that can be used to execute the integration routine along with some typical measured values for the PASC system.

```
$!
$!
$! - Com file to run PASC.EXE on a VAX/VMS system.
$!
$!
$! SET DEF myhome
$!
$ RUN/nodebug PASC
24              ;# of state variables
5.D-01              ;Finish time
1.D-07              ;Delta T
500             ;# steps between output calls
6               ;# of output variables
1,2,3,16,17,18          ;output varibles
5.D-01              ;turns ratio
2.3595D-04          ;Lp
9.438D-04           ;Ls
1.5075D-01          ;Lm
20.D0               ;Rc
10.D0               ;RS1closed
1.D4                ;RS1open
2.d-02              ;RS2pclosed
1.D4                ;RS2popen
1.d6                ;RS2sclosed
1.D6                ;RS2sopen
100.D0              ;Rl
1.6666667D-02           ;Period
60.D0               ;Vsource
t4.dat
$! del t4.dat;*
$!
$ EXIT
```

Figure 50. File to Execute the Integration Routine of Figure 49.